Title
Axial heterogeneity of water, bicarbonate and chloride transport in the rat proximal convoluted tubule

Author
Liu, Fu-Ying,

Publication Date
1986

Peer reviewed|Thesis/dissertation

AXIAL HETEROGENEITY OF WATER, BICARBONATE AND CHLORIDE TRANSPORT IN THE RAT PROXIMAL CONVOLUTED TUBULE

by

FU-YING LIU

DISSERTATION

Submitted in partial satisfaction of the requirements for the degree of

DOCTOR OF PHILOSOPHY

in

Physiology

in the

GRADUATE DIVISION

of the

UNIVERSITY OF CALIFORNIA

San Francisco

Date . . . . . University Librarian

Degree Conferred: JUN 15 1986 . . . . . .

DEDICATED

TO

My husband ----- Guo-Zhang Tan

and

My daughter ----- Wei-Tan

ACKNOWLEDGMENTS

I feel deeply that science means honest and solid knowledge and science is universal.

I wish to extend my deepest gratitude to the following people:

To Dr. Charles A. Noble, Jr., the previous chairman of the clinical internal medicine faculty, because due to his visit to China in 1978, I was introduced to Dr. Floyd C. Rector, Jr.

To Dr. Floyd C. Rector, Jr., for his constant acceptance, support, and guidance. His extraordinary knowledge and his great figure of a scientist are indelibly engraved on my mind.

To Dr. Martin G. Cogan, my supervisor, for his persistence of support, direct guidance, and patience, from the theory of renal physiology to the reality of the laboratory, from year to year.

To Dr. Christine A. Berry, my preceptor, for her special support and concern, special criticism in the knowledge of renal physiology which will endure for my academic career.

To Dr. Chuan-Lu Chiu, my initial teacher of nephrology in China, for his constant concern, encouragement, and moral support.

To Dr. Shan-Yan Lin, my initial director of nephrology in China, for his constant concern and encouragement.

To Dr. Robert J, Alpern, Dr. Patricia Ann Preisig, Kenneth Wong, and Monika Mueller, for their guidance in different techniques in this laboratory.

At last, I am, of course, deeply indebted to my whole family, my husband, my daughter, my parents, my parents-in-law, and others. My husband has helped to teach me to balance the other important aspects of my life.

ABSTRACT

Bicarbonate, chloride and water reabsorption in the early (initial mm) versus the late proximal convoluted tubule (PCT) and change in reabsorption in response to an increase in luminal flow rate or to alkalemia have not been systematically examined. Free-flow bicarbonate, chloride, and water transport as well as osmolality as a function of PCT length were examined by free-flow micropuncture techniques in Munich-Wistar rats. During hydropenia (the control condition), bicarbonate and water reabsorption were 354±21 peq/mm·min and 5.9±0.4 nl/mm·min in the first mm and fell progresively in the remaining 3.8 mm of the tubule. In contrast, chloride reabsorption was only 206±55 peq/mm·min in the first mm but was 50% higher in the rest of the tubule. Tubular fluid osmolality fell along the tubule and by the end PCT was 7.5±0.7 mosmol/kg less than in plasma or 4.7 mosmol/kg less than in Bowman's space. The hydraulic water permeability (P_f) was estimated to be between 0.2 and 2.0 cm/s in the first mm of the tubule and to have fallen to 0.1-0.2 cm/s by the end of the tubule.

As SNGFR was increased in other groups made euvolemic or given atrial natriuretic factor (ANF) or glucagon, bicarbonate reabsorption in both the early and the late PCT was flow-dependent. The early PCT exhibited flow-dependent saturable reabsorptive kinetics up to 520±12 peq/mm·min. Absolute

bicarbonate reabsorption was less in the late PCT but was not saturated at the flow rates studied. Chloride reabsorption increased markedly in the early PCT up to 585±21 peq/mm·min from hydropenia to euvolemia but was without further change following ANF and glucagon. Compared to animals with a normal pH (ANF and glucagon) with comparable filtered bicarbonate load, alkalemia suppressed only late PCT but not early PCT acidification. In conclusion: (1) luminal hypotonicity develops in the rat PCT and must be considered as part of the osmotic driving force for water reabsorption; and (2) free-flow water, bicarbonate and chloride reabsorption in the early PCT is distinguished from that in the late PCT, by being a high capacity, flow-responsive but saturable process relatively unaffected by alkalemia.

TABLE OF CONTENTS

LIST OF FIGURES

CHAPTER 1

BACKGROUND

The kidney plays important functions in the regulation of acid-base balance and extracellular volume. Water and anion transport (especially bicarbonate and chloride) in the proximal convoluted tubule (PCT) are critical for carrying out these functions. The PCT exhibits structural and functional differences along its length (1-4).

The purpose of this thesis is to better understand water, bicarbonate and chloride transport in the rat PCT. These studies were specifically designed to examine the magnitude, kinetics, and regulation of solute and water transport as a function of tubular length.

TRANSPORT

Bicarbonate Reabsorption. Bicarbonate is a critical element in acid-base homeostasis. A major functon of the kidney in the regulation of acid-base balance is in maintaining the plasma concentration of HCO_3^- within a narrow range (24 - 28 meq/L). The renal tubule participates in acid-base homeostasis by

conserving filtered bicarbonate as well as by secreting protons bound to either filtered buffers (as titratable acid) or ammonia (as ammonium ions). The bulk of filtered HCO_3^- is reabsorbed by the proximal convoluted tubule (PCT) (2). The PCT reabsorbs 80-90% of filtered bicarbonate (5) and reduces tubular fluid pH 0.6-0.8 units below that of blood. Cellular hydrogen ion secretion effects the PCT bicarbonate reabsorption, predominantly by sodium/hydrogen exchange (6, 7), and there are also parallel proton and bicarbonate leak pathways of relatively minor quantitative importance (6, 8). The major determinants of net proximal acidification include: luminal and peritubular bicarbonate concentrations and pH (8-13), flow rate (SNGFR) (5, 10, 13, 14), pCO_2 (15-17), renal nerve activity (18), and carbonic anhydrase activity (17, 19, 20). Minor determinants include: extracellular volume status and peritubular protein concentration (5, 10, 11, 21, 22), sodium chloride reabsorption (10, 23), and potassium depletion (10, 13, 24, 25).

Most information presently regarding the kinetics and regulation of PCT acidification have come from analysis of whole PCT or late PCT data. However, rigorous quantitation of absolute bicarbonate reabsorption as a function of proximal tubular length has not been done. The load-dependency and saturability of bicarbonate reabsorption in the PCT has been demonstrated for the late PCT only (8-11, 14). Whether acidification is higher (26), or lower (27) in the early PCT compared to the late PCT, and whether proximal acidification can (8-11, 14) or cannot (28) be saturated as a function of load in the early PCT have not been

resolved.

Chloride Reabsorption. Understanding of mechanisms and regulation of sodium chloride transport in the PCT has been enhanced by recent data from micropuncture, microperfusion, electrophysiologic, and isolated cell membrane studies, but it is still far from clear (29-36).

In the early PCT, electrogenic sodium transport coupled to neutral solutes, such as glucose and amino acids, results in a transepithelial potential difference (PD), lumen negative. If the sodium/chloride permeability ratio were low, this PD would be expected to drive net sodium chloride absorption. If the permeability ratio were high, only sodium re-cycling would occur. It is unknown whether active chloride transport exists in the early PCT. Quantitation of net chloride reabsorption in the early PCT and of change in reabsorption in response to alteration in luminal flow rate has not been attempted in the free-flow state.

Proximal sodium chloride reabsorption in the late PCT is generally accepted to be mediated by an electrically-neutral, active transport system in parallel with passive paracellular reabsorption, predominantly diffusion (4, 6, 29-36) without convection (37). Sodium chloride reabsorption in the late PCT is markedly affected by extracellular volume status, and specifically by the peritubular protein concentration (2, 5, 10, 20, 21, 22, 30). The effect by peritubular protein is on the

active component of sodium chloride reabsorption (3, 22, 28, 30, 38). Sodium chloride concentration is also affected by the magnitude of the lumen-to-blood chloride concentration gradient (4, 10, 19, 20, 30, 32), the principle driving force for the passive, diffusional component of sodium chloride reabsorption (4, 6, 31-36, 39). Finally, renal nerve activity and pCO_2 can affect both sodium chloride reabsorption as well as sodium bicarbonate reabsorption.

Water Reabsorption. The mechanism of water reabsorption in the PCT is controversial. There is no consensus regarding the relative importance of the potential driving forces along the nephron, including contributions by intercellular space cryoscopic hypertonicity, luminal fluid cryoscopic hypotonicity, and effective osmotic gradients due to differential solute reflection coefficients. Equally uncertain is the hydraulic water permeability (P_f) as a function of the PCT length.

Two methods have been used to measure P_f. The most commonly used method in micropuncture and microperfuson studies (in vivo or in vitro) is to calculate P_f by measuring water reabsorption per of tubule length (J_v) and the transepithelial osmotic gradient (Δosmol). P_f is then defined as:

$$P_f = RT(J_v)/AV_w \Delta osmol$$

where R and T have their usual meanings, V_w is the partial molar volume of water, and A is the epithelial area per mm tubule length (assuming a tubule radius of 15 μm). The most accurate

estimates of P_f are between 0.1 and 0.2 cm/sec in the rat PCT (40) and 0.1 and 0.3 cm/sec in the rabbit PCT (41-43). The possibility of axial changes of P_f has not been examined in the PCT.

Heterogeneity of Transport. The structural and functional heterogeneity of the superficial PCT has been documented by many previous studies . The early PCT has a higher capacity for transporting several filtered solutes including glucose (47, 48, 49), amino acids (50), and phosphate (49, 51, 52). But a sytematic examination of anion and water transport has not been undertaken. Furthermore, the kinetics and regulation of transport as a function of PCT length has not been reported previously.

PURPOSE

The first purpose of the present studies was to examine water, bicarbonate and chloride transport as a function of tubule length. The second purpose was to assess the effects of changes in luminal flow rate and alkalemia on segmental solute and water reabsorption.

To achieve these objectives, a new technique of free-flow micropuncture using Munich-Wistar rats was developed to compare the transport properties in the S_1 to S_2 segments of the PCT.

The results of these studies (Chapters 3-5) have been published or submitted for publication:

1. "Axial heterogeneity in the rat proximal convoluted tubule. I. Bicarbonate, chloride, and water transport" Am. J. Physiol. 247 (Renal Fluid Electrolyte Physiol. 16): F816-F821, 1984.

2. "Axial heterogeneity in the rat proximal convoluted tubule. II. Osmolality and osmotic water permeability" Am. J. Physiol. 247 (Renal Fluid Electrolyte Physiol. 16): F822-F826, 1984.

3. "Axial heterogeneity of bicarbonate, chloride and water transport in the rat proximal convoluted tubule. Effects of changes in luminal flow rate and of alkalemia". Submitted for publication J. Clin. Invest. 1986.

The coauthers listed in these publications directed and supervised the research which forms the basis for this dissertation.

CHAPTER 2.

GENERAL METHODOLOGY

MICROPUNCTURE

History. Wearn and Richard (44) were the first to demonstrate the possibility of collecting fluid from single glomerular capsules in the living kidney of the frog in 1921. In the next 20 years, they developed the methods for obtaining tubule fluid from the amphibian kidney and for quantitative analysis of the minute amounts of fluid obtained. Arthur M. Walker and Jean Oliver (45) were the first to collect fluid from the proximal convoluted tubule of the mammalian kidney (in 89 guinea pigs and 56 rats). In their classic paper (45), they described the preparation of the kidney. They first performed right nephrectomy to allow enlargement of the left kidney to be subsequently studied. The animal holder was a copper plate embedded in a sheet of cork and heated from beneath by a 15-watt bulb. A quartz pipette with tip of about 7μm in internal diameter was used for puncture. They observed that the vast majority of the tubule segments appearing on the kidney surface proved to be portions of the proximal convolution, although they occasionally found surface glomeruli in guinea pigs and in 6 of 100 rats.

In the ensuing 45 years, the micropuncture technique has

been improved. A significant discovery by Thurau was that a mutant strain of Wistar rat, the Munich-Wistar rat, had glomeruli consistently situated on the kidney surface which were therefore readily accessible for micropuncture. Our understanding of the process of glomerular filtration has benefited from the discovery of this rat. In 1971, Barry M. Brenner published the first paper using Munich-Wistar rats for investigation of the dynamics of glomerular ulrafiltration (46).

Technique. The experimental preparation and general micropuncture protocol is described in our three published papers (Chapters 3-5). The micropuncture technique used in this thesis is new and the following description with figures is given to help to understand this technque.

The rat was first placed on a thermostatically controlled (37°) micropuncture table. Catheters (PE50) were inserted into the femoral artery for blood pressure measurements and for blood sampling and into a jugular vein for inulin infusion. A tracheostomy was performed. The abdomen was opened by a midline incision, the kidney was stabilized and bathed in warmed saline (37°), and the ureter was cannulated. A surface glomerulus was then located. A small pipette (3-5 µm OD) was inserted into Bowman's space and a small droplet of oil stained with Sudan black was injected (Figure 1). The course of the injected oil droplet was carefully observed and mapped (Figure 2). Only glomeruli that were followed by at least five to seven surface

proximal convolutions were used. The localization pipette was withdrawn and at least one hour was allowed for the hole in Bowman's space to seal. Following inulin infusion and an equilibration period of 45 min, sequential timed 3-7 min collections were begun using 7-9 μm OD glass pipettes. The punctures started at the end-proximal convolution and worked in a retrograde fashion to Bowman's space (Figure 3). After 5 hours, to allow the tubule puncture sites to seal, latex or Microfil (Canton Biomedical products, Boulder, CO) was injected into Bowman's space to fill the entire tubule. At a later time, the kidney was incubated for 30-40 min in 6 N HCl. The cast of the tubule was carefully dissected, with the multiple puncture sites identified using the initial localization map, and it then was photographed (Figure 4). The entire proximal tubule length (glomerulus to the last puncture site) and the length to each puncture site were measured and recorded.

ANALYTIC TECHNIQUES

Osmolality. The osmolality of collected tubular fluid and plasma samples were measured on a nanoliter, melting point Ramsay-Brown osmosmeter. The accurate measurement of the freezing-point depression of very small quantities of aqueous solution is very difficult because of non-homogeneous cooling. The method of Ramsay-Brown avoids this problem by first freezing the sample and

then determining the thawing-point (53).

Five standards (sodium chloride solutions), covering the physiological range of 250 to 330 mosmol, were measured for each experiment. Each standard was measured 6 times. The standard curves relating temperature at melting to osmolality each had a linear regression coefficient of more than 0.998 (n=10) as seen in Figure 5.

The samples were prepared for the osmometer in the following steps. Pipettes were prepared using borosilicate capillary glass, 0.7-1.0 mm outer diameter, which was first pulled and broken to about 20 µm. The pipettes were cleaned with chloroform, rinsed with water, and dried with acetone. The inside of the pipettes were then siliconized with 98% pure 1,1,1,3,3,3-hexamethyldisilazane (Aldrich Chemical Company, Inc., Milwaukee, Wisconsin), heated for 20 minutes on a heating plate, and rinsed and dried again with acetone. The pipettes were filled with Sudan red-stained, water-equilibrated paraffin oil. Three samples were sequentially drawn into one pipette, separated by the same paraffin oil. The outside of the pipettes were washed with chloroform, and the tip sealed with Eastman 910 adhesive. The pipette was put into a 100 µl capillary tube of 4 cm length, which had been first sealed at one end and then filled with clear paraffin oil.

The schematic diagram of the osmometer is shown in Figure 6. The three samples in the measuring pipette were first frozen in a 90% ethanol bath with dry ice for 30 second, thus rapidly transferred to the osmometer bath, which had previously been

cooled to approximately -2°C by lowering a plastic container of dry ice and ethanol into the bath. The container was then removed from the bath. The samples were watched through a single eyepiece microscope. The temperature at which the last ice crystal disappeared in each sample was recorded. Each procedure was repeated 2-3 times for each pipette (containing 3 samples).

Bicarbonate. The total carbon dioxide contents of collected tubular fluid and plasma samples were measured by microcalorimetry (54). A microcalorimeter (picapnotherm) is an apparatus for measuring the heat released when LiOH and CO_2 react. Its sensitivity is less than 10 picomoles of bicarbonate. Total CO_2 was assumed to be principlly bicarbonate since the contribution of dissolved CO_2 and carbonate in the physiological pH range are quite small; at pH 7.4, 95% of the total CO_2 in physiological fluid is HCO_3^-. The overall reaction between CO_2 and LiOH is shown below:

$$2\ LiOH + CO_2 \longrightarrow Li_2CO_3 + H_2O$$
$$\Delta H = -8.96\ 10^4\ J/mole\ CO_2$$

This overall reaction is actually composed of two reactions:

$$2LiOH + 2H_2O \longrightarrow 2LiOH{\cdot}H_2O \qquad (1)$$
$$\Delta H = -1.214\ 10^5\ J/2moles\ H_2O$$
$$2LiOH{\cdot}H_2O + CO_2 \longrightarrow Li_2CO_3 + 3H_2O \qquad (2)$$

$\Delta H = 3.18 \quad 10^4$ J/mole

Figure 7 shows the diagram of the analytical system. Two standards (solutions of Na_2CO_3 with concentrations of either 10 and 25 mM or 25 and 40 mM) were used. The linearity and precision of typical measurements is seen in Figure 8. The correlation coefficient was >0.99 and the standard deviation was 0.5 mM (corresponding to 6.5 picomoles with a 35 nl pipette).

The sample was prepared in the following manner. The collected tubular fluid was transferred into a constant volume pipette filled with paraffin oil (from 12-40 nl). The tip of the pipette was sealed with paraffin oil (Figure 9). The sample was injected into a reaction chamber containing acid (H_3PO_4) through a mercury seal. Carbon dioxide is released as a gas by reacting with phosphoric acid:

$$Na_2CO_3 + 2H_3PO_4 \text{ ----> } 2NaH_2PO_4 + H_2O + CO_2$$

CO_2 is then blown in a column of inert gas into a chamber with LiOH and the resulting heat of the exothermic reaction is measured by a contiguous thermistor bead. Heat release is integrated over time.

Chloride. Chloride concentration, from a small volume (approximately 1 nl) of collected tubular fluid, was measured by electro-

metric titration (55).

The potentiometric end-point titration of chloride with silver depends upon the fact that the concentration of Cl^- ions determines the potential of a silver/silver chloride electrode which dips into the titration vessel. This chloride electrode is connected to a voltmeter, with a reference electrode which completes the circuit. The equipment used for this method is shown schematically in Figure 10. The method involves the following system:

$$Ag \;/\; 0.1\ N\text{-}AgNO_3 \;:\; 0.1\ N\text{-}HNO_3 \;/\; AgCl \;/\; Ag$$

to which an $\sim$0.1 N NaCl sample (in 1 nl) is added:

$$Ag \;/\; 0.1\ N\text{-}AgNO_3 \;:\; 0.1\ N\text{-}HNO_3 \;:\; 0.1\ N\text{-}NaCl \;/\; AgCl \;/\; Ag$$

The addition of NaCl increases the baseline potential to approximately 400 mV. Current is then passed through the AgCl electrode to liberate Ag^+. The Ag^+ complexes with Cl^- and precipitates as AgCl.

$$e^- + Ag^\bullet \text{ -----> } Ag^+$$
$$Ag^+ + Cl^- \text{ -----> } AgCl \downarrow$$

The removal of Cl^- by Ag^+ decreases the voltage in a logarithmic (Nernstian) fashion:

100 meq Cl^- = 400 mV

10 meq Cl^- = 340 mV

1 meq Cl^- = 280 mV

0.1 meq Cl^- = 220 mV

Thus the titration of Ag to Ag^+ is stoichiometrically equal to the reduction in chloride ion, which in turn is very sensitively monited by the change in electrode potential. When a very low Cl^- concentration is reached (i.e., $\leqslant$ 0.1 meq, equivalent to 220 mV), the titration is stopped. The amount of current which had been needed for the titration is then measured, because it had been stored on a capacitor. That current is therefore proportional to the number of Cl^- ions titrated in the sample volume.

In practice, two standard NaCl concentrations bracketing the physiological range (100 meq/L and 130 meq/L) were used. A typical standard curve is shown in Figure 11. The chloride concentration of a sample is calculated from the voltage measurement and standard curve.

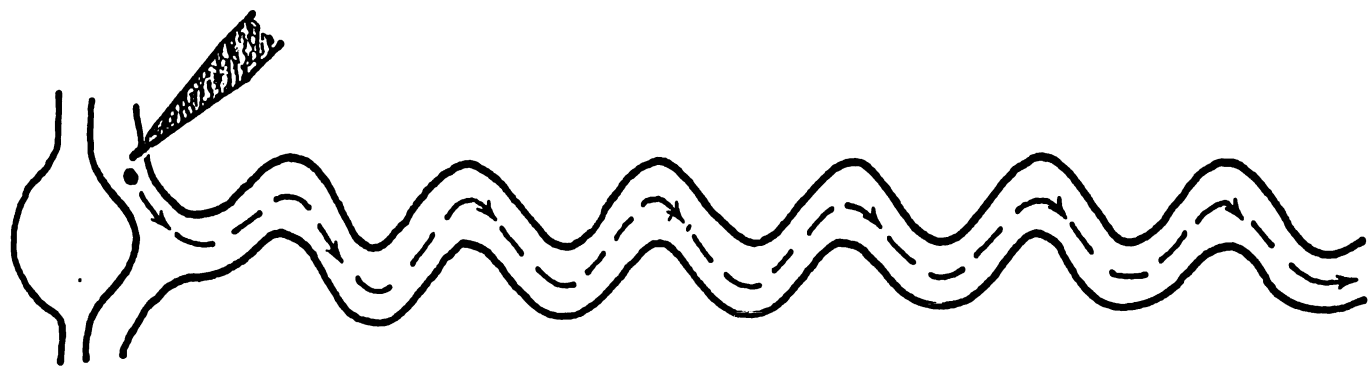

Figure 1. Bowman's space is first punctured and a small oil droplet is injected for mapping.

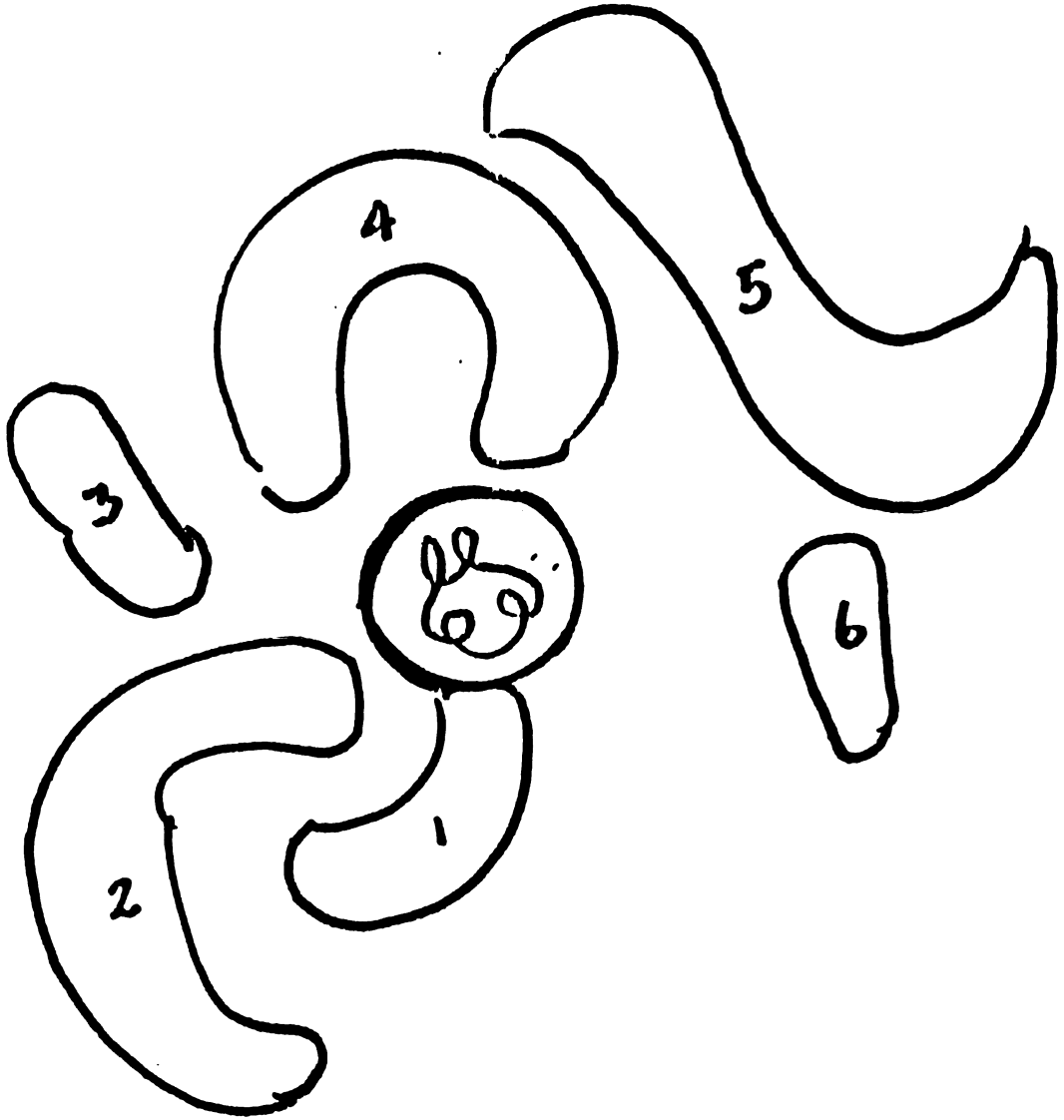

Figure 2. The carefully drawn map of the glomerulus and the surface loops of PCT, following the path of the injected oil droplet. The number marked in each tubule convolution is the sequence of transit by the oil droplet.

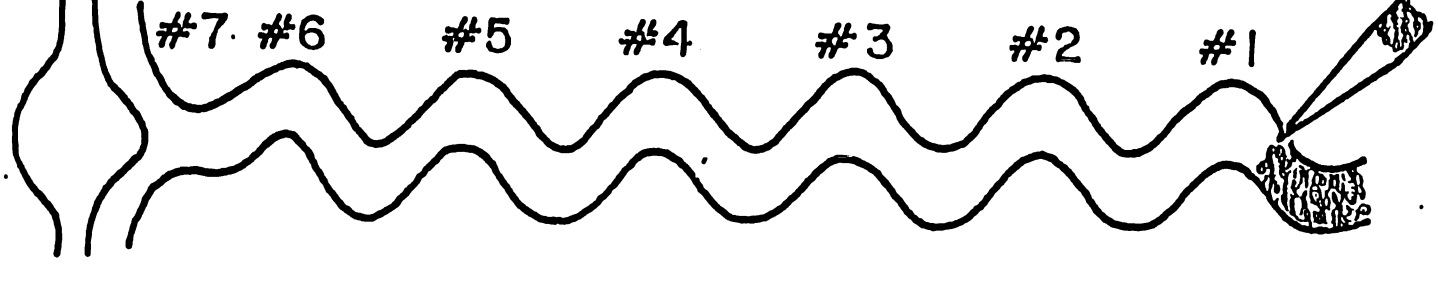

Figure 3. The tubule is punctured sequentially from the end-proximal tubule to Bowman's space for tubular fluid collections.

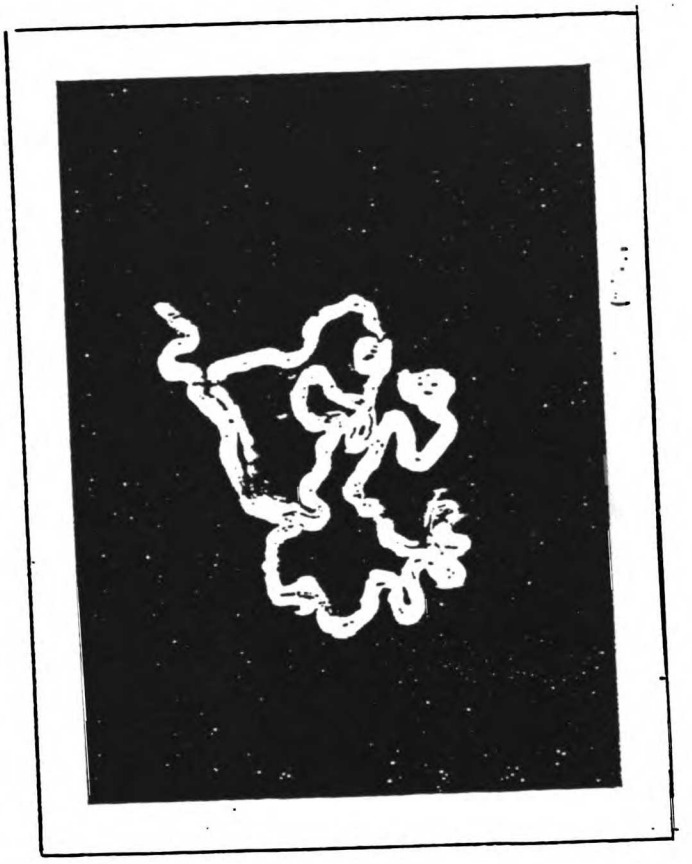

Figure 4. A typical photograph of the proximal convoluted tubule after dissection. Using this photograph, the entire proximal convoluted tubule length (glomerulus to the last puncture site) and the length to each puncture site were measured and recorded.

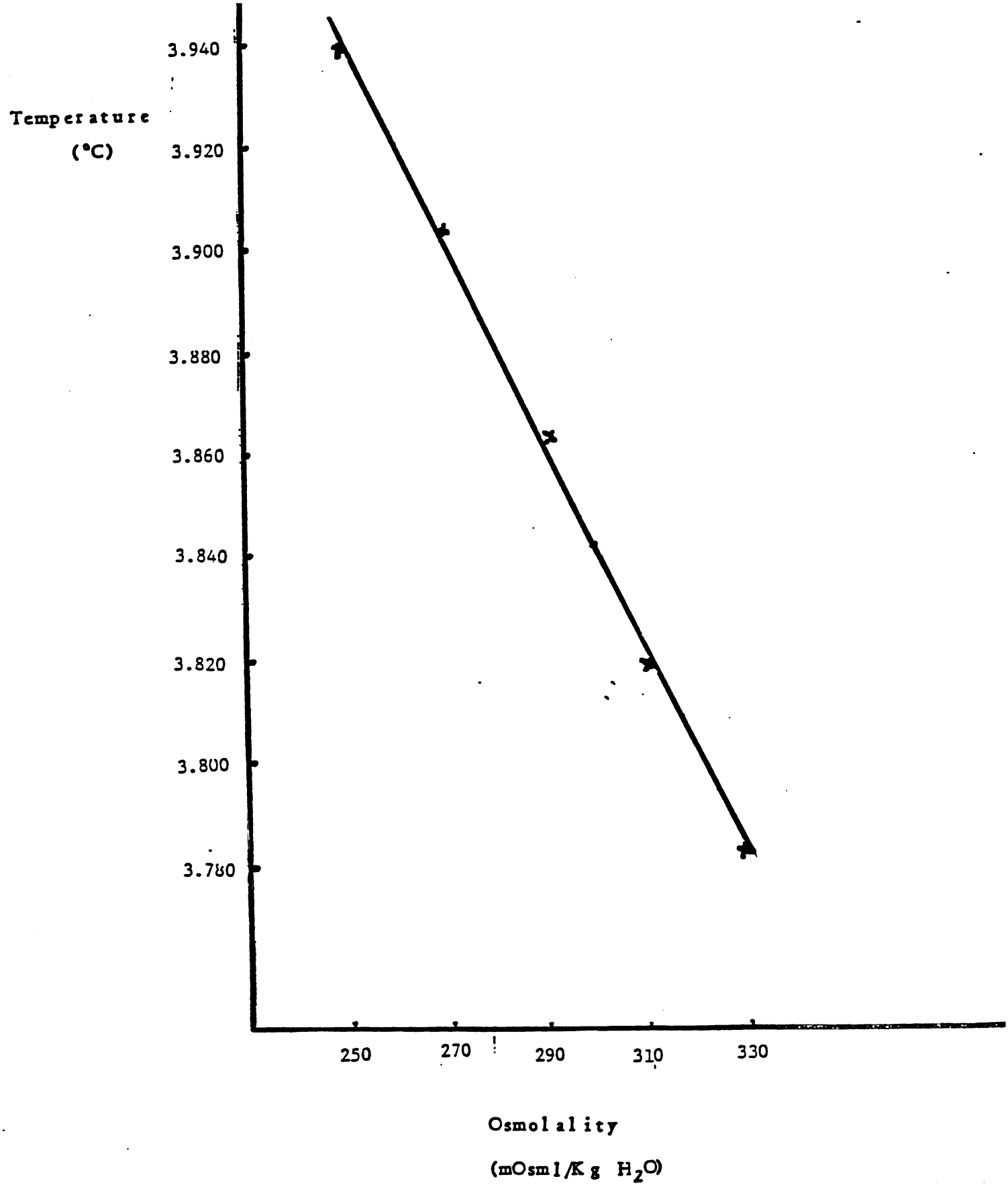

Figure 5. A typical standard curve relating temperature at melting to osmolality (r = 0.999).

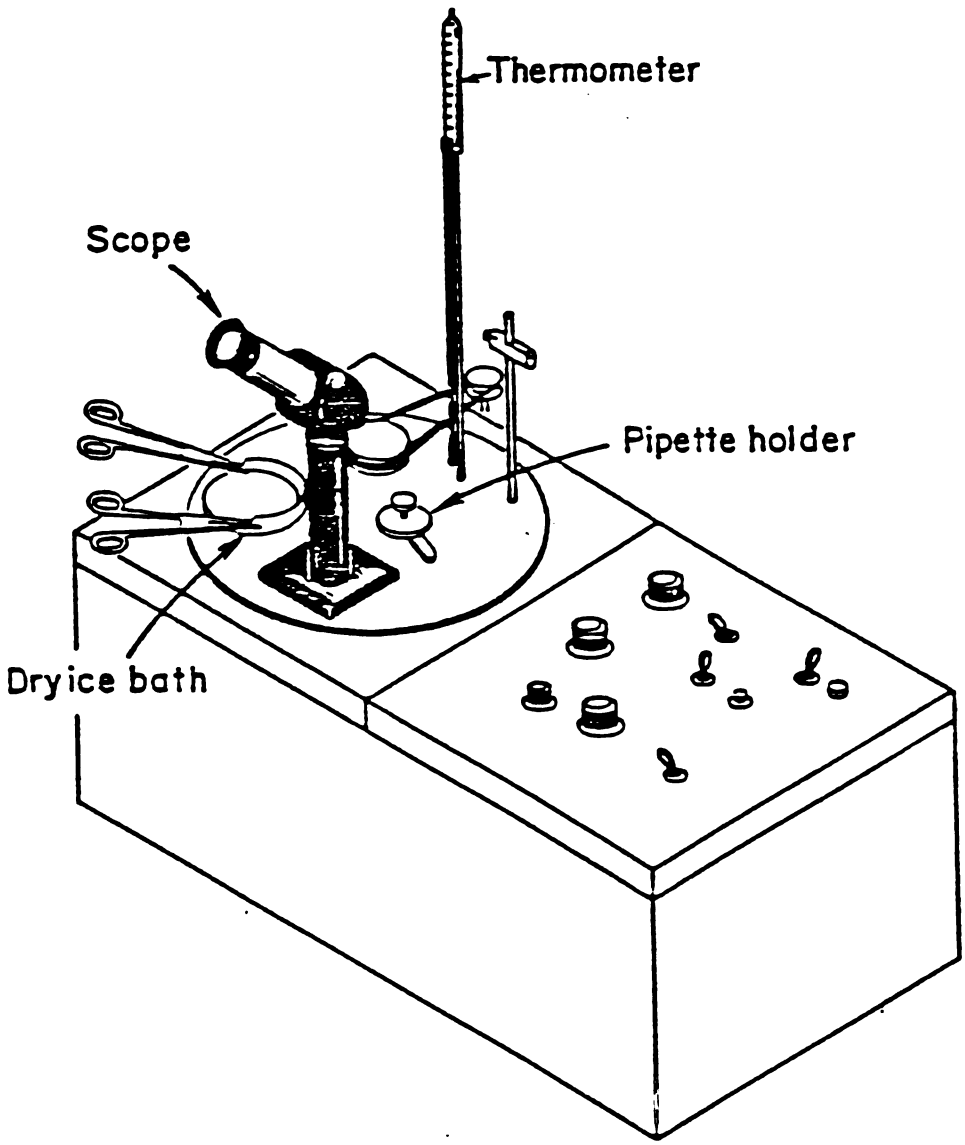

Figure 6. Schematic diagram of the Ramsay-Brown osmometer.

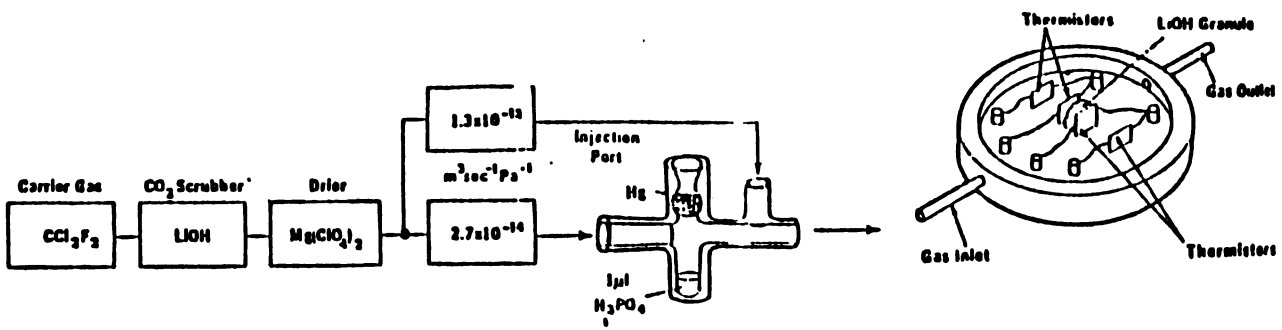

Figure 7. Schematic diagram of the microcalorimeter (picapnotherm).

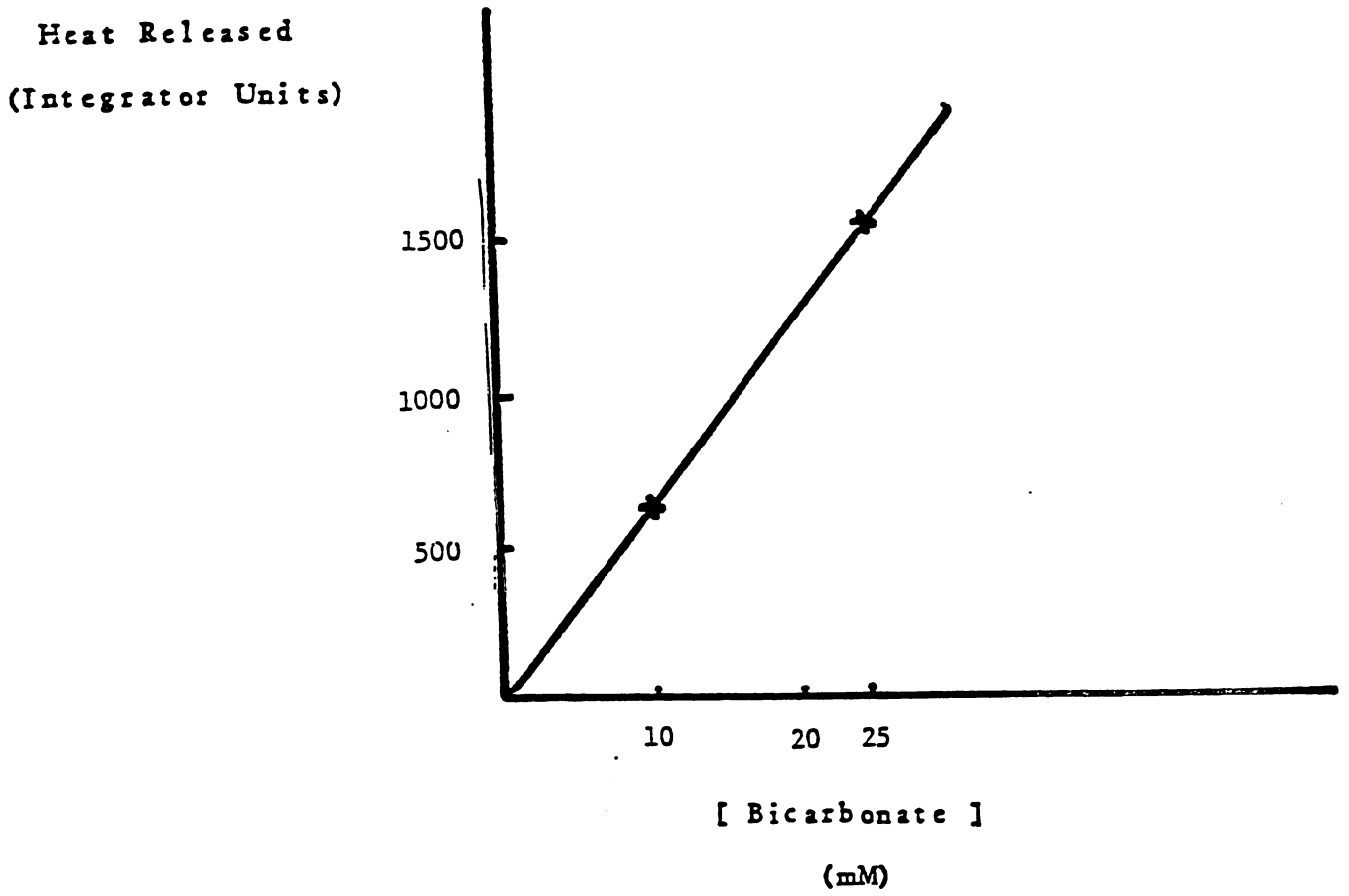

Figure 8. A typical standard curve relating heat released to total CO_2 (r = 0.99).

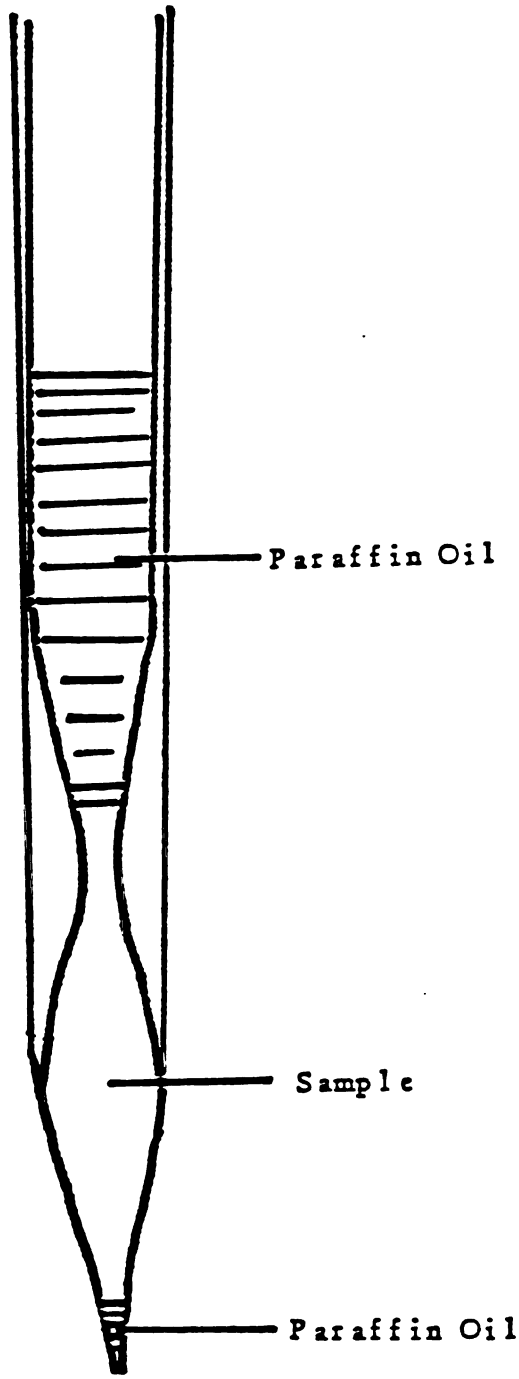

Figure 9. Schematic diagram of the constant volume pipette for bicarbonate measurement.

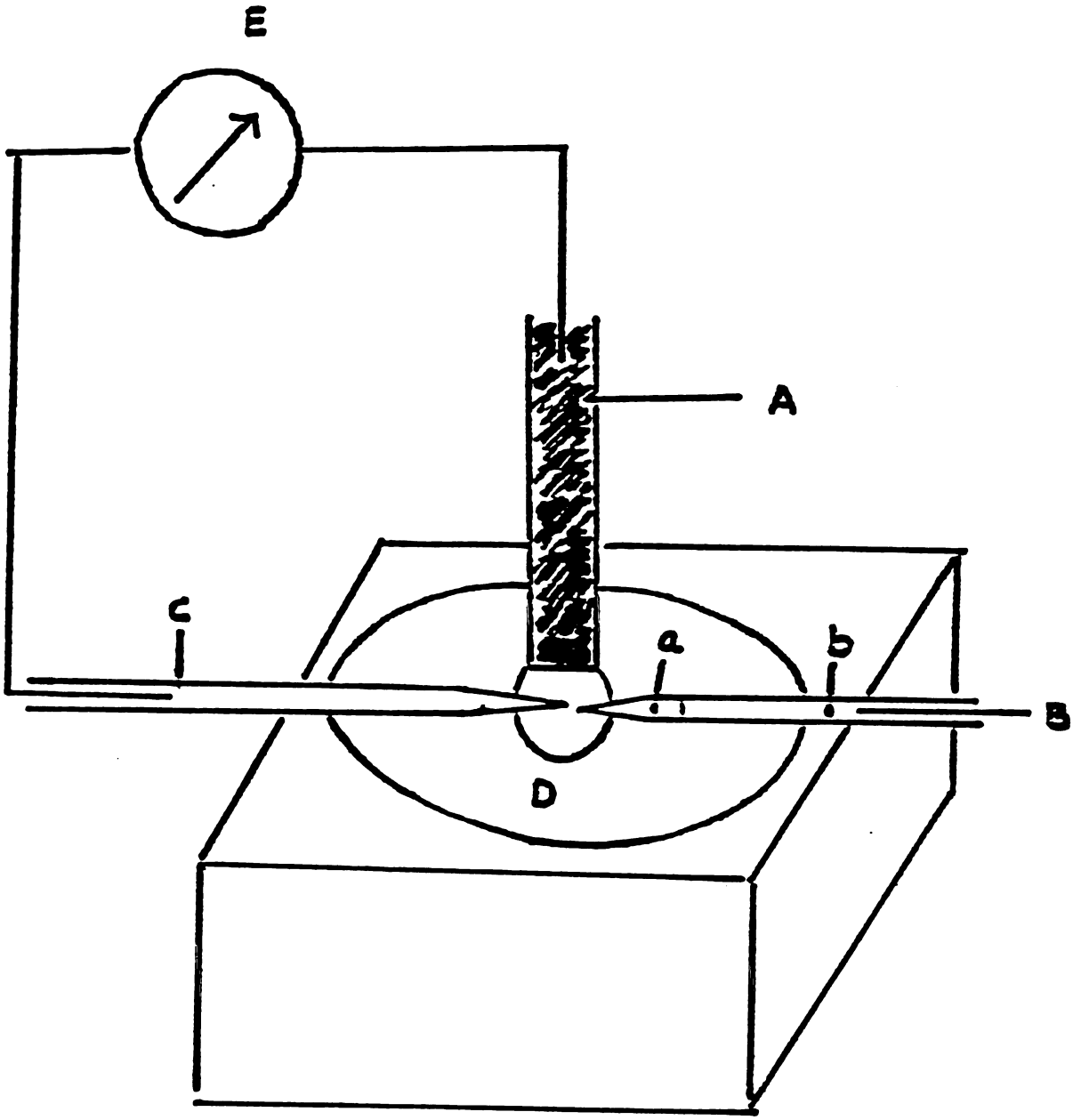

A. Silver Wire Electrode

B. Sample Pipette a. Tubular Fluid (Sample)

C. Reference Electrode (Agar Bridge)

D. Paraffin Oil Bath

E. Voltmeter

Figure 10. Schematic diagram of the microtitrimetric instrument for microchloride measurement (Ramsay technique).

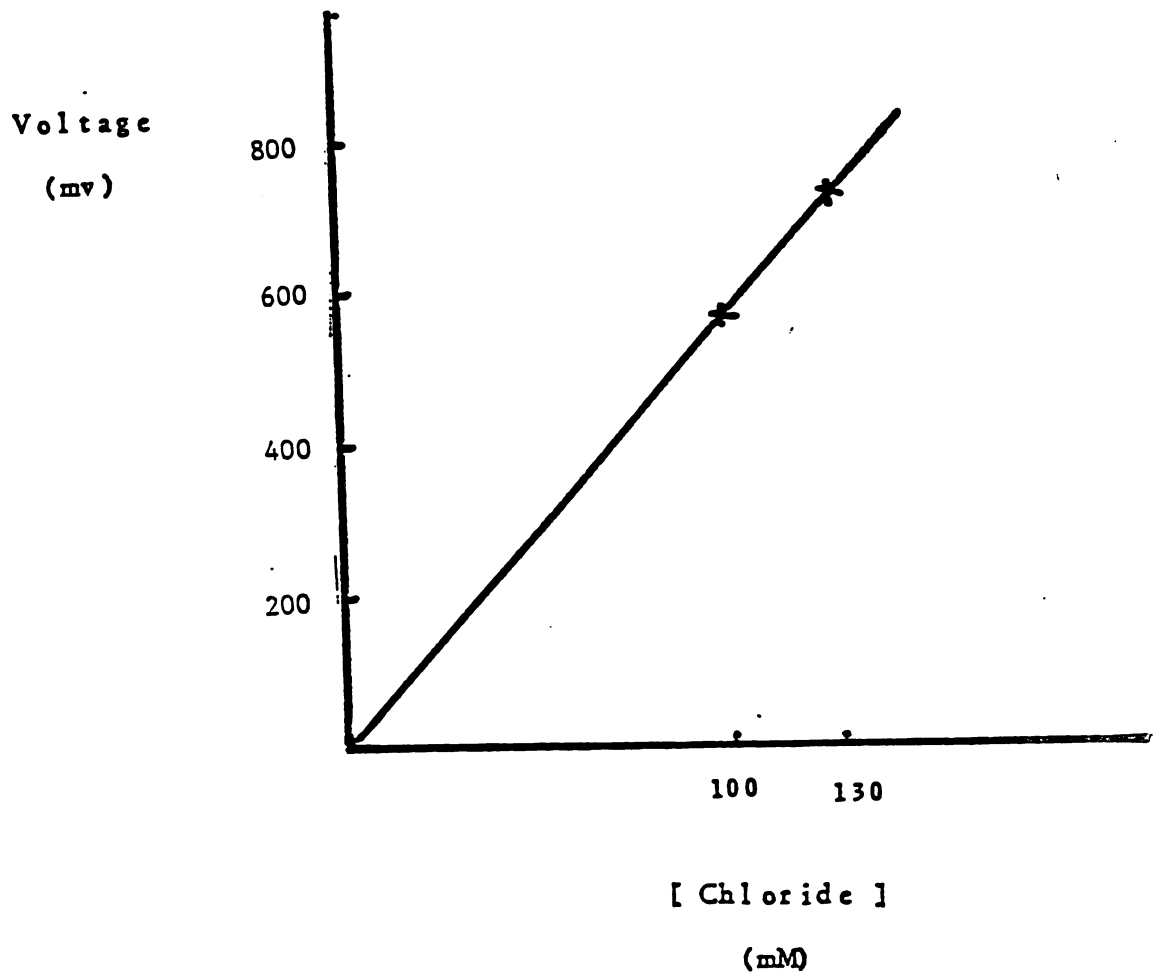

Figure 11. A typical standard curve relating voltage to chloride concentration (r = 0.99).

CHAPTER 3

INTRODUCTION

to

CHAPTER 3

This chapter is a reprint of the material as it appears in "Axial heterogeneity in the rat proximal convoluted tubule. I. Bicarbonate, chloride, and water transport" published in the Am. J. Physiol. 247 (Renal Fluid Electrolyte Physiol. 16): F816-F821, 1984.

AXIAL HETEROGENEITY IN THE RAT PROXIMAL CONVOLUTED TUBULE

I. BICARBONATE, CHLORIDE, AND WATER TRANSPORT

by

Fu-Ying Liu and Martin G. Cogan

Cardiovascular Research Institute and Department of Medicine
University of California, San Francisco
San Francisco, California 94143

Running Head: Heterogeneity of Proximal Transport

Editorial Correspondence and Reprint Requests:

Martin G. Cogan, M.D.
1065 HSE
University of California
San Francisco, California 94143

Portions of this work have been presented in preliminary form at the 16th Annual Meeting of the American Society of Nephrology (Washington, D.C., December 4-7, 1983) and published in abstract form: Kidney Intern., 25:308, 1984.

ABSTRACT

The concentration profiles of bicarbonate, chloride and inulin along the length of the superficial proximal convoluted tubule have not been previously measured simultaneously. For this purpose, free-flow micropuncture measurements were made sequentially from the end-proximal tubule to Bowman's space in ten tubules of hydropenic Munich-Wistar rats. Mean single nephron glomerular filtation rate was 28.7 ± 0.7 nl/min and was stable during the repeated punctures. Bicarbonate and volume reabsorption were 354 ± 21 pmol/mm·min and 5.9 ± 0.4 nl/mm·min in the first mm and fell progressively in the remaining 3.8 mm of tubule, averaging 83 ± 4 pmol/mm·min and 2.3 ± 0.5 nl/mm·min, respectively. The values in the initial mm represent a high transport capacity since they exceed rates that have been observed when comparable or even higher mean luminal substrate concentrations were presented to the late proximal tubule (during free-flow conditions at higher flow rates or using microperfusion). In contrast, chloride reabsorption was only 206 ± 50 peq/mm·min in the first mm and rose to 306 ± 22 peq/mm·min in the rest of the tubule. In conclusion, there is substantial axial transport heterogeneity, with bicarbonate and water reabsorption higher, but chloride reabsorption lower in the early compared with the late superficial proximal convoluted tubule.

Key Words: Acidification; Sodium Transport; Sodium Reabsorption; Micropuncture; Microcalorimetry

INTRODUCTION

Many previous studies have documented the structural and functional heterogeneity of the superficial proximal convoluted tubule (5, 18, 25). The early proximal convoluted tubule has has a higher capacity for transporting several filtered solutes including glucose (3, 26, 33), amino acids (22), and phosphate (8, 26, 32). However, relatively few studies have examined whether the major anions present in the glomerular ultrafiltrate, bicarbonate and chloride, are similarly reabsorbed at a higher rate in the early compared to the later proximal tubule. Observations in vitro have suggested that the bicarbonate reabsorptive rate is in fact lower in the early superficial proximal convoluted tubule than in the late tubule (18). However, opposite results were obtained when segmental proximal acidification was assessed using split droplets (34). Considerable controversy also exists regarding whether the rate of sodium and water reabsorption is slower (7, 26), similar (7, 13, 16, 36) or faster (12, 13, 17) in the early than in the late proximal convoluted tubule.

The purpose of the present free-flow micropuncture study was to define simultaneously the concentration profiles for bicarbonate, chloride and inulin along the accessible proximal convoluted tubule in order to assess whether anion and water reabsorptive heterogeneity exists. The Munich-Wistar rat was used so that measurements could begin at Bowman's space and thus include the earliest portion of the proximal convoluted tubule.

METHODS

Free-flow micropuncture studies were performed in ten tubules from ten hydropenic male Munich-Wistar rats (200-225 g).

Micropuncture Protocol: Rats were prepared for micropuncture as previously described (9-11). Briefly, the animals were allowed free access to food and water prior to being anesthetized with Inactin (100 mg/kg, i.p.). They were placed on a thermostatically controlled (37° C) micropuncture table. Catheters (PE 50) were inserted in the femoral artery for blood pressure measurements and for blood sampling and in a jugular vein for inulin infusion. A tracheostomy was performed. The abdomen was opened by a midline incision, the kidney was stabilized and bathed in warmed saline (37° C), and the ureter was cannulated. A 20 min. equilibration period was then allowed to elapse. Surgically-induced plasma volume losses were not replaced.

A surface glomerulus was then located. A small pipette (3-5μ OD) was inserted into Bowman's space and a small droplet of oil stained with Sudan black injected. The course of the injected oil droplet was carefully observed and mapped. Only glomeruli that were followed by at least 5-7 surface proximal convolutions were used. The localization pipette was withdrawn and at least an hour was allowed for the hole in Bowman's space

to seal. Following an inulin prime (25 uCi), an inulin infusion at 1.6 ml/hr in bicarbonate Ringer's solution was begun (50 μCi/ml). Sequential, timed 3-7 min collections commenced using 7-9μ OD glass pipettes, starting at the end-proximal convolution and working in a retrograde fashion to Bowman's space.

Latex or microfil (Canton Biomedical Products, Boulder, CO) was then injected into Bowman's space to fill the entire tubule. At a later time, the kidney was incubated for 30-40 min in 6 N HCl. The cast of the tubule was carefully dissected, photographed and measured. The entire proximal tubule length (glomerulus to the last puncture site) and the lengths to each puncture site were recorded.

Analysis: The volume of collected tubule fluid samples was determined by injecting them into constant bore capillary glass tubing with a known volume per length and measuring the length occupied. Aliquots of the fluid were used to measure inulin by scintillation counting (Nuclear Chicago), total CO_2 by microcalorimetry (35), and chloride by the microtitrametric method of Ramsay (28).

Calculations: The single nephron glomerular filtration rate (SNGFR) was estimated as the product of the flow rate at a given point multiplied by the corresponding inulin concentration ratio (tubular fluid/plasma water). Water reabsorption at a given point was the flow rate at that point subtracted from the SNGFR.

Anion reabsorption was the filtered load (anion concentration in Bowman's space multiplied by the SNGFR) minus the anion delivery at that point (anion concentration multiplied by the flow rate). Reabsorption at a given length (e.g., 1 mm) was estimated by interpolation between the two closest measured data points to that length for each tubule and expressed as the mean ± SEM. Paired statistical comparisons were made on data from the same tubule and linear and exponential regression analyses were calculated by the method of least squares.

RESULTS

The average length of the tubules was 4.83 ± 0.07 mm, in good agreement with previous measurements of the length of the accessible proximal tubule in the Munich-Wistar rat (13). The Bowman's space total CO_2 concentration was 25.7 ± 0.7 mM and chloride concentration was 118.6 ± 0.6 meq/L, also in good agreement with previously measured values (9-11, 21).

A technical consideration is necessary regarding the validity of flow rate measurements. Before the sample collections, an oil droplet was injected into Bowman's space using a small pipette to map surface convolutions to be subsequently punctured. Although at least an hour elapsed before collections commenced, it was possible that the hole made in Bowman's capsule had not sealed completely and that a leak occurred. To assess this possibility, single nephron glomerular filtration rate (SNGFR) was calculated at each puncture site along the nephron and compared with the first tubule fluid collection site, the end-proximal tubule. If there were a leak of ultrafiltrate from Bowman's space, the calculated SNGFR would be lower than that expected in normal hydropenic rats and/or variable. The average SNGFR in the ten tubules studied was 28.7 ± 0.7 nl/min. This value agrees very well with previously published values for the hydropenic Munich-Wistar rat (9-11). In addition, there was no significant change in SNGFR as a function of length or time in these studies, as shown in Fig. 1. The average difference in

SNGFR at the various puncture sites compared with the end-proximal SNGFR determination was 0.0 ± 0.2 nl/min. Thus, if a leak were introduced with the initial mapping pipette in Bowman's space, it was quite small and relatively constant.

The tubular fluid to glomerular ultrafiltrate concentration ratios (TF/UF) for bicarbonate, chloride and inulin as a function of length are shown in Fig. 2. The TF/UF inulin ratios were relatively linear. The linear regression analysis resulted in the following equation: $y = 0.20x + 1.05$, $r = 0.97$, $p < 0.001$. The TF/UF bicarbonate concentration, on the other hand, fell progressively and could be defined by the exponential equation: $y = 23.0\ e^{-0.32x}$, $r = 0.95$. The TF/UF chloride concentration ratio rose quickly, almost parallelling the TF/UF inulin ratio, to a value of about 1.2 at about 1 mm. The chloride TF/UF then stabilized, and even tended to fall very slightly, over the remaining tubular length.

A comparison of the absolute changes in bicarbonate and chloride concentrations as a function of length are shown in Fig. 3A. Within 1 mm, the chloride concentration rose quickly to values about 20 meq/L higher than existed in the glomerular ultrafiltrate. However, the fall in bicarbonate concentration was slower. At 1 mm, the bicarbonate concentration had fallen by only about 7-8 mM. Furthermore, in the tubule segment greater than 1 mm from the glomerulus, the bicarbonate concentration continued to fall while there was little change in chloride

concentration. Since the changes in chloride and bicarbonate concentrations were not strictly reciprocal, and since changes in osmolality along the tubule have been found to be relatively small (24), it is clear that changes in concentrations of unmeasured solutes were occurring. In Fig. 3B, an attempt is made to quantitate these changes in unmeasured solute concentrations by subtracting the concentrations of bicarbonate plus chloride (each multiplied by an activity coefficient of 1.85) from the simultaneously measured osmolality (24). As can be seen, the unmeasured solute concentration rapidly fell in 8 out of the 10 tubules, reaching a minimimum value at about 1 mm. Presumably this predominantly represented the reabsorption of organic solutes such as glucose, which are known to be avidly reabsorbed in the early proximal tubule (30, 36). Subsequently, the unmeasured solute concentration rose at a rate faster than can be explained by volume reabsorption alone. This increase in unmeasured solute concentration presumably represented secretion of solutes by the proximal tubule (20).

The cumulative absolute rates of bicarbonate, chloride and water reabsorption are shown in Fig. 4. Absolute bicarbonate reabsorption was very high in the first mm, 354 ± 22 pmol/min, and accounted for more than half of the entire tubular bicarbonate reabsorption (673 ± 25 pmol/min). The rate of bicarbonate reabsorption in the tubule following the initial mm was significantly less ($p<0.001$), averaging 84 ± 4 pmol/mm·min. The high rate in the first mm is not simply a consequence of there being

more substrate available for reabsorption. In previous studies, when the late proximal tubule was presented with the a mean luminal bicarbonate concentration (21 mM) comparable to that which existed in the initial mm in the present studies, the rate of bicarbonate reabsorption (176 ± 8 pmol/mm·min) was only about half of the rate in early proximal tubule (2). In fact, when the late proximal tubule has been exposed to substantially higher bicarbonate concentrations and flow rates than existed under the present conditions (by microperfusing the late tubule with bicarbonate concentrations up to 80 mM and at flow rates up to 50 nl/min), the maximal rate of acidification was only 200-210 pmol/mm·min (1, 2). Thus, the early proximal tubule has a higher bicarbonate reabsorptive capacity than has been demonstrated for the late proximal tubule.

In contrast to bicarbonate, the absolute chloride reabsorptive rate in the early (first mm) proximal tubule was relatively low, 206 ± 50 peq/min. The chloride reabsorption for the entire tubule length was 1414 ± 60 peq/min. Thus, the rate of chloride reabsorption rose to 306 ± 22 peq/mm·min for the segment between the initial mm and the end of the tubule.

As predicted by the linear TF/UF inulin values (indicating constant fractional reabsorption), the rate of absolute water reabsorption was found to decrease as function of length. Water reabsorption was very high in the first mm, 5.9 ± 0.4 nl/min, but was only 14.6 ± 0.5 nl/min for the entire tubule. Thus, water

reabsorption in the late tubule, from the end of the first mm to the end of the tubule, was significantly less that in the early tubule ($p<0.001$) and averaged only 2.3 ± 0.5 nl/mm·min. This value for the late tubule is in excellent agreement with volume reabsorptive rates during in vivo microperfusion of late proximal tubules using either an ultrafiltrate-like or sodium chloride solution (1, 2). Thus, as was the case for bicarbonate, the intrinsic sodium and volume reabsorptive capacity is higher in the early proximal tubule.

DISCUSSION

The superficial proximal tubule has been previously described as heterogeneous in several respects (5, 18). The early superficial proximal convoluted tubule has been suggested to be different from the later proximal tubule with regard to many parameters: structure (25); electrophysiological and permeability properties (4, 14, 18, 19, 31); transport capacity of organic solutes (3, 22, 33); transport of phosphate and response to parathormone (8, 17. 26, 32); secretory processes (37); and sodium transport (7, 12, 13, 17, 26). The purposes of the present studies were to extend these observations to the major anions in the glomerular ultrafiltrate, bicarbonate and chloride, and to clarify the pattern of sodium and water reabsorption under free-flow conditions.

Although the bicarbonate concentration profile along the proximal tubule has long been inferred from chloride and pH measurements (15, 36), the present study is the first to quantitate absolute bicarbonate reabsorption as a function of proximal tubule length. Although luminal bicarbonate concentrations along the proximal length were measured by Corman et al. (13), the marked variations in SNGFR and the lack of early punctures (the initial puncture site in those studies was 2.3 $\pm$ 0.2 mm from the glomerulus) make a quantitative assessment of bicarbonate reabsorption difficult. In the present study, bicarbonate reabsorption in the early (initial mm) proximal tubule was found to be

very high, 354 ± 22 pmol/min, accounting for over half of the total proximal bicarbonate reabsorption. This high rate of reabsorption in the early compared to the later tubule was not simply a consequence of exposure to a higher luminal substrate concentration. For instance, when the entire proximal tubule is presented with a comparable mean luminal bicarbonate concentration (18 mM) by increasing flow rate in free-flow conditions, absolute bicarbonate reabsorption does not exceed about 225 pmol/mm·min (10). More explicitly, when the late proximal convoluted tubule has been microperfused with a bicarbonate concentration and flow rate similar to the glomerular ultrafiltrate bicarbonate concentration and SNGFR that existed in the present studies, absolute bicarbonate reabsorption was only 176 ± 8 pmol/mm·min (2). Maximal late proximal rates of acidification have been found to be 200-210 pmol/mm·min (1, 2). Thus, there appears to be a higher reabsorptive capacity for bicarbonate in the early proximal tubule, in agreement with the split droplet studies of Ullrich et al. (34) and similar to previous findings for the reabsorption of glucose (3, 26, 33), amino acids (22) and phosphate (8, 26, 32).

It is unknown whether the increased rate of acidification in the early tubule observed in the present studies represented a maximal rate. It is similarly unclear whether the higher early acidification was due to enhanced activity and/or number of Na^+/H^+ exchangers per unit length or due to the contribution of another transport system confined to that segment (14). The high

absolute transport of bicarbonate in the early tubule would predict that the reabsorbate bicarbonate concentration was quite high (60 meq/l, as estimated by the ratio of absolute bicarbonate to water reabsorption). If bicarbonate diffusion within the insterstitium were relatively constrained, local bicarbonate concentration and pH might be high. Such peritubular alkalinity might then tend to put a self-limiting brake on the acidification process by inhibiting cellular bicarbonate exit (9).

In contrast to bicarbonate, chloride reabsorption in the early proximal convoluted tubule was somewhat less than in the later tubule. To at least some extent, this lower initial rate of chloride reabsorption might be due to the lower mean tubule fluid-to-plasma chloride concentration gradient in the early segment. A lower chloride gradient would diminish diffusional (11, 29) and possibly transcellular, (27, 29) chloride transport. Water abstraction in the early segment (due to organic solute and bicarbonate reabsorption) without proportional fractional chloride reabsorption resulted in an elevation in the tubule fluid chloride concentration by the end of the first mm of tubule, that was 20% higher than plasma, an observation in good agreement with earlier studies (21, 23, 36). This elevated chloride concentration then permits higher rates of passive chloride diffusion as well as active transcellular sodium chloride reabsorption to take place in the late proximal tubule (6, 11, 27, 29). Another consideration is that there may exist intrinsic differences along the length of the tubule for active

sodium chloride transport.

While it is possible that the negative potential difference generated by the high rate of sodium-coupled organic solute reabsorption in the initial part of the tubule (4) might stimulate net sodium chloride reabsorption, enhanced early chloride reabsorption was not observed. The negative transepithelial potential difference in the early proximal tubule would favor net reabsorption of sodium chloride only if the relative chloride/sodium permeability in that segment were relatively high (6). If the chloride/sodium permeability were relatively low, as has been found by Jacobson and Kokko (19), then there would tend to be simply recycling of the transported sodium back into the tubule lumen.

It should be noted from the pattern of concentration changes in Fig. 3 that other solutes are absorbed from luminal fluid in the early proximal tubule and added in the late proximal tubule. This observation is consistent with the known avidity of the early proximal convoluted tubule for organic solutes (3, 30, 36) and with the secretory capacity of the later (S_2) proximal tubule (37). The early reabsorption and later secretion of unmeasured solutes appeared to influence net water reabsorption. While the sum of the measured sodium bicarbonate and sodium chloride reabsorption accounted for only about 60% of the total osmolar flux in the first mm of the tubule, the reabsorption of these ions averaged 105-120% of the net osmolar transport in the

later tubule.

Whether sodium and water reabsorption rates vary along the length of the tubule has been the subject of long-standing controversy (15). The early proximal tubule has been suggested to have an increased (12, 13, 17), similar (7, 13, 16, 36), or decreased (7, 26) sodium reabsorptive capacity compared to the late proximal tubule. The present studies have shown that fractional water reabsorption was relatively constant along the length of the tubule (as reflected by the linearity of the tubular fluid/plasma inulin ratio) so that absolute volume reabsorption was constantly decreasing (Fig. 4). The rate of volume reabsorption in the initial mm of tubule was again not simply due to greater substrate delivery because the value observed, 5.9 nl/mm·min, was more that double that seen when the late proximal tubule has been microperfused with an ultrafiltrate-like solution (2.5 nl/mm·min)(2).

In summary, these free-flow studies have shown a higher reabsorptive capacity for sodium, bicarbonate and water in the early (initial mm) proximal convoluted tubule of the rat compared to the remaining tubule. In contrast, chloride reabsorption was less in the early compared with the late proximal tubule. Under free-flow conditions, the reabsorbate in the early proximal convoluted tubule consists predominantly of organic solutes and sodium bicarbonate while in the later proximal tubule it consists primarily of sodium chloride.

ACKNOWLEDGMENTS

These studies were supported in part by a Clinical Investigator Award (1 KO-8-AM-01015) and a grant (AM-27045) from the National Institute of Arthritis, Diabetes, and Digestive and Kidney Diseases.

REFERENCES

1. Alpern, R. J., M. G. Cogan, and F. C. Rector, Jr. Effect of luminal bicarbonate concentration on proximal acidification in the rat. Am. J. Physiol. 243 (Renal Fluid Electrolyte Physiol. 12): F53-F59, 1982.
2. Alpern, R. J., M. G. Cogan, and F. C. Rector, Jr. Flow dependence of proximal tubular bicarbonate absorption. Am. J. Physiol. 245 (Renal Fluid Electrolyte Physiol. 14): F478-F484, 1983.
3. Barfuss, D. W., and J. A. Schafer. Differences in active and passive glucose transport along the proximal nephron. Am. J. Physiol. 240 (Renal Fluid Electrolyte Physiol. 10): F322-F332, 1981.
4. Barratt, L. J., F. C. Rector, Jr., J. P. Kokko, and D. W. Seldin. Factors governing the transepithelial potential difference across the proximal tubule of the rat kidney. J. Clin. Invest. 53:454-464, 1974.
5. Berry, C. A. Heterogeneity of tubular transport processes in the nephron. Ann. Rev. Physiol. 44:181-201, 1982.
6. Berry, C. A., and F. C. Rector, Jr. Active and passive sodium transport in the proximal tubule. Mineral Electrolyte Metab. 4:149-160, 1980
7. Bishop, J. H. V., R. Green, and S. Thomas. Free-flow

reabsorption of glucose, osmoles and water in rat proximal convoluted tubule. J. Physiol. 288:331-351, 1979.

8. Brunette, M. G., L. Taleb, and S. Carriere. Effect of parathyroid hormone on phosphate reabsorption along the nephron of the rat. Am. J. Physiol. 225:1076-1081, 1973.
9. Cogan, M. G., and F.-Y. Liu. Metabolic alkalosis in the rat: Evidence that reduced glomerular filtration rather than enhanced tubular bicarbonate reabsorption is responsible for maintaining the alkalotic state. J. Clin. Invest. 71:1141-1160, 1983.
10. Cogan, M. G., D. A. Maddox, M. S. Lucci, and F. C. Rector, Jr. Control of proximal bicarbonate reabsorption in normal and acidotic rats. J. Clin. Invest. 64:1168-1180, 1979.
11. Cogan, M. G. and F. C. Rector, Jr. Proximal reabsorption during metabolic acidosis in the rat. Am. J. Physiol. 242 (Renal Fluid Electrolyte Physiol. 11): F499-F507, 1982.
12. Corman, B., N. Roinel, and C. de Rouffignac. Water reabsorption capacity of the proximal convoluted tubule: A micorperfusion study of rat kidney. J. Physiol. 316:379-392, 1981.
13. Corman, B., R. Thomas, R. McLeod, and C. de Rouffignac. Water and total CO_2 reabsorption along the rat proximal convoluted tubule. Pfluegers Arch. 389:45-53, 1980.
14. Fromter, E. and K. Gessner. Effect of inhibitors and diuretics on electrical potential differences in rat kidney proximal tubule. Pfluegers Arch. 357:209-224, 1975.
15. Gottschalk, C. W. Renal tubular function: Lessons from

micropuncture. Harvey Lectures 58:99-124, 1963.

16. Gyory, A. Z., J. M. Lingard, and J. A. Young. Relation between active sodium transport and distance along the proximal convolutions of rat nephrons: Evidence for homogeneity of sodium transport. Pfluegers Arch. 348:205-210, 1974.

17. Hamburger, R. J., N. L. Lawson, and J. H. Schwartz. Response to parathyroid hormone in defined segments of proximal tubule. Am. J. Physiol. 230:286-290, 1976.

18. Jacobson, H. R. Functional segmentation of the mammalian nephron. Am. J. Physiol. 241 (Renal Fluid Electrolyte Physiol. 10): F203-F218, 1981.

19. Jacobson, H. R., and J. P. Kokko. Intrinsic differences in various segments of proximal convoluted tubules. J. Clin. Invest. 57:818-825, 1976.

18. Lassiter, W. E., C. W. Gottschalk, and M. Mylle. Micropuncture study of net transtubular movement of water and urea in nondiuretic mammalian kidney. Am. J. Physiol. 200:1139-1146, 1961.

21. LeGrimellec, C. Micropuncture study along the proximal convoluted tubule. Electrolyte reabsorption in first convolutions. Pfluegers Arch. 354:133-150, 1975.

22. Lingard, J., G. Rumrich, and J. A. Young. Reabsorption of L-glutamine and L-histidine from various regions of the rat proximal convolution studied by stationary microperfusion: Evidence that the proximal convolution is not homogeneous. Pfluegers Arch. 342:1-12, 1973.

23. Litchfield, J. B. and P. A. Bott. Micropuncture study of

renal excretion of water, K, Na, and Cl in the rat. Am. J. Physiol. 203:667-670, 1962.

24. Liu, F.-Y., M. G. Cogan, and F. C. Rector, Jr. Axial heterogenetiy in the rat proximal convolute tubule. II. Osmolality and osmotic water permeability. Am. J. Physiol. (Renal Fluid Electrolyte Physiol.), Submitted for Publication, 1984.

25. Maunsbach, A. B. Observation on the segmentation of the proximal tubule in the rat kidney. J. Ultrastructure Research 16:239-258, 1966.

26. McKeown, J. W., P. C. Brazy, and V. W. Dennis. Intrarenal heterogeneity for fluid, phosphate and glucose absorption in the rabbit. Am. J. Physiol. 237 (Renal Fluid Electrolyte Physiol. 6): F312-F318, 1979.

27. Neumann, K. H., and F. C. Rector, Jr. Mechanism of NaCl and water reabsorption in the proximal convoluted tubule of rate kidney. Role of chloridek concentration gradients. J. Clin. Invest. 58:1110-1118, 1976.

28. Ramsay, J. A., R. H. J. Brown, and P. C. Croghan. Electrometric titration of chloride in small volume. J. Exp. Biol. 32:822-829, 1955.

29. Rector, F. C., Jr. Sodium, bicarbonate, and chloride absorption by the proximal tubule. Am. J. Physiol. 244 (Renal Fluid Electrolyte Physiol. 13): F461-471, 1983.

30. Rohde, and P. Deetjen. Die glucoseresorption in der rattenniere. Pfluegers Arch. 302:219-232, 1968.

31. Seely, J. F. Variation in electrical resistance along length

of rat proximal convoluted tubule. Am. J. Physiol.225:48-57, 1973.

32. Staum, B. B., R. J. Hamburger, and M. Goldberg. Tracer microinjection study of renal tubular phosphate reabsorption in the rat. J. Clin. Invest. 41, 2271-2276, 1972.

33. Turner, R. J., and A. Moran. Heterogeneity of sodium-dependent D-glucose transport sites along the proximal tubule: Evidence from vesicle studies. Am. J. Physiol. 242 (Renal Fluid Electrolyte Physiol. 11): F406-F414, 1982.

34. Ullrich, K. J., G. Rumrich, and K. Baumann. Renal proximal tubular buffer-(glycodiazine) transport. Inhomogeneity of local transport rate, dependence on sodium, effect of inhibitors and chronic adaptation. Pfluegers Arch. 357:149-163, 1975.

35. Vurek, G. G., D. G. Warnock, and R. Corsey. Measurement of picomole amounts of carbon dioxide by calorimetry. Anal. Chem. 47:765-767, 1975

36. Walker, A. M., P. A. Bott, J. Oliver, and M. C. MacDowell. The collection and analysis of fluid from single nephrons of the mammalian kidney. Am. J. Physiol. 134:580-595, 1941.

37. Woodhall, P. B., C. C. Tisher, C. A. Simonton, and R. R. Robinson. Relationship between para-aminohippurate secretion and cellular morphology in rabbit proximal tubules. J. Clin. Invest. 61:1320-1329, 1978.

FIGURE LEGENDS

1. The ratio of the single nephron glomerular filtration rate at each measured point x ($SNGFR_x$) to that measured at the end of the proximal tubule ($SNGFR_{EP}$) as a function of length.

2. Tubular fluid/glomerular ultrafiltrate (TF/UF) concentration ratios for inulin, bicarbonate and chloride as a function of length in the superficial proximal convoluted tubule of the Munich-Wistar rat.

3. Top panel (A) shows the absolute changes in concentration for chloride and bicarbonate as a function of length in the superficial proximal tubule. Note that the two curves do not mirror each other. The bottom panel (B) shows the unmeasured osmoles as a function of length. The unmeasured osmoles were calculated as the difference of the total luminal fluid osmolality (Ref. L/C/R) and the sum of the NaCl and $NaHCO_3$ osmotic activities (estimated as 1.85 times the chloride plus bicarbonate concentrations). Note the disappearance of unmeasured osmoles in the first mm of the tubule and reappearance in the later tubule.

4. Cumulative absolute reabsorption of water, bicarbonate and chloride as a function of length in the superficial proximal convoluted tubule of the Munich-Wistar rat.

TABLE 1. *Tubular fluid concn and delivery and reabsorption rate of bicarbonate, chloride, and water as a function of length*

	Bowman's Space	First Millimeter	Second Millimeter	Third Millimeter	Fourth Millimeter	Fifth Millimeter
			Tubular fluid			
$[HCO_3^-]$, mM	25.7 ± 0.7	16.9 ± 0.8	10.4 ± 0.6	8.6 ± 0.6	6.8 ± 0.7	5.7 ± 1.0
$[Cl^-]$, meq/liter	118.5 ± 0.6	138.9 ± 1.8	140.7 ± 2.4	139.4 ± 1.8	140.1 ± 1.9	138.5 ± 2.5
			Delivery rate			
HCO_3^-, pmol/min	740 ± 31	385 ± 24	199 ± 16	151 ± 15	110 ± 15	86 ± 17
Cl^-, peq/min	3,363 ± 88	3,157 ± 375	2,674 ± 308	2,392 ± 276	2,144 ± 250	1,952 ± 229
H_2O, nl/min	28.7 ± 0.7	22.8 ± 0.7	19.0 ± 0.5	17.3 ± 0.5	15.6 ± 0.5	14.4 ± 0.6
			Reabsorption rate			
HCO_3^-, pmol·mm^{-1}·min^{-1}		354 ± 21	186 ± 17	48 ± 10	41 ± 7	24 ± 3
Cl^-, peq·mm^{-1}·min^{-1}		206 ± 55	483 ± 94	282 ± 42	248 ± 40	192 ± 35
H_2O, nl·mm^{-1}·min^{-1}		5.9 ± 0.4	3.8 ± 0.4	1.7 ± 0.2	1.7 ± 0.2	1.2 ± 0.2

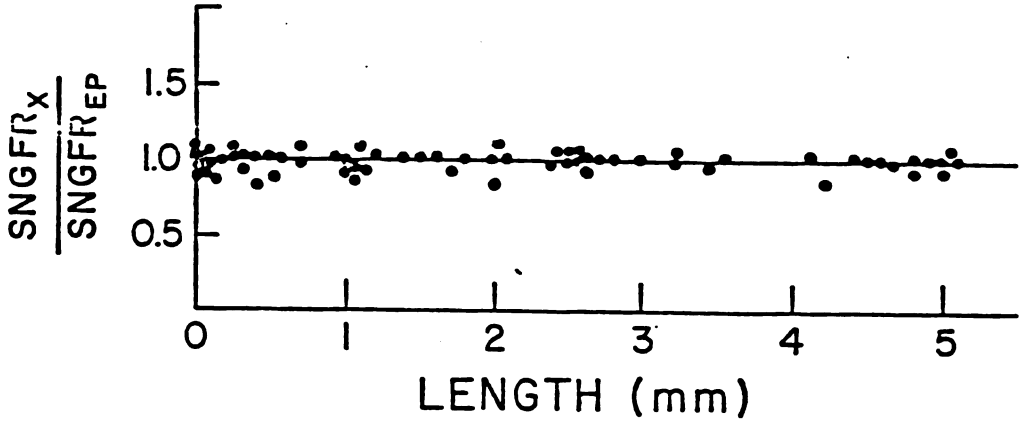

FIGURE 1

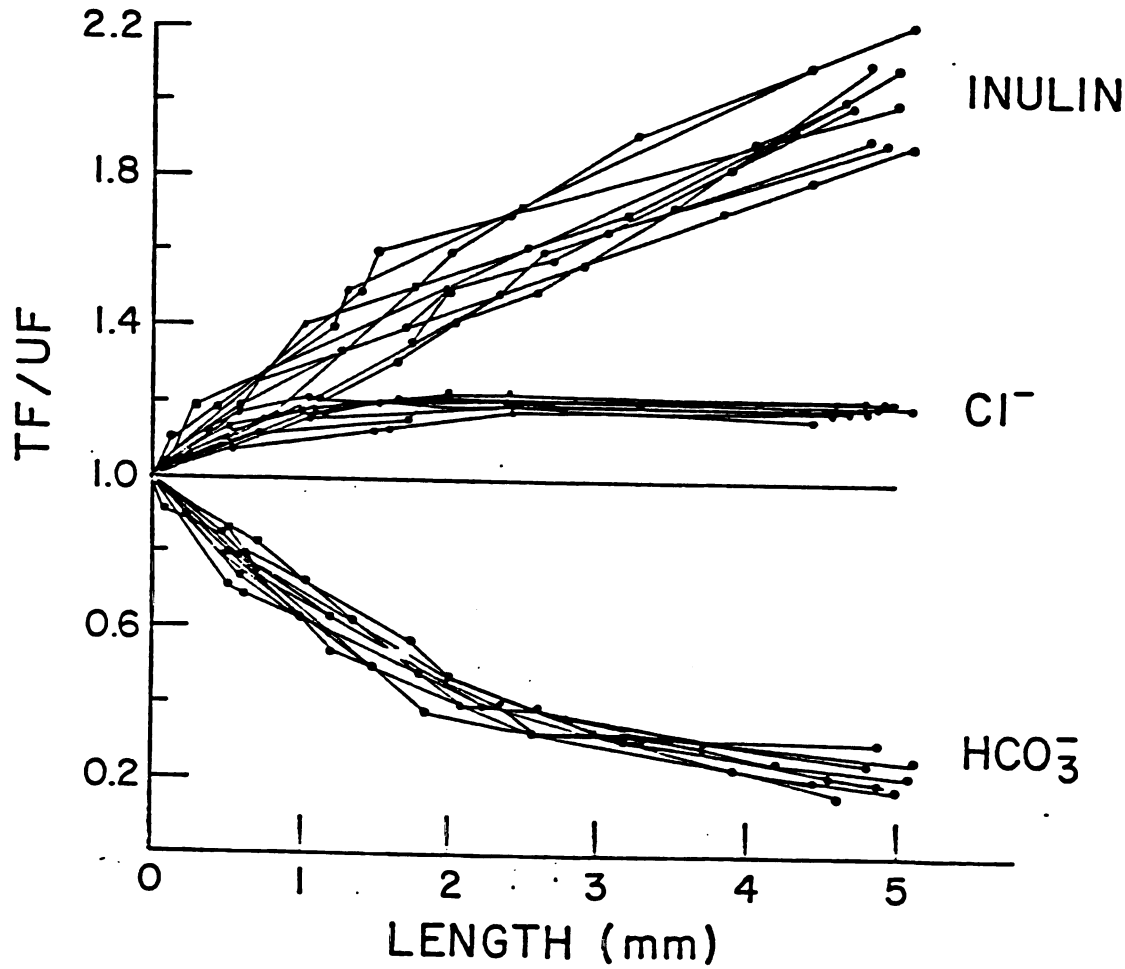

FIGURE 2

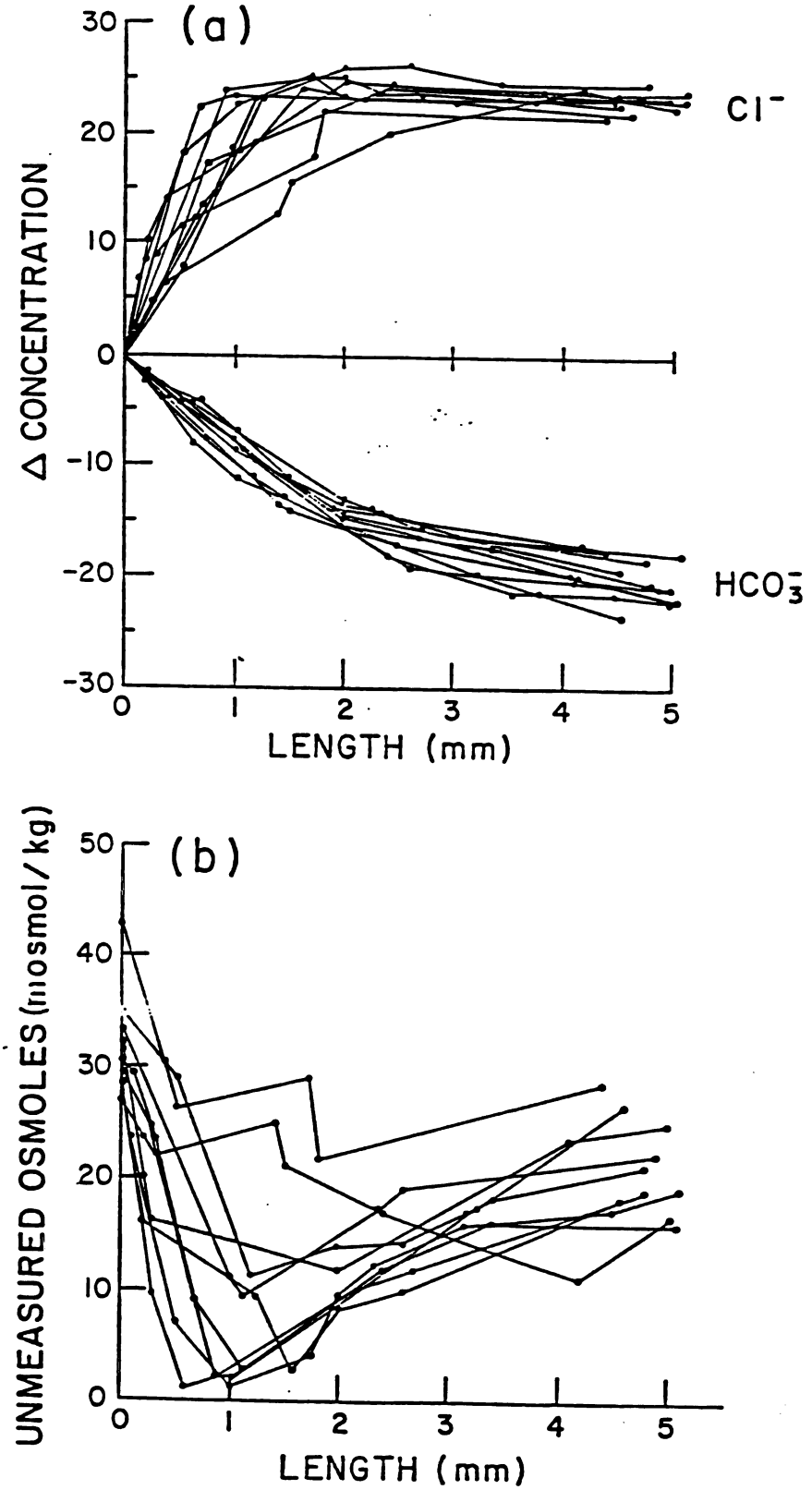
(a)
30
20
10
0
-10
-20
-30
Δ CONCENTRATION
Cl⁻
HCO₃⁻
0
1
2
3
4
5
LENGTH (mm)
(b)
50
40
30
20
10
0
UNMEASURED OSMOLES (mOsmol/kg)
0
1
2
3
4
5
LENGTH (mm)

FIGURE 3

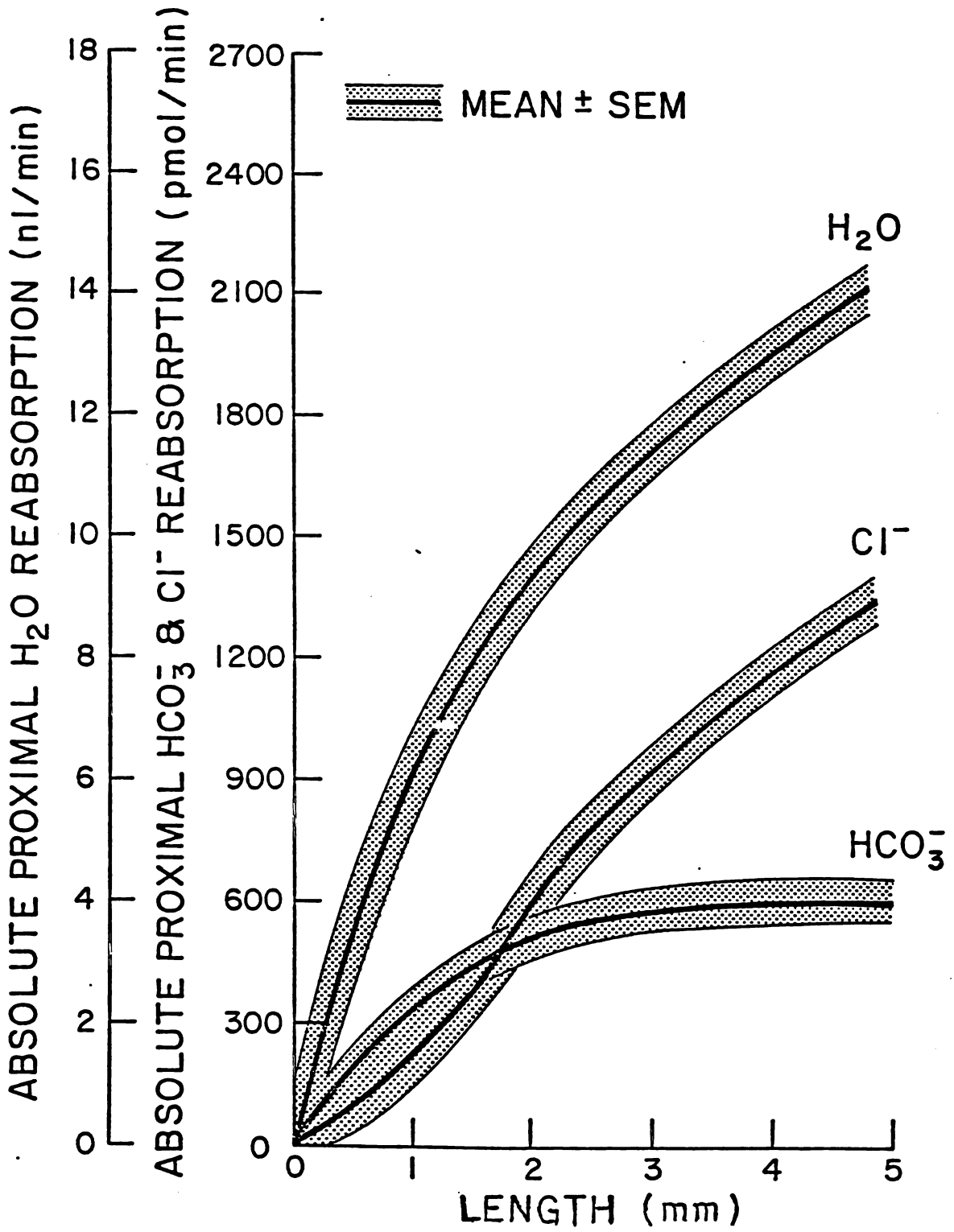
ABSOLUTE PROXIMAL H_2O REABSORPTION (nl/min)
ABSOLUTE PROXIMAL HCO_3^- & Cl^- REABSORPTION (pmol/min)
MEAN ± SEM
H_2O
Cl^-
HCO_3^-
LENGTH (mm)
0
2
4
6
8
10
12
14
16
18
300
600
900
1200
1500
1800
2100
2400
2700
1
2
3
4
5

FIGURE 4

CHAPTER 4

INTRODUCTION

to

CHAPTER 4

This chapter is a reprint of the material as it appears in "Axial heterogeneity in the rat proximal convoluted tubule. II. Osmolality and osmotic water permeability" published in the Am. J. Physiol. 247 (Renal Fluid Electrolyte Physiol. 16): F822-F826, 1984.

AXIAL HETEROGENEITY IN THE RAT PROXIMAL CONVOLUTED TUBULE

II. OSMOLALITY AND OSMOTIC WATER PERMEABILITY

by

Fu-Ying Liu, Martin G. Cogan, and Floyd C. Rector, Jr.

Cardiovascular Research Institute and Departments of Medicine and Physiology
University of California, San Francisco
San Francisco, California 94143

Running Head: Proximal Osmolality and P_f

Editorial Correspondence and Reprint Requests:

Martin G. Cogan, M.D.
1065 HSE
University of California
San Francisco, California 94143

Portions of this work have been presented in preliminary form at the 16th Annual Meeting of the American Society of Nephrology (Washington, D.C., December 4-7, 1983) and published in abstract form: Kidney Int., 25:308, 1984.

ABSTRACT

There is substantial disagreement over whether the luminal fluid in the proximal convoluted tubule becomes hypotonic with respect to plasma. To address this question, free-flow micropuncture measurements were made sequentially from the end-proximal tubule to Bowman's space in ten tubules of hydropenic Munich-Wistar rats. Osmolality in Bowman's space was 2.8 ± 0.3 mosmol less than plasma. Tubular fluid osmolality fell along the tubule and by the end-proximal tubule was 7.5 ± 0.7 mosmol less than plasma, or 4.7 mosmol less than Bowman's space. Since luminal fluid became hypotonic, the reabsorbate was hypertonic. Absolute water reabsorption was measured simultaneously, allowing estimation of the transepithelial osmotic water permeability (P_f). The osmotic gradient responsible for water reabsorption was assumed to be either lumen-to-reabsorbate or lumen-to-peritubular plasma, with a reflection coefficient for sodium chloride of 0.7 or 1.0. The P_f was then estimated to be between 0.2 and 2.0 cm/sec in the first mm of tubule and to have fallen to 0.1-0.2 cm/sec by the end of the tubule. A constant P_f along the tubule could explain observed rates of water absorption if reabsorbate hypertonicity were not dissipated and if the reflection coefficient for sodium chloride were less than unity; otherwise P_f must be higher in the early than in the late proximal convoluted tubule. In conclusion, luminal hypotonicity develops in the rat proximal convoluted tubule and must be considered as part of the osmotic driving force for water reabsorption.

INTRODUCTION

Water reabsorption in the proximal convoluted tubule occurs due to the transepithelial osmotic pressure gradient generated by solute transport (7). There has been on-going controversy, however, regarding the magnitudes of both the osmotic gradient generated and the osmotic water permeability (P_f) of the proximal tubule. Since the earliest measurements of Walker et al. (25) in the rat, it has been assumed that luminal fluid osmolality is not measurably different from that of plasma. If the luminal fluid remained exactly isosmotic with plasma, then water absorption would require local hypertonicity in some poorly mixed intraepithelial compartment (10). This hypothesis, however, has been difficult to prove and, in fact, has been subject to serious criticism (2, 3, 13, 23). Schafer and Andreoli, on the other hand, have reported very high P_f values for the proximal convoluted and straight tubules and, on the basis of these high values, proposed that observed rates of water transport could be driven by small degrees of luminal hypotonicity that would be difficult to detect by existing methods (2, 3, 23). Thus, the resolution of this question depends on whether or not the luminal fluid and the reabsorbate are truly isosmotic with plasma. In microperfusion studies in the rat proximal convoluted tubule, luminal fluid became overtly hypotonic (12) while in isolated perfused rabbit tubules a hypertonic reabsorbate has been demonstrated (5). On the other hand, measurements of tubular

fluid osmolality in free-flow micropuncture studies in rats have yielded conflicting results: small degrees of luminal hypotonicity have been observed in some (4, 8, 15, 16, 25) but not in all studies (14, 16).

Given the functional transport heterogeneity that has been demonstrated along the proximal convoluted tubule (17), it was the purpose of the present studies to examine whether a change in osmolality also develops along the rat proximal convoluted tubule under free-flow conditions. Using the luminal osmolality and measured rates of water reabsorption with estimates of contraluminal osmolality, the P_f could be calculated and expressed as a function of tubule length.

METHODS

Free-flow micropuncture studies were performed in ten tubules from ten hydropenic male Munich-Wistar rats (200-225 g).

Micropuncture Protocol: Rats were prepared for micropuncture as described in the accompanying paper (17). Briefly, the animals were allowed free access to food and water prior to being anesthetized with Inactin (100 mg/kg, i.p.). They were placed on a thermostatically controlled (37° C) micropuncture table. Catheters (PE 50) were inserted in the femoral artery for blood pressure measurements and for blood sampling and in a jugular vein for inulin infusion. A tracheostomy was performed. The abdomen was opened by a midline incision, the kidney was stabilized and bathed in warmed (37° C) saline, and the ureter was cannulated. A 20 min. equilibration period was then allowed to elapse. Surgically-induced plasma volume losses were not replaced.

A surface glomerulus was then located. A small pipette (3-5 μ OD) was inserted into Bowman's space and a small droplet of oil stained with Sudan black was then injected. The course of the injected oil droplet was carefully observed and mapped. Only glomeruli that were followed by at least 5-7 surface proximal convolutions were used. The localization pipette was then withdrawn and at least an hour was allowed for the hole in Bowman's

space to seal. Following an inulin prime (25 μCi) an inulin infusion at 1.6 ml/hr in bicarbonate Ringer's solution was then begun (50 μCi/ml). Sequential, timed 3-7 min collections commenced using 7-9μ OD glass pipettes, starting at the end-proximal convolution and working in a retrograde fashion to Bowman's space. Blood collections were made at the beginning, middle and end of the micropuncture period.

Latex was then injected into Bowman's space to fill the entire tubule. At a later time, the kidney was incubated for 30-40 min in 6 N HCl. The latex cast of the tubule was carefully dissected, photographed and measured. The entire proximal tubule length (glomerulus to the last puncture site) and the lengths to each puncture site were recorded.

Analysis: The volume of collected tubule fluid samples was determined by injecting them into constant bore capillary glass tubing with a known volume per length and measuring the length occupied. Inulin was measured by scintillation counting. Osmolality was measured by the method of Ramsay and Brown (21). Chloride concentration in tubule fluid was measured by the microtitrametric method (22). Six aliquots of each tubule fluid or plasma sample were prepared and measured three at a time. Standards were used that spanned the physiologic range (250-330 mosmol). The ten standard curves relating temperature at melting to osmolality each had a linear regression coefficient >0.998. To assess the accuracy of osmolality determination, measurements

were made of 18 unknowns with osmolalities similar to the ones found experimentally (290-310 mosmol). The difference between the observed and expected values was 0.6 ± 0.6 (SD) mosmol. The coefficient of variation on these unknowns was 0.2%. Since the range of measurement error was 0-1.5 mosmol, the accuracy of tubule fluid measurements was well within 1.5 mosmol.

Calculations: Water reabsorption was calculated as previously described (17). The osmolality and flow rates at a given length (e.g., 1 mm) were estimated by interpolation between the two closest measurements. The reabsorbate osmolality was calculated by mass balance:

$$\text{Reabsorbate Osmolality} = (Osm_1 \cdot V_1 - Osm_2 \cdot V_2)/(V_1 - V_2) \quad (1)$$

where Osm_1 and V_1 and Osm_2 and V_2 are the osmolalities and flow rates at points 1 and 2, respectively.

Osmotic water permeability (P_f) for each mm of tubule was calculated as:

$$P_f = RT(J_v)/AV_w \, \Delta osmol \quad (2)$$

where R and T have their usual meanings, J_v represents the water reabsorbed along each mm segment of tubule, A is the epithelial area per mm tubule length (assuming a tubule radius of 15 u), V_w is the partial molar water volume and Δ osmol is the osmotic

pressure difference developed in that segment. The osmotic gradients were taken as either the plasma-to-lumen or reabsorbate-to-lumen osmolal differences, each assuming the reflection coefficient for sodium chloride to be 0.7 or 1.0. For the gradient reabsorbate-to-lumen with a sodium chloride reflection coefficient of 0.7, it was necessary to calculate the reabsorbate chloride concentration using the measured luminal concentration and mass balance, similar to equation (1) above for reabsorbate osmolality.

All results are expressed as mean ± SEM.

RESULTS

The mean single nephron glomerular filtration rate in these ten tubules was 29 ± 1 nl/min. The length of these accessible superficial proximal convoluted tubules was 4.8 ± 0.1 mm. Segmental water reabsorption under these hydropenic conditions has been considered separately (17), and was, for each mm starting from Bowman's space: 5.9 ± 0.4, 3.7 ± 0.4, 1.7 ± 0.2, 1.7 ± 0.2, and 1.2 ± 0.2 nl/mm·min.

The osmolality in Bowman's space was 299.5 ± 0.6 mosmol, which was significantly below the simultaneously measured arterial plasma osmolality (302.3 ± 0.5 mosmol) by 2.8 ± 0.3 mosmol. As illustrated in Fig. 1, the osmolality declined in a roughly linear fashion in most tubules. By the end of the tubule, luminal osmolality reached 7.5 ± 0.7 mosmol below plasma levels, or 4.7 mosmol below the value observed in Bowman's space. Thus, hypotonicity developed; when all tubules are considered, the change in osmolality was about -1 mosmol per mm of tubule length. However, in a few tubules a rapid fall and then relative stabilization of luminal osmolality was observed, in accord with recent theoretical predictions (26). However, a rise in osmolality following an initial decline was not observed (8).

Since luminal osmolality and volume flux were measured simultaneously along the tubule, it was possible to calculate the osmotic water permeability (P_f) if the effective contraluminal

osmolality could be assumed. However, the correct contraluminal osmolality that should be used for these calculations is not known. One possibility is that the reabsorbate hypertonicity (which exists because the luminal fluid has become hypotonic to plasma) could participate in volume absorption if reabsorbed solute concentration gradients are not dissipated by diffusive mixing with peritubular capillary plasma. On the other hand, if the reabsorbate hypertonicity is not sustained and does not participate in solute-solvent coupling, then the appropriate interstitial osmolality approaches that of plasma. Bounds for the osmotic gradient were therefore taken to be peritubular plasma-to-lumen (solid lines in Fig. 2) or reabsorbate-to-lumen (dashed lines in Fig. 2). The former represents the lower limit of an osmotic driving force and assumes that the interstitium is well mixed and has rapid solute diffusion, so that local reabsorbate hypertonicity cannot be sustained. The latter represents the upper limit of an osmotic driving force in which solute diffusion is restricted so that the reabsorbate hypertonicity can be maintained. A further variable that contributes to uncertainty in estimating effective osmotic gradients is the reflection coefficients of the luminal and contraluminal constituents. We therefore assumed that sodium chloride might exert either its full osmotic pressure on each side of the epithelium, with a reflection coefficient of 1.0 (circles in Fig. 2) or a reduced pressure, with a reflection coefficient of 0.7 (squares in Fig. 2.). All other solutes, such as bicarbonate and organics, were assumed to have reflection coefficients of unity.

The results of these calculations are shown in Fig. 2. It can be seen that the estimated P_f at the beginning of the proximal tubule might be from 0.2 - 2.0 cm/sec, depending on the osmotic gradient and the reflection coefficient for sodium chloride chosen. If the reabsorbate-to-lumen osmotic gradient is used with a sodium chloride reflection coefficient of 0.7 (dashed line with squares), the calculated P_f is relatively stable at 0.2. In all other circumstances, the P_f declined along the tubule, and reached values from 0.1 - 0.2 cm/sec by the end of the tubule.

DISCUSSION

The results of these studies demonstrate that luminal hypotonicity does develop in the rat proximal convoluted tubule. While the contribution of luminal hypotonicity to the osmotic driving force for water reabsorption can be determined with reasonable accuracy, the degree of contraluminal hypertonicity is unknown, rendering it possible only to estimate the range of the transepithelial P_f at this time.

The finding of luminal hypotonicity under free-flow conditions is consistent with microperfusion data indicating that luminal hypotonicity and reabsorbate hypertonicity does occur (5, 12). The present observation that the tubular fluid/plasma osmolality decreased to 0.975 by the end of the proximal tubule is also in accord with most other mid- and end-proximal measurements of 0.97-0.99 in the rat (4. 15. 16), Psammomys (18) and Rhesus monkey (6), but are less than some measurements of 1.00-1.02 (14, 16). However, observed luminal hypotonicity in some studies was interpreted as being indistinguishable from isotonicity because of uncertainty regarding the accuracy of the measurements. For instance, a closer reading of the early experiments of Walker et al. (25), in which isotonic luminal fluid was said to be found, actually reveals that eight of nine tubular fluid samples from rats were hypotonic to plasma. The fall in osmolality found in the current experiments is at odds with the apparant increase with length from hypotonic to isotonic values found by Bishop et

al. (8), although the significant linear regression in those experiments was not strong (r=0.22). An initial fall with stabilization in osmolality could not be excluded in some of the tubules in the present studies (26).

A comment should be made regarding the osmolality in Bowman's space, which was 2.8 mosmol lower that plasma. A certain degree of hypotonicity in the glomerular ultrafiltrate is expected because of the Donnan equilibrium that exists across the glomerular capillary wall. The predicted osmotic disequilibrium is 1.4 mosmol for a Donnan distribution of 1.05. This Donnan factor of 1.05 has been established by simultaneous comparisons of the bicarbonate concentration in plasma and in Bowman's space in 100 experiments in Munich-Wistar rats (ref. 9 and unpublished observations). The difference between the observed and expected osmolality in the glomular ultrafiltrate, 1.4 mosmol, was at the threshold of detection in our hands (1.5 mosmol). The small discrepancy might be explained by fact that protein was present in plasma samples but not in tubular fluid. Protein might affect the structuring of water in the sample and change the freezing point.

While it is clearly established that luminal hypotonicity contributes to the osmotic driving force for volume reabsorption, it is uncertain whether the reabsorbate, which may be hypertonic, also contributes to the driving force for volume flux. The reabsorbate will be hypertonic to the lumen when the luminal

fluid osmolality is decreasing, as was the case in most of the tubules (Fig. 1). If the osmolality in the tubular fluid is stable and not decreasing, the reabsorbate will be same as that in the lumen. When mean values are considered for the early tubule, the reabsorbate can be calculated to be 4.2 mosmol/kg hypertonic to plasma. A lower transepithelial P_f would be calculated if this contraluminal hyperosmolality, acting in concert with the luminal hypotonicity, participated in the osmosis of water than if the plasma isosmolality-to-luminal hypotonicity were the relevant gradients. It is unknown whether the hypertonicity established by transport persists in the interstitium, thus effecting solute-solvent coupling, or whether it would be dissipated by diffusive mixing with peritubular plasma. The theoretical presence of an interstitial compartment substantially hypertonic to plasma has been both promoted (10) and refuted (2, 3, 13, 23). The ability for the solutes in the reabsorbate to maintain a hypertonic environment would depend on the existance of diffusion barriers, either in channels within the cell or perhaps in a gel surrounding the cell. Such contraluminal barriers to solute diffusion have not been proven to exist but have some support (1, 7).

In addition to uncertainty regarding the true cryoscopic osmotic gradient, there is also debate regarding the reflection coefficients for the solutes comprising these gradients. Assumption of a lower reflection coeffient for sodium chloride (e.g., 0.7) than for other solutes like bicarbonate and organics (1.0)

would also affect the magnitude of the effective osmotic gradients established across the epithelium. The effective gradient is increased and the calculated P_f is reduced, when the reflection coefficient for sodium chloride is less than unity, although the major site of the effect along the tubule is different depending on whether the plasma or the reabsorbate is chosen to represent the contraluminal osmolality. If the plasma-to-lumen osmolality gradient is the driving force for water absorption, a reflection coefficient for sodium chloride less than for bicarbonate will have the greatest effect near the end of the tubule, where the luminal fluid consists principally of sodium chloride, whereas the plasma contains bicarbonate. In the early tubule, the luminal and plasma solutions are of similar composition so that the low sodium chloride reflection coefficient has little effect in adding to the effective driving force. On the other hand, if the reabsorbate-to-lumen osmolality gradient is the relevant driving force, the end-proximal reabsorbate and luminal fluids are symmetric sodium chloride solutions whereas the early reabsorbate contains more bicarbonate (about 60 mM) than the luminal fluid (about 25 mM). In this situation, the lower reflection coefficient for sodium chloride amplifies the osmotic gradient in the earliest portion of the tubule.

We have attempted to cover all of these possibilities in Fig. 2, which depicts the calculated P_f as function of length when the gradients are assumed to be defined by the osmotic gradients from lumen-to-plasma or lumen-to-reabsorbate, with a

reflection coefficient for sodium chloride in the fluids in each case assumed to be either 0.7 or 1.0. The values for P_f at the end of the tubule converge to about 0.1 - 0.2 cm/sec, in good agreement with recent estimates of 0.12 - 0.17 cm/sec using in vivo microperfusion of the late proximal tubule (20). Other estimates of P_f in the rat late proximal tubule have varied from 0.14 - 0.35 (11, 12, 19, 24), but these also suffer from uncertainty regarding the true transepithelial driving force (7). The values at the beginning of the tubule may be higher, ranging from 0.2 - 2.0 cm/sec depending on which gradients are presumed to apply. Such a higher P_f in the early compared to the late proximal convoluted tubule is consistent with the data of Welling et al., possibly attributable to the greater membrane surface area in the earliest tubule (27).

Thus, as shown in Fig. 2, a constant P_f along the tubule could explain observed rates of water absorption only if reabsorbate hypertonicity were not dissipated and the reflection coefficient for sodium chloride were less than unity; otherwise, P_f in the early proximal tubule must be higher than in the late proximal convoluted tubule. In any case, these studies demonstrate that luminal hypotonicity exists in the rat proximal convoluted tubules and must be considered as part of the osmotic driving force for volume reabsorption.

ACKNOWLEDGMENTS

These studies were supported in part by a Clinical Investigator Award (1 KO-8-AM-01015) and a grant (AM-27045) from the National Institute of Arthritis, Diabetes, and Digestive and Kidney Diseases.

REFERENCES

1. Alpern, R. J. Effect of volume flux (Jv) on bicarbonate flux (JHCO3) in the in vivo perfused rat proximal convoluted tubule (PCT). Kidney Intern. 25:270, 1984.
2. Andreoli, T. E., and J. A. Schafer. Volume absorption in the pars recta. III. Luminal hypotonicity as a driving force for isotonic volume absorption. Am. J. Physiol. 234 (Renal Fluid Electrolyte Physiol. 4): F349-F355, 19778.
3. Andreoli, T. E., J. A. Schafer, and S. L. Troutman. Perfusion rate-dependence of transepithelial osmosis in isolated proximal convoluted tubules: Estimation of the hydraulic conductance. Kidney Int. 14:263-269, 1978.
4. Atherton, J. C. Comparison of chloride concentration and osmolality in proximal tubular fluid, peritubular capillary plasma and systemic plasma in the rat. J. Physiol. 273:765-773, 1977.
5. Barfuss, D. W., and J. A. Schafer. Collection and analysis of absorbate from proximal straight tubules. Am. J. Physiol. 241 (Renal Fluid Electrolyte Physiol. 10): F597-F604, 1981.
6. Bennett, C. M., B. M. Brenner, and R. W. Berliner. Micropuncture study of nephron function in the Rhesus monkey. J. Clin. Invest. 47:203-216, 1968.
7. Berry, C. A. Water permeability and pathways in the proximal tubule. Am. J. Physiol. 245 (Renal Fluid Electrolyte Physiol. 14): F279-F294, 1983.
8. Bishop, J. H. V., R. Green, and S. Thomas. Free-flow reabsorption of glucose, sodium, osmoles and water in rat proxi-

mal convoluted tubule. J. Physiol. 288:331-351, 1979.

9. Cogan, M. G., D. A. Maddox, M. S. Lucci, and F. C. Rector, Jr. Control of proximal bicarbonate reabsorption in normal and acidotic rats. J. Clin. Invest. 64:1168-1180, 1979.

10. Curran, P. F., and J. R. MacIntosh. A model system for biological water and solute transport. Nature London 193:347-348, 1962.

11. DiBona, G. F. Effect of magnesium on water permeability of the rat nephron. Am. J. Physiol. 223:1324-1326, 1972.

12. Green, R. and G. Giebisch. Luminal hypotonicity: a driving force for fluid absorption from the proximal tubule. Am. J. Physiol 246 (Renal Fluid Electrolyte Physiol. 15): F167-F174, 1984.

13. Hill, A. E. Solute-solvent coupling in epithelia: acritical examination of the standing-gradient osmotic flow theory. Proc. R. Soc. London Ser. B. 190:99-114, 1975.

14. Lassiter, W. E., C. W. Gottschalk, and M. Mylle. Micropuncture study of net transtubular movement of water and urea in nondiuretic mammalian kidney. Am. J. Physiol. 200:1139-1146, 1961.

15. Lechene, C., F. Morel, M. Guinnebault, and C. de Rouffignac. Etude par microponction de l'elaboration de l'urine. I. Chez le rat dans differents etats de diurese. Nephron 6:457-477, 1969.

16. Le Grimellec, C., N. Roinel, and F. Morel. Simultaneous Mg, Ca, P, K, Na and Cl analysis in rat tubular fluid. I. During perfusion of either inulin or ferrocyanide. Pfluegers

Arch. 340:181-196, 1973.

17. Liu, F.-Y., and M. G. Cogan. Axial heterogeneity in the rat proximal convoluted tubule. I. Bicarbonate, chloride and water transport. Am. J. Physiol. (Renal Fluid Electrolyte Physiol.): Submitted for publication, 1984.

18. Morel, F., C. de Rouffignac, D. Marsh, M. Guinnebault, and C. Lechene. Etude par microponction de l'elaboration de l'urine. II. Chez le Psammomys non diuretique. Nephron 6:553-570, 1969.

19. Persson, E., aand H. R. Ulfendahl. Water permeability in rat proximal tubules. Acta Physiol. Scand. 78:353-363, 1970.

20. Preisig, P. A., and C. A. Berry. Pathway of transepithelial osmotic water flow in the rat proximal convoluted tubule (PCT). Kidney Int. 25:313, 1984.

21. Ramsay, J. A., and R. H. J. Brown. Simplified apparatus and procedure for freezing-point determinations upon small volumes of fluid J. Sci Instr. 32:372-375, 1955.

22. Ramsay, J. A., R. H. J. Brown, and P. C. Croghan. Electrometric titration of chloride in small volume. J. Exp. Biol. 32:822-829, 1955.

23. Schafer, J. A., C. S. Patlak, S. L. Troutman, and T. E. Andreoli. Volume absorption in the pars recta. II. Hydraulic conductivity coefficient. Am. J. Physiol. 234 (Renal Fluid Electrolyte Physiol. 4): F340-F348, 1978.

24. Ullrich, K. J., G. Rumrich, and G. Fuchs. Wasserpemeabilitat und transtubularer wasserfluxx corticaler nephronabschnitte bei verschiedenen diuresezustanden. Pfluegers Arch. 280:99-

119, 1964.

25. Walker, A. M., P. A. Bott, J. Oliver, and M. C. MacDowell. The collection and analysis of fluid from single nephrons of the mammalian kidney. Am. J. Physiol. 134:580-595, 1941.

26. Weinstein, A. M. Nonequilibrium thermodynamic model of the rat proximal tubule epithelium. Biophys. J. 44:153-170, 1983.

27. Welling, L. W., D. J. Welling, and T. J. Ochs. Video measurement of basolateral membrane hydraulic conductivity in the proximal tubule. Am. J. Physiol. 245 (Renal Fluid Electrolyte Physiol. 14): F123-F129, 1983.

FIGURE LEGENDS

1. The luminal fluid osmolality (top panel, A) and the difference in tubular fluid osmolality compared to plasma (bottom panel, B) as a function of length in the proximal convoluted tubule of the rat.

2. The estimated transepithelial osmotic water permeability as function of proximal tubule length assuming four osmotic gradients: plasma-to-lumen (solid lines) or reabsorbate-to-lumen (dashed lines) with sodium chloride reflection coefficients of 1.0 (circles) or 0.7 (squares).

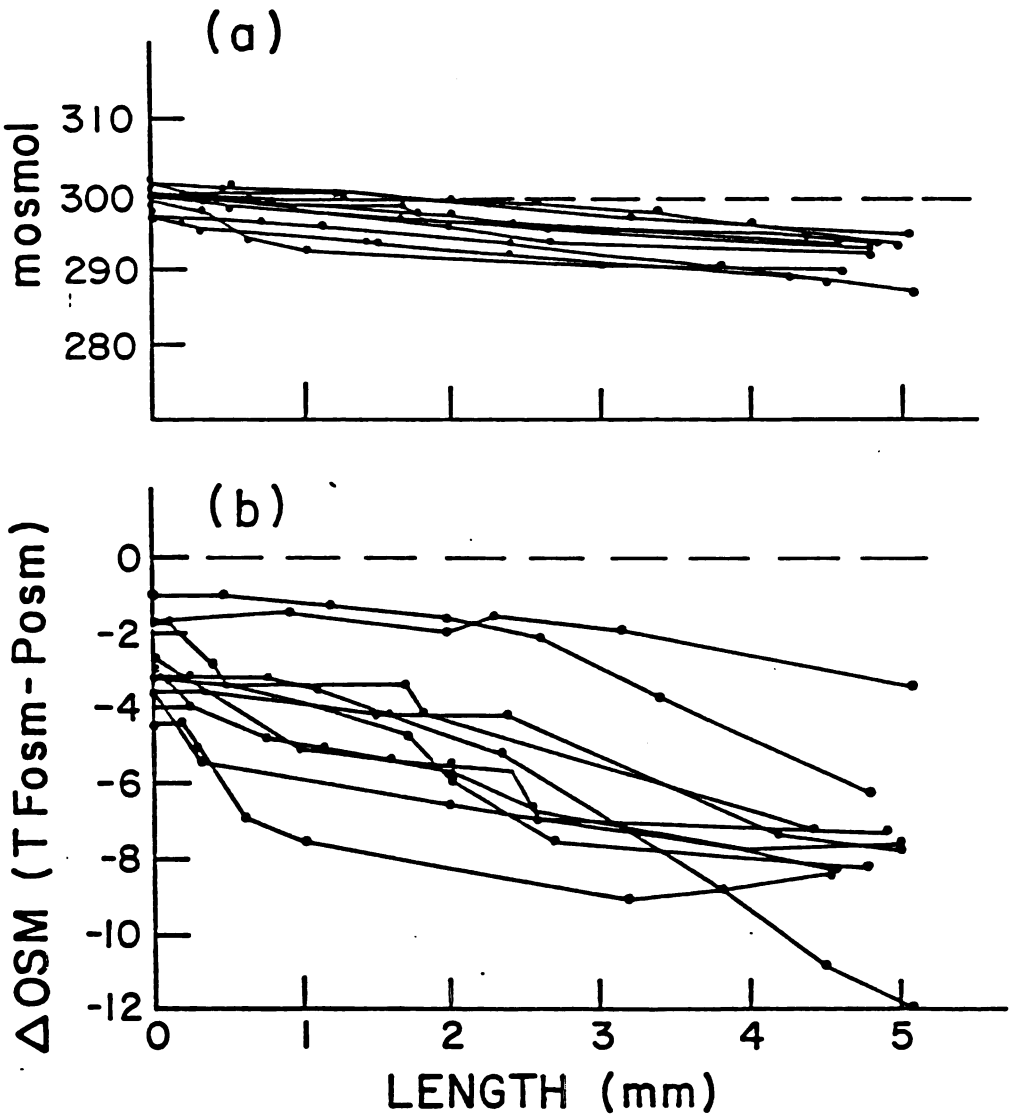
(a)
mosmol
310
300
290
280
(b)
ΔOSM (TFosm-Posm)
0
-2
-4
-6
-8
-10
-12
0
1
2
3
4
5
LENGTH (mm)

FIGURE 1

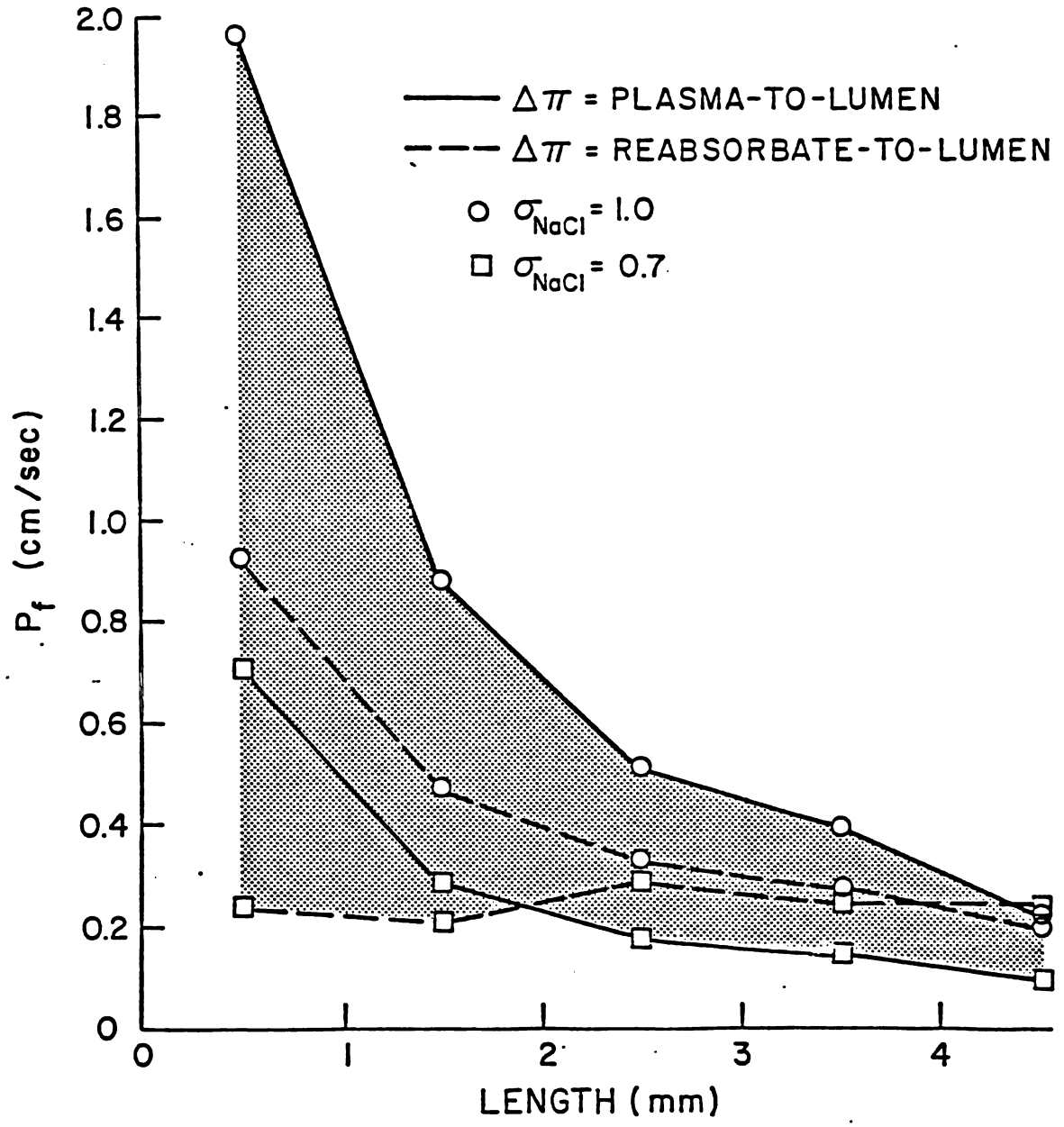
2.0
1.8
1.6
1.4
1.2
1.0
0.8
0.6
0.4
0.2
0
P_f (cm/sec)
0
1
2
3
4
LENGTH (mm)
$\Delta\pi$ = PLASMA-TO-LUMEN
$\Delta\pi$ = REABSORBATE-TO-LUMEN
σ_{NaCl} = 1.0
σ_{NaCl} = 0.7

CHAPTER 5

INTRODUCTION

to

CHAPTER 5

This chapter is a pre-print of the material as it appears in "Axial heterogeneity of bicarbonate, chloride and water transport in the rat proximal convoluted tubule. Effects of changes in luminal flow rate and of alkalemia", submitted for publication, J. Clin. Invest. 1986.

AXIAL HETEROGENEITY OF BICARBONATE, CHLORIDE AND WATER TRANSPORT IN THE RAT PROXIMAL CONVOLUTED TUBULE

Effects of Change in Luminal Flow Rate and of Alkalemia

Fu-Ying Liu and Martin G. Cogan

Cardiovascular Research Institute and Department of Medicine
University of California, San Francisco, California 94143

Running Head: Proximal Anion Transport Heterogeneity

Editorial Correspondence and Reprint Requests:

Martin G. Cogan, M.D.
Division of Nephrology
1065 HSE
University of California
San Francisco, California 94143
(415) 476-2172

Portions of this work were presented at the Western Section and National Meetings of the American Federation for Clinical Research and published in abstract form: 1986. Clin. Res. 34: 109A.

ABSTRACT

Changes in bicarbonate, chloride and water reabsorption in the early versus late rat superficial proximal convoluted tubule (PCT) were examined in response to alteration in luminal flow rate and in peritubular bicarbonate concentration. As SNGFR was increased from 28.7 ± 0.7 nl/min in hydropenia to 41.5 ± 0.4 nl/min in euvolemia, bicarbonate reabsorption in the early (1st mm) PCT increased proportionally, from 354 ± 21 to 520 ± 12 peq/mm·min. This high acidification rate did not increase further when SNGFR went to 51.2 ± 0.7 or 50.7 ± 0.6 nl/min following atrial natriuretic factor (ANF) or glucagon administration, respectively, nor was it inhibited by alkalemia in another group of rats with chronic metabolic alkalosis. Late PCT bicarbonate reabsorption was also flow-dependent, though at a much lower absolute level, but was inhibitable by alkalemia. Chloride reabsorption in the early PCT increased from 206 ± 55 peq/mm·min in hydropenia to 585 ± 21 peq/mm·min in euvolemia, but no further following ANF or glucagon. Chloride transport in the late PCT was lower and exhibited less flow-dependence. Water reabsorption increased proportionally (i.e., glomerulo-tubular balance was exhibited), from 5.9 ± 0.4 to 10.1 ± 0.4 nl/mm·min in the transition from hydropenia to euvolemia, but no further following ANF or glucagon. Water reabsorption in the late PCT was lower and showed less flow-dependence. In conclusion, the early superficial PCT is distinguished from the late PCT by having high capacity, flow-responsive but saturable anion and volume reabsorptive processes relatively unaffected by alkalemia.

INTRODUCTION

The rat proximal convoluted tubule (PCT)[1] exhibits structural and functional differences along its length (1-3). The early PCT is distinguished by having cells (S_1 subtype) with greater membrane surface area and more mitochondria (1) and by having greater avidity for reabsorption of several solutes, including glucose, amino acids, and phosphate, than cells (S_2) resident in the late PCT (2, 3).

We recently extended this description of axial heterogeneity by examining free-flow anion reabsorption along the length of the superficial PCT in hydropenic rats. The early PCT reabsorbed bicarbonate at a greater rate than has been observed in the late PCT (4), even when the latter has been presented with similar bicarbonate loads by means of microperfusion (5, 6). The high rate of acidification in the early PCT has been confirmed (7, 8). In addition, we demonstrated that the early PCT was capable of reabsorbing chloride at a substantial rate (4), a surprising finding since minimal chloride transport in this nephron segment was expected based on previous theoretical considerations (9).

However, the reabsorptive kinetics of these robust anion transport processes in the early PCT in response to change in luminal flow and substrate delivery rate have not been clearly defined. Conflicting conclusions have been advanced recently regarding the saturability of early PCT bicarbonate reabsorption under physiological conditions as load is increased (8, 10).

While microperfusion studies have demonstrated saturability of acidification in the late PCT in vivo (5, 6), the early PCT has not been examined. Another issue which has not yet been addressed is whether chloride transport in the early PCT can increase when flow rises (11). Flow-dependence of chloride transport has been found to occur in some (12-14), but not other (14-16), microperfusion studies of the late PCT in vivo.

In addition to the quantitative and possible kinetic differences with regard to luminal determinants of anion transport in the early versus late PCT, there may also be axial differences in control of transport by peritubular factors. It has been proposed, for instance, that alkalemia suppresses late, but not early, acidification (17, 18). Such differential regulation has been posited because of the findings that bicarbonate absorption in the late PCT determined by in vivo microperfusion was markedly inhibited during metabolic alkalosis (19), whereas total bicarbonate reabsorption over the entire length of the PCT determined by free-flow micropuncture was not substantially altered by alkalemia (20).

The first purpose of the present studies was to compare the flow-dependency of bicarbonate, chloride, and water reabsorption in the early versus late superficial PCT. Anion and water transport was examined over the entire length of the tubule by the retrograde, sequential free-flow micropuncture technique (developed in this laboratory) as single nephron glomerular filtration

rate (SNGFR) was systematically altered in increments of about 10 nl/min. Axial PCT transport during the volume-contracted, low-SNGFR condition of hydropenia was compared to proximal transport during the normal-SNGFR condition of euvolemia and finally to the high-SNGFR condition induced by administration of either atrial natriuretic hormone (ANF) or glucagon. The use of vasoactive hormones, ANF and glucagon, for this purpose is predicated on the assumption that they raise SNGFR but do not independently alter proximal transport. The lack of direct effect by ANF on the proximal tubule is supported by several lines of evidence: (1) there are no extra-glomerular cortical ANF receptors (21, 22); (2) the second messenger for ANF, cyclic GMP, is not produced by the PCT either in vivo (23) or in vitro (21, 24, 25) and the PCT has no particulate guanylate cyclase (21, 25); (3) and all micropuncture and microperfusion studies to date both in vivo (26-29) and in vitro (30) have failed to show any direct effect by ANF on solute or volume transport in the PCT independent of flow rate. Similarly, glucagon causes no increase in its second messenger, cyclic AMP, in the proximal tubule (24, 31) and does not affect proximal sodium transport (32).

Our second purpose was to test the prediction that acidification in the late, but not early, PCT is suppressed by alkalemia (17, 18). For this purpose, bicarbonate reabsorption in the early and late PCT was compared during normal and alkalotic conditions at comparable filtered bicarbonate loads.

METHODS

Free-flow micropuncture studies were performed in 27 Munich-Wistar rats. We employed the technique previously developed in this laboratory by which multiple punctures are made sequentially along the entire length of the superficial PCT in a retrograde fashion, from the end-proximal tubule to Bowman's space (4). This technique permits assessment of the axial profiles of bicarbonate, chloride and volume transport.

Protocols

The first four protocols were designed to systematically alter SNGFR from subnormal to normal to supernormal levels to assess the effect of changes in luminal flow rate on segmental anion and water reabsorption. The last protocol, in which chronic metabolic alkalosis was induced, was performed to permit comparison of segmental bicarbonate reabsorption in alkalotic and normal animals with similar filtered bicarbonate loads.

Group 1: Hydropenia. The results of studies in 10 hydropenic rats on a normal diet have been reported previously (4) and are repeated here for comparison with the other groups. Surgically-induced plasma volume loss was not replaced so that SNGFR was subnormal (33).

Group 2: Euvolemia. 6 rats were studied in which the plasma volume contraction incurred by the micropuncture prepara-

tory surgery was corrected by isoncotic plasma infusion, as previously described (8,33). Isoncotic plasma obtained from donor sibling rats maintained identically to the rat under study was given as an infusion of 1.3% body weight over 45 min and then as a sustaining infusion of 5 µl/min to maintain a normal plasma volume and SNGFR.

Group 3: ANF. Following the achievement of the euvolemic state in 5 rats, an intravenous infusion was begun of synthetic, rat ANF (Auriculin B, 25 amino acids: arg^{126} to tyr^{150} residues, generously provided by Dr. J. Lewicki, California Biotechnology, Inc., Palo Alto, CA). ANF was given as a bolus of 5 µg/kg followed by a sustaining rate of 0.5 µg/kg/min in a bicarbonate Ringer's solution at a rate (30 µl/min) sufficient to replace urinary solute and volume losses (23, 26, 29). ANF used in this manner causes a stable state of glomerular hyperfiltration (23, 26, 29).

Group 4: Glucagon. The same protocol as Group 3 was followed except that glucagon was given as a bolus of 10 µg/kg followed by a sustaining rate of 1.0 µg/kg/min at 50 µl/min.

Group 5: Chronic Metabolic Alkalosis. As previously described (20), 6 rats were maintained for 2 weeks on a standard liquid electrolyte-deficient diet (40 ml/day) supplemented with Na_2SO_4 (2.6 meq/d) and injected with 0.5 mg/d deoxycorticosterone acetate i.m. Surgically-induced plasma volume losses were reple-

nished prior to micropuncture. Rats prepared in this way have hyperbicarbonatemia with reduction in SNGFR.

Micropuncture Technique

The rats were prepared for micropuncture as previously described (4, 20, 23, 26, 33, 34). Briefly, the animals were anesthetized with Inactin (100 mg/kg, i.p.) and placed on a thermostatically controlled (37°C) micropuncture table. Catheters (PE-50) were inserted into the femoral artery for blood sampling and into a jugular vein for inulin infusion. A tracheostomy was performed. The abdomen was opened by a midline incision, the kidney was stabilized and bathed in warmed saline (37°C), and the ureter was cannulated. A 20-min equilibration was allowed to elapse.

A surface glomerulus was then located. A small pipette (3-5 μm OD) was inserted into Bowman's space and a small droplet of oil stained with Sudan black was injected. The course of the injected oil droplet was carefully observed and mapped. Only glomeruli followed by at least six to seven surface proximal convolutions were used. The localization pipette was withdrawn and 1 h was allowed to elapse, which we have previously shown is sufficient time for the hole in Bowman's space to seal (4). The plasma volume in Groups 2-4 was then replenished as described above and a ^{3}H-methoxyinulin infusion commenced (25-50 μCi bolus, then 50-100 μCi/h in bicarbonate Ringer's solution at 0.8-1.6 ml/h).

Following an equilibration time of at least 1 hour, sequential, timed 3-8 min collections were begun using 7-9 μm OD glass pipettes. They started at the end-proximal convolution and worked in a retrograde fashion to Bowman's space. Because of the special interest in these studies in early PCT transport, care was taken to obtain at least one sample within the estimated initial mm of the tubule.

After 5 h, to allow the tubule puncture sites to seal, Microfil (Canton Biomedical Products, Boulder, CO) was injected into Bowman's space to fill the entire tubule. At a later time, the kidney was incubated for 30-40 min in 6 N HCl. The cast of the tubule was dissected, with the multiple puncture sites identified using the initial localization map, and it then was photographed. The entire accessible proximal tubule length (glomerulus to the last puncture site) and the length to each puncture site were measured and recorded.

Analysis

The volume of collected tubule fluid samples was determined by injecting them into constant-bore capillary glass tubing with a known volume per length and measuring the length occupied. Aliquots of the fluid were used to measure inulin by scintillation counting, total CO_2 by microcalorimetry (35), and chloride by the microtitrimetric method of Ramsay et al. (36), as previously described (4, 20, 23, 26, 33, 34). For ease of

presentation, bicarbonate is used to represent total CO_2 content of tubular fluids and urine under physiologic conditions.

Calculations

The SNGFR was estimated as the product of the flow rate at a given point multiplied by the corresponding inulin concentration ratio (tubular fluid/plasma water). SNGFR values in the text refer to mean determinations but there were no systematic changes in SNGFR as a function of length or time, as previously documented (4). Water reabsorption at a given point was the flow rate at that point subtracted from the SNGFR. Bicarbonate and chloride reabsorption were the filtered load (anion concentration in Bowman's space multiplied by the SNGFR) minus the anion delivery at that point (anion concentration multiplied by the flow rate). Reabsorption at a given length (e.g., 1 mm) was estimated by interpolation between the two closest measured data points to that length for each tubule. The fractional reabsorption for a given nephron mm segment was calculated as the anion or volume reabsorption of that mm segment divided by the delivery of anion or volume to that segment. All data are expressed as mean $\pm$ SEM. Statistical comparisions between groups were made using the unpaired t-test.

RESULTS

General

As shown in Table 1, all groups had similar values for animal weight and for total length of the accessible superficial PCT (about 5 mm). Mean values for SNGFR in Groups 1, 2, and 3-4 differed from each other by increments of approximately 10 nl/min while plasma anion concentrations were stable. In Group 5 with chronic metabolic alkalosis, hyperbicarbonatemia and glomerular hypofiltration were present. No differences in plasma protein concentration or hematocrit were found between groups. Blood pressure was stable during the observation period in each group, though about 5-10 mmHg less in Groups 3 and 4 than in Groups 1 and 2.

In the following description of results, data will be presented by mm increments. To be concise, transport rates in the third-to-fifth mm of the late PCT have been consolidated in the figures since results for these segments were relatively homogeneous. The impact of altering luminal flow rate or peritubular anion composition on segmental bicarbonate, chloride or water transport will be displayed in three ways: (1) absolute transport as a function of length; (2) absolute transport as a function of delivered load; and (3) fraction of the delivered load reabsorbed as a function of the delivered load. There were no statistical differences in any of the transport data between the hyperfiltration Groups 3 and 4.

Flow-Dependence of Bicarbonate Transport

As shown in Table 2 and Figs. 1A and 1B, a progressive increase in luminal flow rate in Groups 1-4 resulted in lesser depression in the luminal bicarbonate concentration and tubular fluid/glomerular ultrafiltrate (TF/UF) concentration ratio as a function of length.

In the transition from hydropenia to euvolemia (Groups 1 and 2), the rise in filtered bicarbonate load (740 ± 31 to 1135 ± 9 peq/min) resulted in a proportional increase in bicarbonate reabsorption in the first mm of the PCT, from 354 ± 21 to 520 ± 12 peq/mm·min ($p<0.001$) (hexagons and squares, Figs. 2 and 3). Fractional reabsorption therefore remained constant at 0.5 in the initial mm segment (hexagons and squares, Fig. 4). In the second mm, the increase in flow rate resulted in a smaller rise in transport and fractional reabsorption of the delivered load fell. In the third-to-fifth mm, bicarbonate reabsorption was lower than in the first mm in hydropenia, expressed in both absolute (Figs. 2 and 3) and fractional (Fig. 4) terms, but increased in proportion to load in euvolemia.

When ANF (Group 3) or glucagon (Group 4) caused a further increase in SNGFR and filtered bicarbonate load (to 1424 ± 24 and 1430 ± 36 peq/min, respectively), bicarbonate reabsorption remained static in the first mm of the PCT, 542 ± 14 and 547 ± 29 peq/mm·min (triangles, Figs. 2 and 3). Therefore, fractional

reabsorption declined in this segment to about 0.4 (triangles, Fig. 4). A similar response, though at lower levels, was observed in the second mm. In qualitative contrast, the third-to-fifth mm of the PCT showed a further increase in absolute bicarbonate transport in response to the increased delivered bicarbonate load with only a slight fall in the fraction of delivered load reabsorbed for each mm. The present free-flow bicarbonate reabsorptive data in the late (third-to-fifth mm) PCT agree quite well with previous microperfusion data (dotted lines in Figs. 3 and 4) (6).

Effect of Alkalemia on Bicarbonate Transport

During chronic metabolic alkalosis (Group 5), the rise in glomerular ultrafiltrate bicarbonate concentration was offset by the fall in SNGFR (Table 2), so that the filtered bicarbonate load (1437 $\pm$ 28 peq/min) was not significantly different than that of Groups 3 and 4 which had normal acid-base status. As shown in Table 3 and Fig. 5, bicarbonate reabsorption was similar in the alkalotic group (circles) in the first mm, 565 $\pm$ 12 peq/mm·min, compared to the normal pH groups (triangles). The same was true for the second mm. However, bicarbonate reabsorption was significantly reduced ($p<0.05$) by 20-40% in the alkalotic animals in each of the third-to-fifth mm segments despite higher luminal bicarbonate concentrations (Table 2). As a result of this inhibition of late PCT acidification, cumulative absolute bicarbonate reabsorption along the entire PCT length was significantly ($p<0.05$) reduced in Group 5 (1115 $\pm$ 46) compared to the

Groups 3 and 4 (1201 ± 33 and 1180 ± 39 peq/min).

Bicarbonate transport as a function of load in the first mm in all five groups are combined in Fig. 6. It is apparent that acidification can rise to very high levels, to about 550 peq/mm·min, but then saturates when load is raised further by an increase in flow or concentration.

Flow-Dependency of Chloride Transport

The transepithelial chloride concentration gradient tended to decrease slightly as flow and filtered chloride load increased in Groups 1 to 2 to 3 and 4 (Table 2 and Figs 1A and 1B) and increased somewhat in the alkalotic Group 5 animals (Fig 1C).

Compared to hydropenia (solid hexagons), when filtered chloride load was increased in euvolemia (Group 2), chloride transport in the first mm almost tripled, to 585 ± 21 peq/mm·min (solid squares, Figs. 7 and 8), and fractional chloride reabsorption actually increased to 0.12 (Fig. 9). This flow-induced stimulation of chloride transport occurred to a similar degree but at a lesser delivered chloride load in the second mm (stippled symbols, Figs. 8 and 9). Chloride transport was changed relatively little in response to the increase in flow up to euvolemic values in the third-to-fifth mm of the PCT in Groups 1 and 2 (open hexagons and squares, Figs. 7 and 8). Fractional chloride transport in these groups therefore declined (Fig. 9). With a further increase in luminal flow rate and chloride deli-

very following ANF or glucagon administration (Groups 3 and 4), no further augmentation of absolute chloride reabsorption was observed in either the early or late PCT (open and solid triangles, Figs. 7 and 8) and hence fractional chloride reabsorption as a function of delivered chloride load declined in all PCT segments (Fig. 9). The relatively modest load-dependence of chloride transport in the late PCT is in reasonable agreement with microperfusion studies in which the late PCT has been perfused at varying rates with sodium chloride-containing solutions (dotted lines, Figs. 8 and 9) (12). Chloride transport in the first mm in Group 5 was similar to Group 1 (Table 3 and hexagons and circles, Figs. 7 and 8) at comparable filtered loads, suggesting that alkalemia did not obviously affect this transport system.

Flow-Dependence of Water Transport

As SNGFR rose from hydropenia to euvolemia (Groups 1 and 2), absolute water reabsorption in the first mm of the PCT increased markedly, from 5.9 $\pm$ 0.4 to 10.1 $\pm$ 0.4 nl/mm·min (Table 3 and hexagons and squares, Figs. 10 and 11). The fraction of water reabsorbed in the first mm actually rose slightly as flow increased, from 0.21 to 0.25 (Fig. 12). A quantitatively less flow-dependent response in absolute water reabsorption was observed in the remaining PCT (Figs. 10 and 11) so that water reabsorption as a fraction of delivered volume load for the third-to-fifth mm declined (Fig. 12). A further increase in SNGFR by ANF and glucagon (Groups 3 and 4) evoked no change in

absolute water reabsorption in the first mm and only small increments in reabsorption in the remaining PCT (triangles, Figs. 10 and 11) so that fractional reabsorption of delivered volume load declined in all mm studied (Fig. 12). The relatively poor load-dependence of water transport in the late PCT agrees reasonably well with data previously obtained by in vivo microperfusion (dotted lines, Figs. 11 and 12) (6).

DISCUSSION

These studies examined the response of the early versus late PCT transport systems for bicarbonate, chloride and water to alterations in luminal flow rate and to luminal and peritubular anionic composition. In the following discussion, the early PCT will refer principally to the first mm of the superficial PCT. Maunsbach has stated that the initial mm of the rat PCT contains exclusively S_1 cells (1). The third-to-fifth mm of the accessible superficial PCT, which will subsequently be referred to as the late PCT, contains only S_2 cells (1). The transition from S_1 to S_2 cells is not abrupt according to Maunsbach (1). The second mm of the PCT probably contains a mixture of both cell types and would therefore be expected to exhibit transport characteristics intermediate between the early and late PCT, as was observed in the present studies.

Axial Heterogeneity of Bicarbonate Reabsorption: Response to Alteration in Luminal Flow Rate

Bicarbonate reabsorption in the rat late PCT is effected by proton secretion and exhibits saturation kinetics (5, 6, 11, 17, 17-20). Major independent determinants of acidification in the late PCT include the luminal bicarbonate concentration (5), luminal flow rate (6), and peritubular bicarbonate concentration/pH (19). The present free-flow micropuncture study as well as others (8, 10) quantitatively demonstrated the flow-dependence of

bicarbonate reabsorption in the late PCT previously shown using in vivo microperfusion (compare dotted line representing previous microperfusion data and symbols representing present data in the third-to-fifth mm of the PCT in Figs. 3 and 4). While microperfusion studies indicate that bicarbonate absorption in the late PCT is saturable at about 200 peq/mm·min (5, 6, 19), this level cannot be reached under physiologic free-flow conditions due to insufficient bicarbonate delivery rates even following ANF and glucagon (Groups 3 and 4).

With increasing bicarbonate load caused by glomerular hyperfiltration induced by either ANF or glucagon, bicarbonate reabsorption in the early PCT qualitatively resembled that in the late PCT by showing saturation kinetics (Figs. 3 and 6). The saturability of early PCT bicarbonate reabsorption in the physiologic range of filtered bicarbonate loads is consistent with the conclusion reached by Corman et al. (10), though they did not directly measure bicarbonate reabsorption in the early PCT, but is in apparent contradiction with the conclusion of Maddox and Gennari (8). In the latter work, however, a systematic examination of bicarbonate reabsorption in the initial mm of the PCT at high bicarbonate deliveries was not undertaken. At a filtered bicarbonate load of 1200-1600 peq/min, Maddox and Gennari reported that bicarbonate reabsorption at 1 mm of tubule length was about 550 peq/min, in excellent agreement with our results. When filtered bicarbonate load exceeded 1600 peq/min, they presented only three data points for bicarbonate reabsorption in

the first mm; one of the points was below and two were above the line describing bicarbonate reabsorption at filtered load of 1200-1600 peq/min.

There are two interesting differences between the acidification rates in the early and late PCT. The first difference is that the level of saturation of bicarbonate transport is achieved in the early but not late PCT by the filtered bicarbonate load that occurs in a normal euvolemic animal. An increment in filtered bicarbonate load above normal (e.g., as induced by ANF or glucagon) results in further bicarbonate reabsorption solely in the late PCT. Maintenance of proximal glomerulotubular balance for bicarbonate reabsorption (flow-dependent acidification) at supernormal flow rates is therefore a function of the late but not early PCT. The second, more important, difference is that the absolute magnitude of the bicarbonate reabsorptive capacity in the early PCT, about 550 peq/mm·min, is 2.5-3 times the maximal rate in the late PCT (5, 6, 19). In fact, early PCT acidification capacity is more than an order of magnitude higher than maximal rates which have been reported in any distal nephron segment under normal conditions (2, 3).

The present studies did not elucidate whether such high rates of acidification in the early PCT were effected by amplification of the same processes resident in the late PCT. S_1 cells have greater membrane surface area (1) and could potentially contain more of the same luminal and peritubular transporters

required for acidification in the S_2 cells. It is also possible that the early PCT might recruit a different mechanism for boosting bicarbonate reabsorption (37). Further work will be required to identify the mechanism(s) responsible for the higher early PCT acidification process and to provide a more precise definition of the kinetics of transport in this segment than can be obtained using free-flow micropuncture techniques.

When taken together, the micropuncture and microperfusion data have shown that bicarbonate reabsorption of the entire superficial PCT can eventually be saturated in response to progressively increasing luminal flow. If maximal rates of transport in each of the five mm segments are sequentially taken as 550, 350, 200, 200 and 200 peq/mm·min from Fig. 3, a maximal reabsorptive capacity of the entire PCT would be approximately 1500 peq/min. This rate of bicarbonate reabsorption is never reached under physiologic free-flow conditions because the requisite SNGFR ($\geq$75 nl/min) and filtered bicarbonate load ($\geq$2000 peq/min) cannot be acutely achieved. At lower, physiologic SNGFRs, bicarbonate reabsorption in the entire proximal convoluted tubule demonstrates very good flow-dependence (8, 17, 33). Nevertheless, it would seem reasonable to consider bicarbonate transport kinetically similar (load-dependent but saturable) to transport processes for other sodium co-transported solutes in the PCT (e.g., glucose and amino acids).

Axial Heterogeneity of Bicarbonate Reabsorption: Response to Alkalemia.

In agreement with previous predictions from this laboratory (17, 18), late but not early PCT bicarbonate reabsorption was found to be inhibited by alkalemia. The suppressed rate of bicarbonate reabsorption in the late PCT during alkalemia in the present studies agreed very well with that previously defined by in vivo microperfusion, about 80 peq/mm·min (19). Inhibition of bicarbonate reabsorption was observed despite concurrent high luminal bicarbonate concentration (2-3 times normal), potassium deficiency, and extracellular volume contraction (5, 17). Alkalemia resets the maximal rate of late PCT acidification and prohibits further stimulation by yet higher luminal bicarbonate concentration (19). Alkalemia suppresses late PCT acidification (19, 38, 39), presumably by impairing bicarbonate exit from the cell (due to the hyperbicarbonatemia or possibly the reabsorbate alkalinity) resulting in cellular alkalinization (R. J. Alpern, personal communication). The reason for the relative sparing of the early PCT from this inhibitory effect of alkalemia is unknown but certainly deserving of further study. It should be noted, however, that when more prolonged metabolic alkalosis and hypokalemia occurs in association with tubular hypertrophy, the quantitative and perhaps qualitative effects of alkalemia on segmental bicarbonate reabsorption can be altered (40).

The results considered collectively suggest that bicarbonate reabsorption during chronic metabolic alkalosis may be maximal in

both the early and late PCT. In the early PCT, bicarbonate reabsorption was already at a maximal level (about 550 peq/mm·min) during the normal state (Groups 2-4) and was not reduced by alkalemia (Group 5); in the late PCT, bicarbonate reabsorption was reduced by alkalemia and rendered unresponsive to further stimulation by a high luminal bicarbonate concentration and delivery. The thesis that absolute bicarbonate reabsorption over the entire proximal convoluted tubule length is at a maximal level during chronic metabolic alkalosis is supported by observations that an increase in SNGFR and filtered bicarbonate load by volume expansion (20) or by ANF (34) resulted in no reabsorptive stimulation. It has therefore been proposed that the glomerular hypofiltration which occurs during chronic metabolic alkalosis (20, 34) is critical for the maintenance of the alkalotic state by preventing filtered bicarbonate load from exceeding the PCT reabsorptive capacity.

Axial Heterogeneity of Chloride Transport

Chloride transport in the late PCT is effected by parallel active and passive processes (9, 11, 41, 42). Transcellular transport of chloride is electroneutral and exquisitely sensitive to the peritubular protein concentration (9, 11, 41). Paracellular chloride transport is governed by the magnitudes of the junctional chloride permeability and the transepithelial electrochemical gradient, principally the chloride concentration gradient (9, 11). Contradictory microperfusion evidence has been presented on whether active chloride transport in the late PCT is

(1214) or is not (14-16) flow-dependent. Even when found, the magnitude of the rise in chloride transport is small compared to the increase in chloride load, similar to the present free-flow results (compare dotted line representing previous microperfusion data and symbols representing present data in the third-to-fifth mm in Figs. 8 and 9) (12). A rigorous statement regarding flow-dependence of late PCT chloride transport is not possible for several reasons. First, the transepithelial chloride gradients in these studies were not equivalant (the late PCT transepithelial chloride gradient declined from about 23 to 20 to 18 meq/L in hydropenia, euvolemia, and ANF and glucagon groups, respectively, and was $\geq$30 meq/L in the microperfusion studies). A small flow-induced change in active transport might have been offset by a directionally opposite change in chloride diffusion. Second, peritubular factors may also have been changed, which could affect active chloride transport. Nevertheless, while a definitive mechanistic conclusion cannot be reached, inspection of Figs. 7-9 reveals that the relatively low rate of absolute chloride reabsorption in the late PCT under free-flow conditions (<300 peq/mm·min) increased only modestly, with a decline in the fraction reabsorbed, as delivery rose.

Chloride transport in the early PCT differed from that in the late PCT both quantitatively and qualitatively. First, there was a marked augmentation in chloride transport in transition from the low filtered chloride loads of Groups 1 and 5 to the normal level of Group 2 (Figs. 7 and 8), unrelated to chemical

concentration gradients. The fractional chloride reabsorption actually rose to as high as 0.12 (Fig. 9). Indeed, as chloride load increased to the euvolemic level, most of the increment in absolute chloride reabsorption for the entire PCT, 544 peq/min (from 1404 ± 189 to 1948 ± 175 peq/min), was attributable to enhancement of chloride transport in the initial mm (379 peq/min). A further increase in chloride load with ANF or glucagon induced no more chloride transport, indicating apparant saturation of this process. Puzzling aspects of the load-dependent chloride reabsorptive response in the early PCT include the fact that the fractional rate of transport actually increased as delivery rose and transport in the second mm required a lower delivered load for augmenting transport than the first mm. Second, the maximum rate of chloride reabsorption in the first mm was very high, 585 peq/mm·min, similar to the rate of bicarbonate reabsorption in this segment and even rivalling the rate of chloride transport in the thick ascending limb of Henle (43).

The mechanism(s) responsible for this robust and flow-dependent chloride reabsorptive process in the early PCT was not defined in the present experiments. The early PCT may possess more of the presently unidentified transporters that effect chloride transport in the late PCT (e.g., more apical NaCl co-transporters or parallel exchangers such as Na^+/H^+ and Cl^-/OH^- or Na^+/H^+ and Cl^-/formate$^-$ with appropriate increase in peritubular transport systems) (42, 44). Alternatively, a different mechanism may be responsible for this early flow-dependent PCT

chloride transport. For instance, there may substantial electrodiffusion of chloride in the early PCT, driven by the lumen-negative potential difference generated by sodium-coupled organic reabsorption. Such a mechanism for chloride transport coupled to electrogenic organic reabsorption has been thought unlikely for the rabbit early PCT (9) because a lumen-negative potential difference in the setting of a high sodium/chloride permeability would simply result in sodium recycling. However, appropriate permeability measurements have not yet been performed in the rat.[2] Such a mechanism would explain the early PCT chloride transport flow-dependence and saturability (since transport of glucose and other organic solutes is flow-dependent and saturable). Clearly, further study of this important transport mechanism is required.

Axial Heterogeneity of Water Transport

Water reabsorption in the PCT is effected principally by the osmotic gradient (luminal hypotonicity and possibly peritubular hypertonicity) generated by reabsorption of sodium bicarbonate, sodium chloride, and organic solutes (11, 45). Flow-dependence of volume reabsorption in the PCT has been of great investigative interest for may years (46). In the late PCT during microperfusion, water reabsorption increases with load. However, the proportionality between water reabsorption and delivery has often been found not to be well maintained (46) (i.e., glomerulotubular balance has been less than perfect), in accord with the present results (compare dotted lines representing microperfusion

data and symbols representing present free-flow data in Figs. 11 and 12). In any event, the absolute rate of water reabsorption (<3 nl/mm·min) and the reabsorbed fraction of water delivered in the late PCT as a function of water delivery (<0.1) were relatively low under all free-flow conditions.

In the early PCT, on the other hand, a rise in SNGFR and filtered solute loads from a hydropenic to a euvolemic level was accompanied by excellent load-dependent solute transport and water reabsorption. Water reabsorption increased to 10.1 nl/mm·min in the euvolemic state, a rate 4-5 times higher than observed under normal conditions in the late PCT (58). This water reabsorptive rate exceeds that which normally occurs in any other segment of the entire nephron. In addition, the increase in absolute water reabsorption in the early PCT in the transition from the hydropenic to euvolemic state was proportional to the increased SNGFR; maintenance of excellent fractional water reabsorption at a high level (0.20-0.25). Glomerulo-tubular balance was perfect and fully a quarter of the glomerular ultrafiltrate was reabsorbed in the first mm of the nephron under conditions of low-to-normal SNGFR.

The early PCT reabsorbed a greater fraction of delivered volume than the late PCT and tended to exhibit better glomerulo-tubular balance in the low-to-normal SNGFR range. However, a further increase in SNGFR with ANF or glucagon revealed no higher water reabsorptive capacity and fractional water reabsorption

then declined. This lack of flow-dependent reabsorption in both the early and late PCT when the SNGFR rose above normal caused a disproportionately large fraction (~80%) of the increment in filtered sodium and water load to be transmitted out of the PCT.

These findings emphasize the complicated nature of water reabsorption in the PCT: (1) there is an axial gradient in the capacity for solute and water reabsorption; (2) there appears to be a heterogeneous, non-linear, water reabsorptive response as a function of length to a change in luminal flow and anion composition; (3) and there can be differential regulation of solute and water reabsorption in the early versus late tubule by peritubular factors. Such complex kinetics and determinants of transport as a function of length may explain some of the disparity in reported results regarding flow-dependency of whole PCT volume reabsorption (46).

In conclusion, the early superficial PCT is distinguished from the late PCT by having high capacity, flow-responsive but saturable, anion and volume reabsorptive processes relatively unaffected by alkalemia.

ACKNOWLEDGMENTS

We thank Floyd C. Rector, Jr., M.D. for his continuing support and advice. These studies were performed by Dr. Liu in partial fulfillment of the requirements for the the Ph.D. Degree in Physiology, University of California, San Francisco. These studies were supported in part by a Clinical Investigator Award (1-K08-AM-10115) and grants from the National Institute of Arthritis, Diabetes, and Digestive Diseases (Am-37423 and AM-27045) and from Wyeth Laboratories.

REFERENCES

1. Maunsbach, A. B. 1966. Observations on the segmentation of the proximal tubule in the rat kidney. J. Ultrastruct. Res. 16:239-258.

2. Berry, C. A. 1982. Heterogeneity of tubular transport processes in the nephron. Annu. Rev. Physiol. 44:181-201.

3. Jacobson, H. R. 1981. Functional segmentation of the mammalian nephron. Am. J. Physiol. 241 (Renal Fluid Electrolyte Physiol. 10):F203-F218.

4. Liu, F.-Y., and M. G. Cogan. 1984. Axial heterogeneity in the rat proximal convoluted tubule. I. Bicarbonate, chloride and water transport. Am. J. Physiol. 247 (Renal Fluid Electrolyte Physiol. 16):F816-F821.

5. Alpern, R. J., M. G. Cogan, and F. C. Rector, Jr. 1982. Effect of luminal bicarbonate concentration on proximal acidification in the rat. Am. J. Physiol. 243 (Renal Fluid Electrolyte Physiol. 12): F53-F59.

6. Alpern, R. J., M. G. Cogan, and F. C. Rector, Jr. 1983. Flow dependence of proximal tubular bicarbonate absorption. Am. J. Physiol. 245 (Renal Fluid Electrolyte Physiol. 14): F478-F484.

7. Maddox, D. A., L. J. Atherton, W. M. Deen, and F. J. Gennari. 1984. Proximal HCO_3^- reabsorption and the determinants of tubular and capillary P_{CO_2} in the rat. Am. J. Physiol. 247 (Renal Fluid Electrolyte Physiol. 16): F73-F81.

8. Maddox, D. A., and F. J. Gennari. 1985. Load dependence of HCO_3 and H_2O reabsorption in the early proximal tubule of

the Munich-Wistar rat. Am. J. Physiol. 248 (Renal Fluid Electrolyte Physiol. 17): F113-F121.

9. Berry, C. A., and F. C. Rector, Jr. 1980. Active and passive sodium transport in the proximal tubule. Mineral Electrolyte Metab. 4:149-160.

10. Corman, B., R. Thomas, R. McLeod, and C. de Rouffignac. 1980. Water and total CO_2 reabsorption aong the rat proximal convoluted tubule. Pfluegers Arch. Eur. J. Physiol. 389:45-53.

11. Rector, F. C., Jr. 1983. Sodium, bicarbonate, and chloride absorption by the proximal tubule. Am. J. Physiol. 244 (Renal Fluid Electrolyte Physiol. 13): F461-F471.

12. Green, R., R. J. Moriarty, and G. Giebisch. 1981. Ionic requirements of proximal tubular fluid reabsorption: Flow dependence of fluid transport. Kidney Int. 20:580-587.

13. Senekjian, H.O., T. F. Knight, S. C. Sansom, and E. J. Weinman. 1980. Effect of flow rate and the extracellular fluid volume on proximal urate and water absorption. Kidney Int. 17:155-161.

14. Wiederholt, M., K. Hierholzer, E. E. Windhager, and G. Giebisch. 1967. Microperfusion study of fluid reabsorption in proximal tubules of rat kidneys. Am. J. Physiol. 213:809-818.

15. Morgan, T., and R. W. Berliner. 1969. In vivo perfusion of proximal tubules of the rat: glomerulotubular balance. Am. J. Physiol. 217:992-997.

16. Morel, F., and Y. Murayama. 1970. Simultaneous measurement

of unidirectional and net sodium fluxes in microperfused rat proximal tubules. Pfluegers Arch. Eur. J. Physiol. 320:1-23.

17. Cogan, M. G., and R. J. Alpern. 1984. Regulation of proximal bicarbonate reabsorption. Am. J. Phyiol. 247 (Renal Fluid Electrolyte Physiol. 16): F387-F395.

18. Alpern, R. J., and F. C. Rector, Jr. 1985. A model of proximal tubular bicarbonate absorption. Am. J. Physiol. 248 (Renal fluid Electrolyte Physiol. 17): F272-F281.

19. Alpern, R. J., M. G. Cogan, and F. C. Rector, Jr. 1983. Effects of extracellular volume and plasma bicarbonate concentration on proximal acidification in the rat. J. Clin. Invest. 71:736-746.

20. Cogan, M. G., and F.-Y. Liu. 1983. Metabolic alkalosis in the rat. Evidence that reduced glomerular filtration rather than enhanced tubular bicarbonate reabsorption is responsible for maintaining the alkalotic state. J. Clin. Invest. 71:1141-1160.

21. Cantin, M., and J. Genest. 1985. The heart and the atrial natriuretic factor. Endocrine Rev. 6:107-127.

22. Biachi, G., G. Gutkowska, G. Thibault, R. Garcia, J. Genest, and M. Cantin. 1985. Radioautographic localization of ^{125}I-atrial natriuretic factor (ANF) in rat tissues. Histochem. 82:441-452.

23. Huang, C.-L., H. E. Ives, and M. G. Cogan. 1986. Atrial natriuretic factor causes glomerular hyperfiltration, blunted tubulo-glomerular feedback, and increased glomeru-

lar cGMP generation. Kidney Int. 29:384.

24. Stokes, T. J., and K. J. Martin. 1986. Atriopeptin III increases cGMP in glomeruli but not in proximal tubules of dog kidney. Am. J. Physio. 250 (Renal Fluid Electrolyte Physiol. 19): F27-F31.

25. Tremblay, J., R. Gerzer, P. Vinay, S. C. Pang., R. Beliveau, and P. Hamet. 1985. The increase of cGMP by atrial natriuretic factor (ANF) correlates with the distribution of particulate guanylate cyclase. FEBS Letters 181:17.

26. Huang, C.-L., J. Lewicki, L. K. Johnson, and M. G. Cogan. 1985. Renal mechanism of action of rat atrial natriuretic factor. J. Clin. Invest. 75:769-773.

27. Sonnenberg, H., and W. A. Cupples. 1982. Intrarenal localization of the natriuretic effect of cardiac atrial extract. Can. J. Physiol. Pharmacol. 60:1149-1152.

28. Briggs, J. P., B. Steipe, G. Schubert, and J. Schnermann. 1982. Micropuncture studies on the renal effects of atrial natriuretic substance. Pfluegers Arch. Eur. J. Physiol. 395:271-276.

29. Cogan, M. G. 1986. Atrial natriuretic factor can increase renal solute excretion primarily by raising glomerular filtration. Am. J. Physiol. 250 (Renal Fluid Electrolyte Physiol. 19): Fxxx-Fxxx.

30. Baum, M., and R. Toto. 1986. Lack of direct effect of atrial natriuretic factor in the rabbit proximal tubule. Am. J. Physiol. 250 (Renal Fluid Electrolyte Physiol. 19): F66-F69.

31. Bailly, C., M. Imbert-Teboul, D. Chabardes, A. Hus-Citharel, M. Montegut, A. Clique, and F. Morel. 1980. The distal nephron of rat kidney: A target site for glucagon. Proc. Natl. Acad. Sci. USA 77:3422-3424.

32. Levy, M., and N. L. Starr. 1972. The mechanism of glucagon-induced natriuresis in dogs. Kidney Int. 2:76-84.

33. Cogan, M.G., D. A. Maddox, M. S. Lucci, and F. C. Rector, Jr. 1979. Control of proximal bicarbonate reabsorption in normal and acidotic rats. J. Clin. Invest. 64:1168-1180.

34. Cogan, M. G. 1985. Atrial natriuretic factor ameliorates chronic metabolic alkalosis by increasing glomerular filtration. Science 2229:1405-1407.

35. Vurek, G. G., D. G. Warnock, and R. Corsey. 1975. Measurement of picomole amounts of carbon dioxide by calorimetry. Anal. Chem. 47:765-767.

36. Ramsay, J. A., R. H. J. Brown, and P. C. Croghan. 1955. Electrometric titration of chloride in small volumes. J. Exp. Biol. 32:822-829.

37. Fromter, E., and K. Gessner. 1975. Effect of inhibitors and diuretics on electrical potential differences in rat kidney proximal tubule. Pfluegers Arch. Eur. J. Physiol. 357:209-224.

38. Sasaki, S., C. A. Berry, and F. C. Rector, Jr. 1982. Effect of luminal and peritutublar HCO_3^- concentrations and P_{CO_2} on HCO_3^- reabsorption in rabbit proximal convoluted tubules perfused in vitro. J. Clin. Invest. 70:639-649.

39. Blumenthal, S. S., R. A. Ware, and J. G. Kleinman. 1985.

Proximal tubule hydrogen ion transport processes in diuretic-induced metabolic alkalosis. J. Lab. Clin. Med. 106:17-22.

40. Maddox, D. A., and F. J. Gennari. 1986. Load dependence of proximal tubular bicarbonate reabsorption in chronic metabolic alkalosis in the rat. J. Clin. Invest., In press.

41. Berry, C. A., and M. G. Cogan. 1981. Influence of peritubular protein on solute absorption in the rabbit proximal tubule. A specific effect on NaCl transport. J. Clin. Invest. 68:506-516.

42. Warnock, D. G, and J. Evçloff. 1982. NaCl entry mechanisms in the luminal membrane of the renal tubule. Am. J. Physiol. 242 (Renal Fluid Electrolyte Physiol. 11) F561-F574.

43. Burg, M. B. 1982. Thick ascending limb of Henle's loop. Kidney Int. 22:454-464.

44. Karniski, L. P., and P. S. Aronson. 1985. Chloride/formate exchange with formic acid recycling: A mechanism of active chloride transport across epithelial membranes. Proc. Natl. Acad. Sci. USA:

45. Liu, F.-Y., and M. G. Cogan. 1984. Axial heterogeneity in the rat proximal convoluted tubule. II. Osmolality and osmotic water permeability. Am. J. Physiol. 247 (Renal Fluid Electrolyte Physiol. 16): F822-F826.

46. Wilcox, C. S., and C. Baylis. 1986. Glomerular-tubular balance and proximal regulation. In: Seldin, D. W., and G. Giebish, Eds. The Kidney: Physiology and Pathophysiology. New York, Raven Press, pp. 985-1012.

Table 1. General Characteristics

	Group	Animal Weight (g)	Tubule Length (mm)	SNGFR (nl/min)	Plasma $[HCO_3^-]$ (meq/L)	Plasma $[Cl^-]$ (meq/L)
1.	Hydropenia	216±3	4.83±0.07	28.7±0.7	24.1±0.5	105±1
2.	Euvolemia	217±6	4.98±0.10	41.5±0.4	24.1±0.5	109±1
3.	ANF	213±3	5.18±0.06	51.2±0.7	24.5±0.5	104±1
4.	Glucagon	210±5	5.10±0.07	50.7±0.6	24.7±0.1	104±1
5.	Alkalosis	207±5	4.88±0.07	30.9±0.6	41.3±0.9	93±1

Table 2. Anion Concentration and Delivery Rates as a Function of PCT Length

Anion Concentrations

Group	Bowman's Space	1st mm	2nd mm	3rd mm	4th mm	5th mm
HCO_3^- (mEq/L)						
1. Hydropenia	25.7±0.7	16.9±0.8	10.4±0.6	8.6±0.6	6.8±0.7	5.7±0.3
2. Euvolemia	27.3±0.2	19.6±0.4	13.9±0.4	10.8±0.5	8.6±0.3	6.4±0.4
3. ANF	27.8±0.5	21.5±0.5	17.1±0.4	14.3±0.3	11.5±0.2	9.1±0.3
4. Glucagon	28.2±0.6	21.3±0.7	16.7±0.7	14.4±0.7	11.7±0.3	9.3±0.4
5. Alkalosis	46.6±1.5	36.1±1.4	28.5±1.2	27.0±1.1	25.5±1.0	23.9±0.8
Cl^- (mEq/L)						
1. Hydropenia	118.6±0.6	138.9±1.8	140.7±2.4	139.4±1.8	140.1±1.9	138.5±2.5
2. Euvolemia	113.4±0.4	131.8±1.3	132.9±2.2	132.2±2.1	134.1±2.1	135.5±2.5
3. ANF	107.6±1.2	121.1±0.7	123.2±1.2	124.2±1.0	125.1±0.7	125.6±1.2
4. Glucagon	107.4±0.9	117.5±0.3	120.5±0.9	123.5±1.2	125.1±1.1	124.9±1.5
5. Alkalosis	96.8±0.6	115.4±1.4	125.9±0.7	127.2±1.3	129.7±2.8	133.1±5.1

Delivery Rates

Group	Bowman's Space	1st mm	2nd mm	3rd mm	4th mm	5th mm
HCO_3^- (peq/min)						
1. Hydropenia	740±31	385±24	199±16	151±15	110±15	86±15
2. Euvolemia	1135±9	615±18	382±15	272±15	196±10	133±10
3. ANF	1424±24	882±14	628±17	484±9	359±6	266±13
4. Glucagon	1430±36	883±25	622±34	485±30	358±13	263±12
5. Alkalosis	1437±28	871±28	569±21	481±19	396±18	323±17
Cl^- (peq/min)						
1. Hydropenia	3363±88	3157±118	2674±97	2392±87	2144±79	1952±70
2. Euvolemia	4704±37	4141±43	3634±39	3311±47	3056±61	2802±55
3. ANF	5503±56	4966±48	4524±42	4209±38	3907±48	3661±49
4. Glucagon	5443±66	4886±44	4489±52	4157±50	3839±80	3547±112
5. Alkalosis	2992±71	2794±58	2526±69	2270±61	2016±63	1796±61
H_2O (nl/min)						
1. Hydropenia	28.7±0.7	22.8±0.7	19.0±0.5	17.3±0.5	15.6±0.5	14.4±0.6
2. Euvolemia	41.5±0.4	31.4±0.5	27.4±0.4	25.1±0.5	22.8±0.5	20.7±0.7
3. ANF	51.2±0.7	41.0±0.3	36.7±0.2	33.9±0.1	31.2±0.3	29.2±0.4
4. Glucagon	50.7±0.6	41.6±0.4	37.3±0.6	33.7±0.5	30.7±0.5	28.4±0.7
5. Alkalosis	30.9±0.6	24.3±0.7	20.1±0.6	17.7±0.4	15.5±0.3	13.5±0.3

Table 3. Absolute Anion and Water Transport Rates as a Function of PCT Length

Group	1st mm	2nd mm	3rd mm	4th mm	5th mm
HCO_3^- (peq/mm·min)					
1. Hydropenia	354±21	186±17	48±10	41±7	24±3
2. Euvolemia	520±12	233±22	109±11	76±6	73±10
3. ANF	542±14	254±16	144±11	125±12	93±8
4. Glucagon	547±29	261±38	137±17	127±17	95±17
5. Alkalosis	565±12	302±12	89±8	85±7	73±9
Cl^- (peq/mm·min)					
1. Hydropenia	206±55	483±94	282±42	248±40	192±35
2. Euvolemia	585±21	507±70	323±26	254±22	254±17
3. ANF	537±18	443±54	315±32	302±21	246±22
4. Glucagon	557±22	397±13	332±8	319±38	291±45
5. Alkalosis	198±32	268±24	256±18	253±16	220±23
H_2O (nl/mm·min)					
1. Hydropenia	5.9±0.4	3.8±0.4	1.7±0.2	1.7±0.2	1.2±0.2
2. Euvolemia	10.1±0.4	4.1±0.5	2.3±0.2	2.3±0.1	2.1±0.2
3. ANF	10.2±0.5	4.3±0.5	2.9±0.2	2.6±0.2	2.1±0.1
4. Glucagon	9.1±0.4	4.3±0.2	3.6±0.2	3.0±0.4	2.3±0.3
5. Alkalosis	6.7±0.3	4.2±0.3	2.3±0.2	2.2±0.2	2.0±0.2

FIGURE LEGENDS

1. Axial profiles for tubular fluid/ultrafiltrate (TF/UF) concentration ratios for inulin, chloride and bicarbonate in Panel A for euvolemic Group 2; Panel B for ANF and glucagon hyperfiltration Groups 3 and 4; and Panel C for alkalotic Group 5. Solid lines in each case depict mean values for hydropenic Group 1.

2. Bicarbonate transport as a function of PCT length for hydropenic Group 1 (hexagons), euvolemic Group 2 (squares), ANF-treated Group 3 (triangles), and glucagon-treated Group 4 (inverted triangles).

3. Bicarbonate transport by each PCT segment as a function of the delivered bicarbonate load to that segment for hydropenic Group 1 (hexagons), euvolemic Group 2 (squares), ANF-treated Group 3 (triangles), and glucagon-treated Group 4 (inverted triangles). Dotted line derived from microperfusion data of Alpern et al. (6).

4. Reabsorbed fraction of delivered bicarbonate load by each PCT segment as a function of the delivered bicarbonate load to that segment for hydropenic Group 1 (hexagons), euvolemic Group 2 (squares), ANF-treated Group 3 (triangles) and glucagon-treated Group 4 (inverted triangles). Dotted line derived from microperfusion data of Alpern et al. (6).

5. Bicarbonate transport as a function of PCT length for normal ANF-treated Group 3 (triangles) and glucagon-treated Group 4 (inverted triangles) compared with alkalotic Group 5 (circles).

6. Bicarbonate transport in the first mm of the PCT as a function of the filtered bicarbonate load for hydropenic Group 1 (hexagons), euvolemic Group 2 (squares), ANF-treated Group 3 (triangles), glucagon-treated Group 4 (inverted triangles), and alkalotic Group 5 (circles).

7. Chloride transport as a function of PCT length for hydropenic Group 1 (hexagons), euvolemic Group 2 (squares), ANF-treated Group 3 (triangles), glucagon-treated Group 4 (inverted triangles), and alkalotic Group 5 (circles).

8. Chloride transport by each PCT segment as a function of the delivered chloride load to that segment for hydropenic Group 1 (hexagons), euvolemic Group 2 (squares), ANF-treated Group 3 (triangles), glucagon-treated Group 4 (inverted triangles), and alkalotic Group 5 (circles). Dotted line derived from microperfusion data of Green et al. (12).

9. Reabsorbed fraction of delivered chloride load by each PCT segment as a function of the delivered bicarbonate load to that segment for hydropenic Group 1 (hexagons), euvolemic Group 2 (squares), ANF-treated Group 3 (triangles), glucagon-treated

Group 4 (inverted triangles), and alkalotic Group 5 (circles). Dotted line derived from microperfusion data of Green et al. (12).

10. Water transport as a function of PCT length for hydropenic Group 1 (hexagons), euvolemic Group 2 (squares), ANF-treated Group 3 (triangles), and glucagon-treated Group 4 (inverted triangles).

11. Water transport by each PCT segment as a function of the delivered water load to that segment for hydropenic Group 1 (hexagons), euvolemic Group 2 (squares), ANF-treated Group 3 (triangles), and glucagon-treated Group 4 (inverted triangles). Dotted line derived from microperfusion data of Alpern et al. (6).

12. Reabsorbed fraction of delivered water load by each PCT segment as a function of the delivered water load to that segment for hydropenic Group 1 (hexagons), euvolemic Group 2 (squares), ANF-treated Group 3 (triangles), and glucagon-treated Group 4 (inverted triangles). Dotted line derived from microperfusion data of Alpern et al. (6).

FOOTNOTES

1. Abbreviations used in this paper: PCT, proximal convoluted tubule; GFR, glomerular filtration rate; SNGFR, single nephron GFR; ANF, atrial natriuretic factor.

2. The quantity of organics reabsorbed in the early PCT can be estimated if it is assumed: (1) that the constituents of the reabsorbate beside sodium bicarbonate and sodium chloride are principally organics solutes; and (2) that the reabsorbate is approximately isosmotic (300 mOsm/kg H_2O) (44). The organic solute flux can then be estimated as:

$$(300)(H_2O \text{ reabsorption}) - 2(HCO_3^- + Cl^- \text{ reabsorption})$$

and was 656, 820, 902 and 522 pmol/mm·min in the first mm of the PCT in Groups 1-4, respectively. These organic solute reabsorption rates would be more than sufficient to account for the quantity of chloride reabsorbed if the paracellular pathway in this nephron segment were relatively chloride-selective (9).

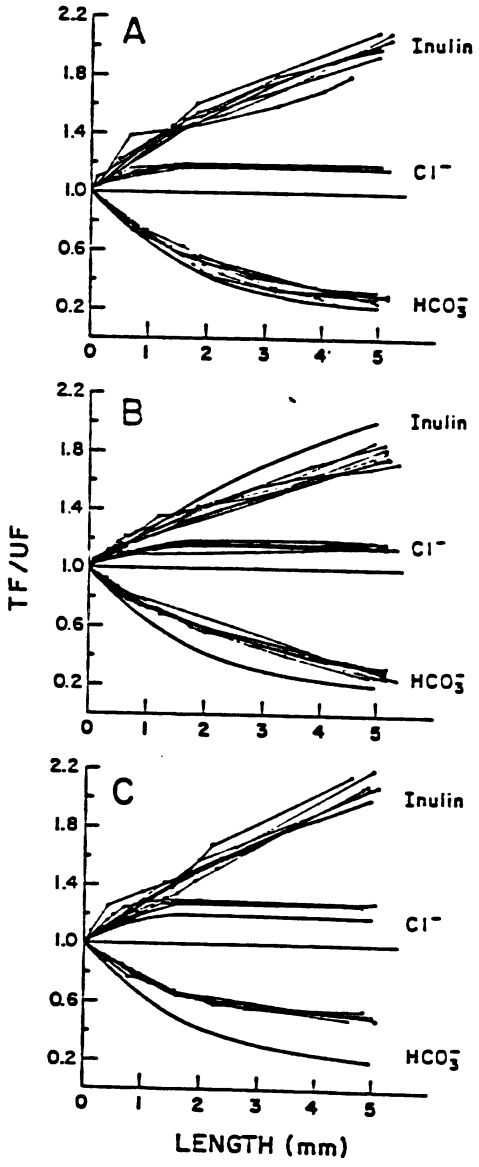

Fig. 1

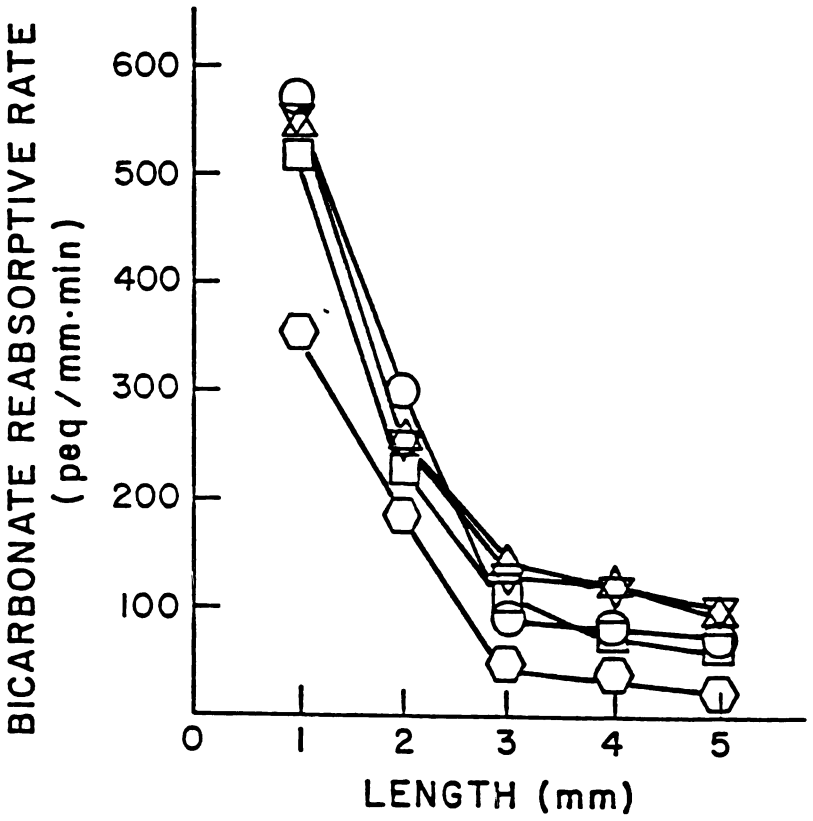
BICARBONATE REABSORPTIVE RATE
(peq/mm·min)
600
500
400
300
200
100
0
1
2
3
4
5
LENGTH (mm)

Fig. 2

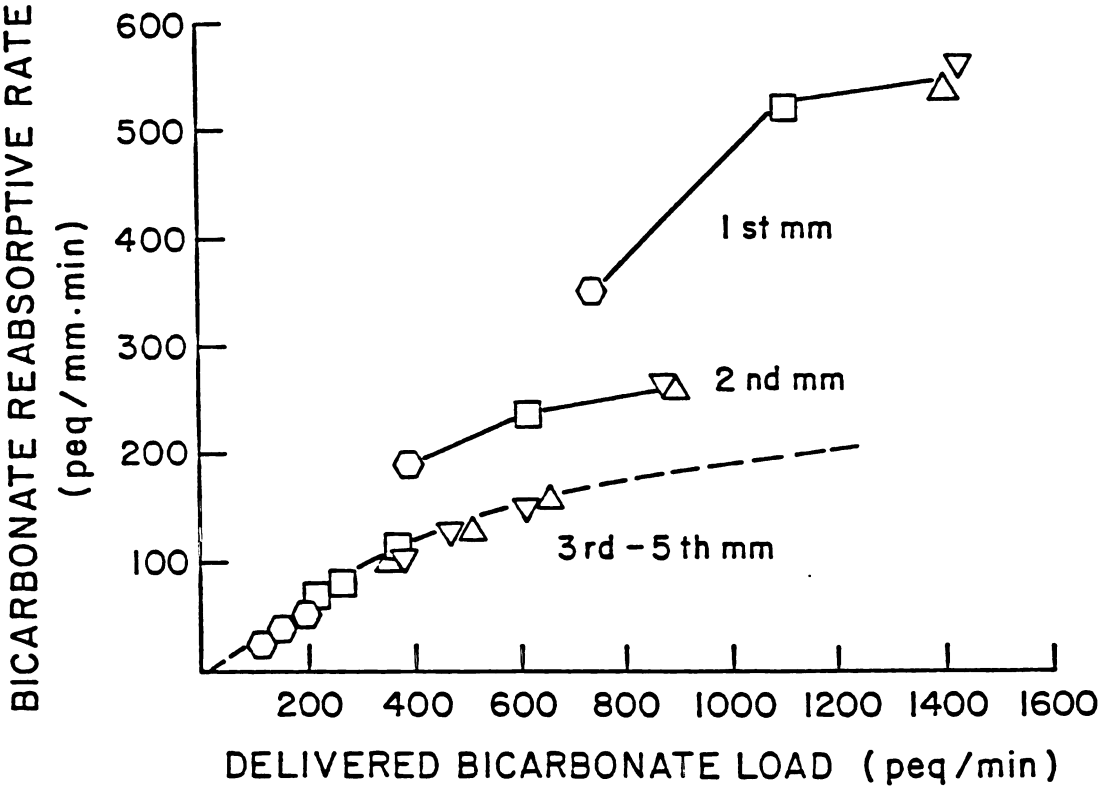
BICARBONATE REABSORPTIVE RATE
(peq/mm·min)
600
500
400
300
200
100
1 st mm
2 nd mm
3 rd - 5 th mm
200
400
600
800
1000
1200
1400
1600
DELIVERED BICARBONATE LOAD (peq/min)

Fig. 3

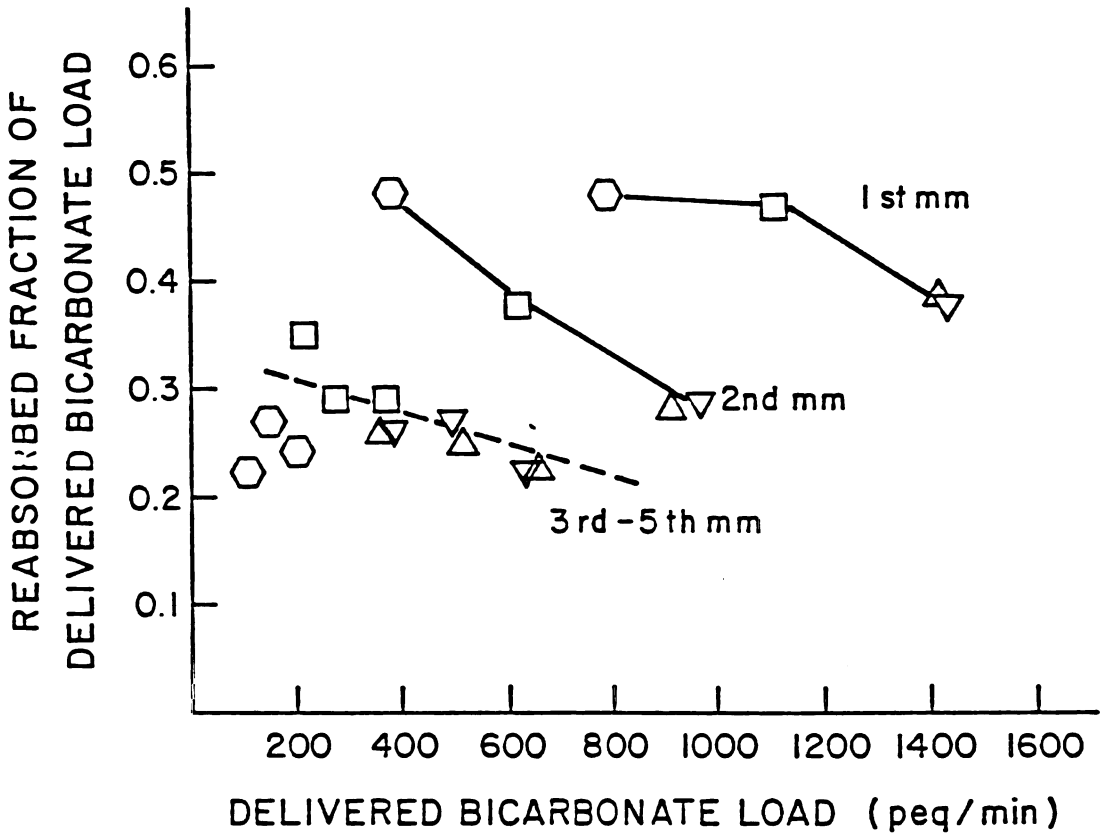
REABSORBED FRACTION OF
DELIVERED BICARBONATE LOAD
0.6
0.5
0.4
0.3
0.2
0.1
1st mm
2nd mm
3rd-5th mm
200
400
600
800
1000
1200
1400
1600
DELIVERED BICARBONATE LOAD (peq/min)

Fig. 4

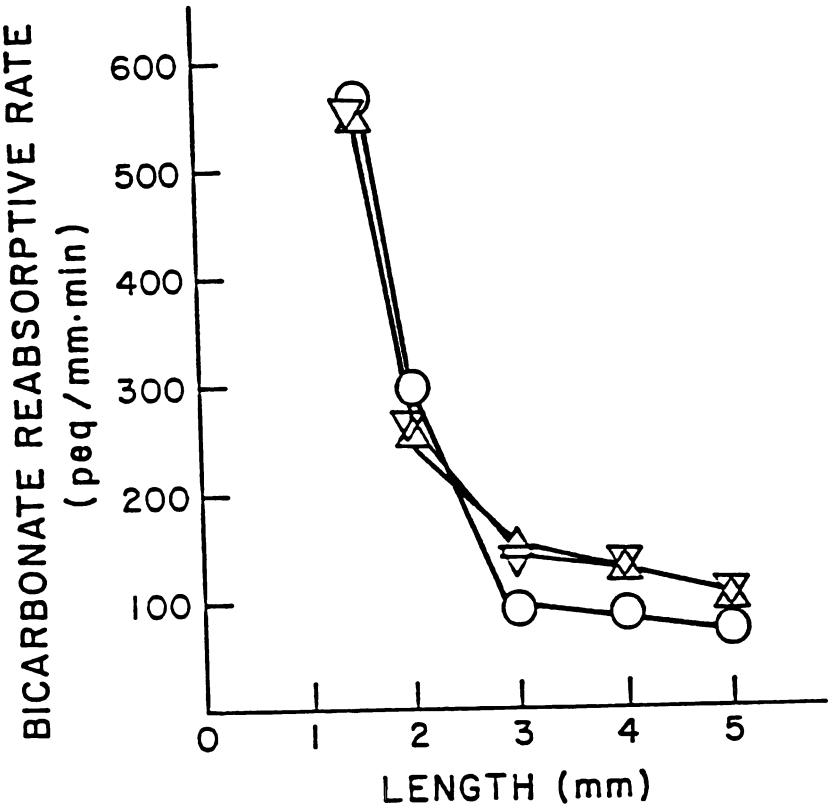
BICARBONATE REABSORPTIVE RATE
(peq/mm·min)
600
500
400
300
200
100
0
1
2
3
4
5
LENGTH (mm)

Fig. 5

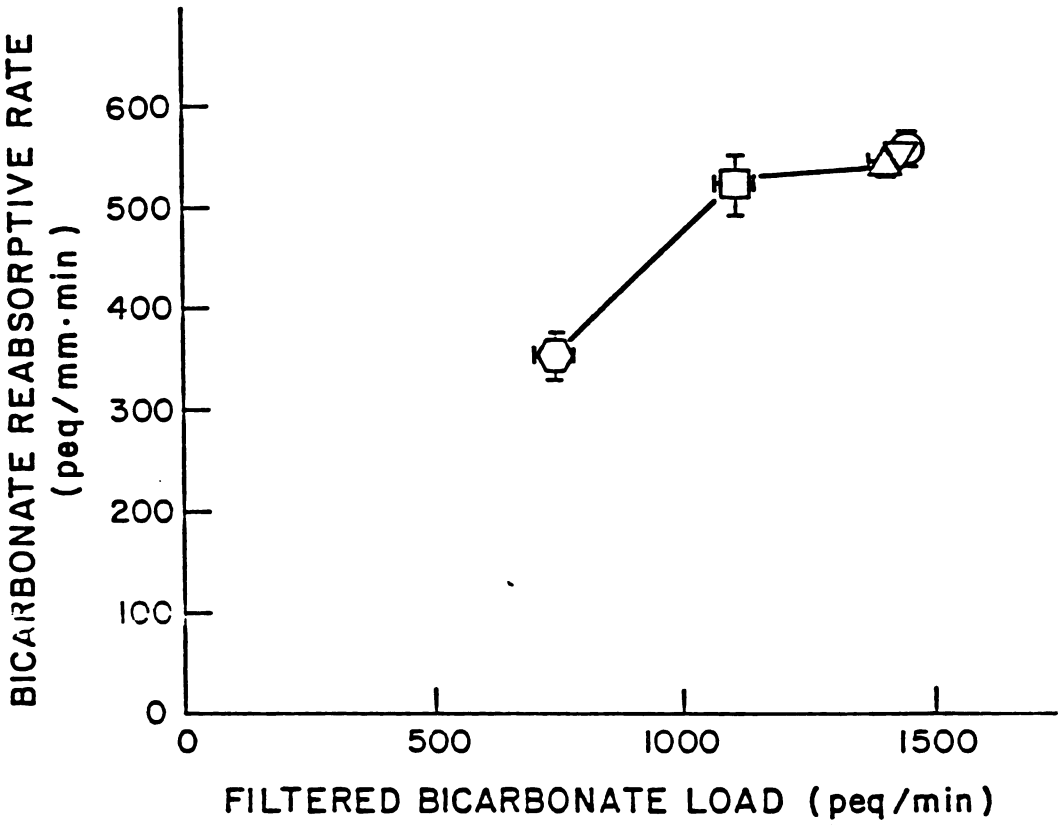
BICARBONATE REABSORPTIVE RATE
(peq/mm·min)
600
500
400
300
200
100
0
0
500
1000
1500
FILTERED BICARBONATE LOAD (peq/min)

Fig. 6

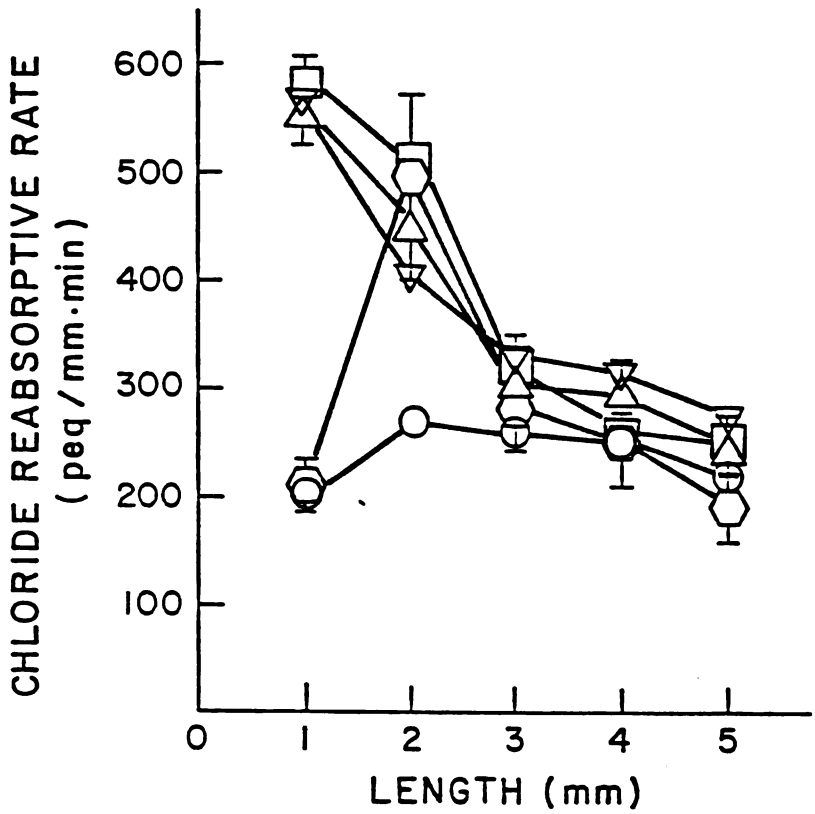
CHLORIDE REABSORPTIVE RATE
(peq / mm·min)
600
500
400
300
200
100
0
1
2
3
4
5
LENGTH (mm)

Fig. 7

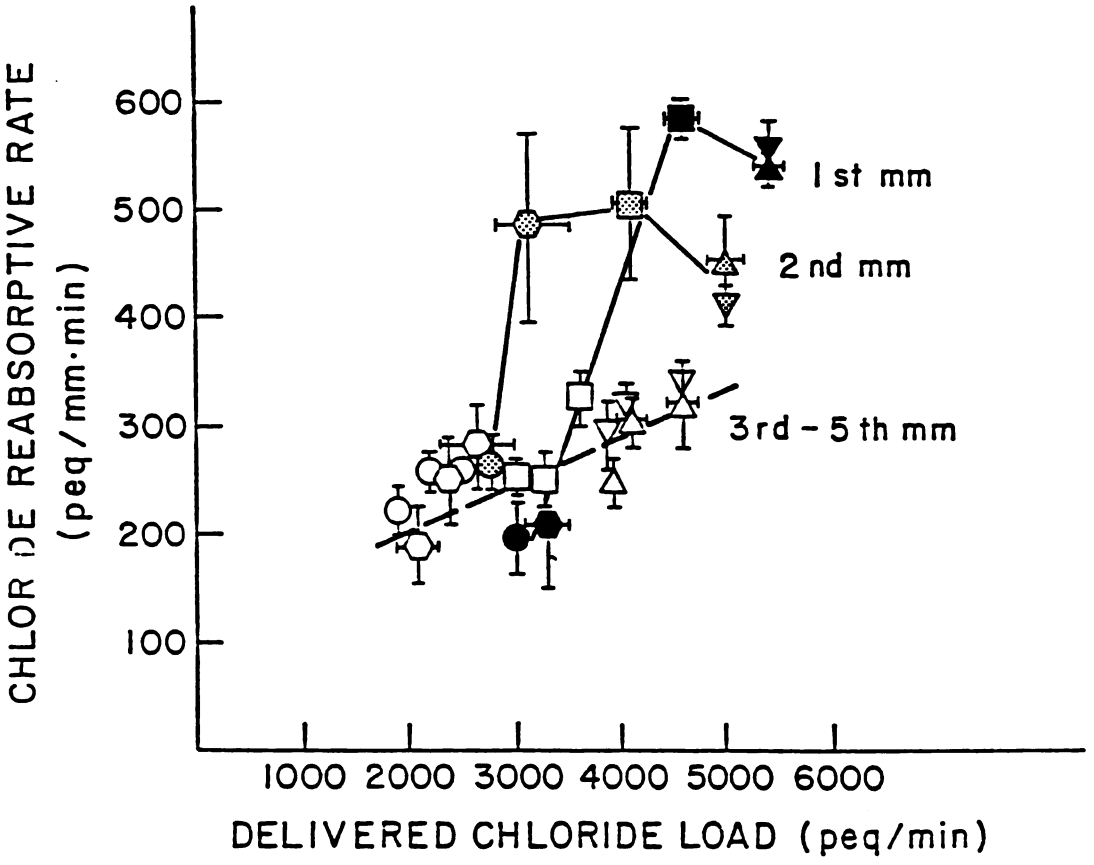
CHLORIDE REABSORPTIVE RATE
(peq/mm·min)
600
500
400
300
200
100
1st mm
2nd mm
3rd - 5th mm
1000 2000 3000 4000 5000 6000
DELIVERED CHLORIDE LOAD (peq/min)

Fig. 8

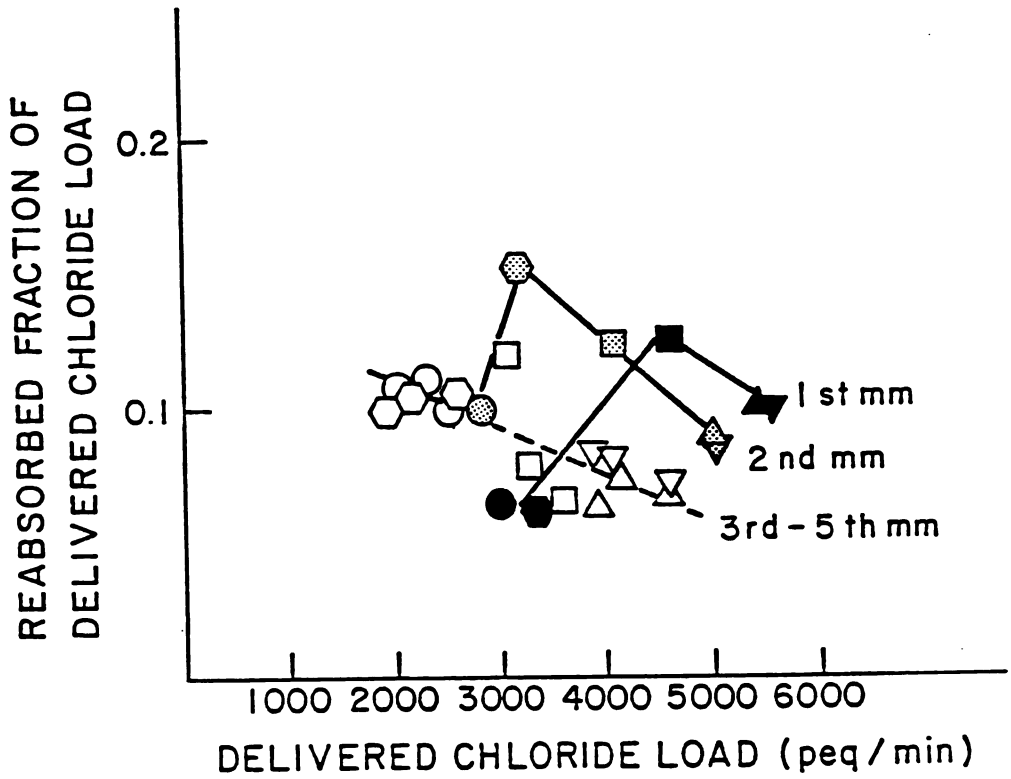
REABSORBED FRACTION OF
DELIVERED CHLORIDE LOAD
0.2
0.1
1st mm
2nd mm
3rd - 5th mm
1000 2000 3000 4000 5000 6000
DELIVERED CHLORIDE LOAD (peq / min)

Fig. 9

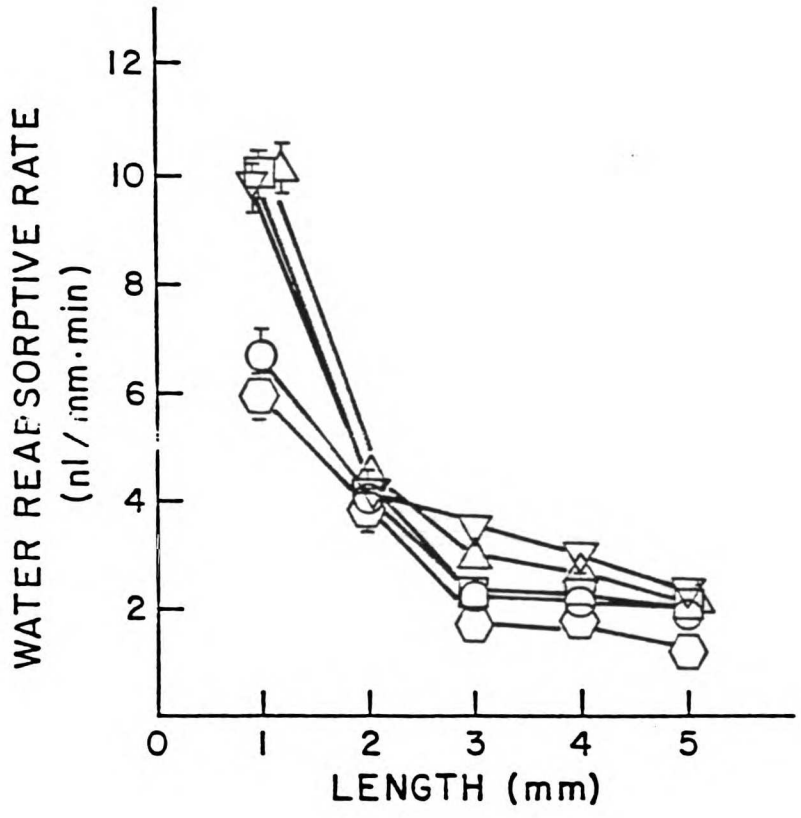
WATER REABSORPTIVE RATE
(nl / mm·min)
12
10
8
6
4
2
0
1
2
3
4
5
LENGTH (mm)

Fig. 10

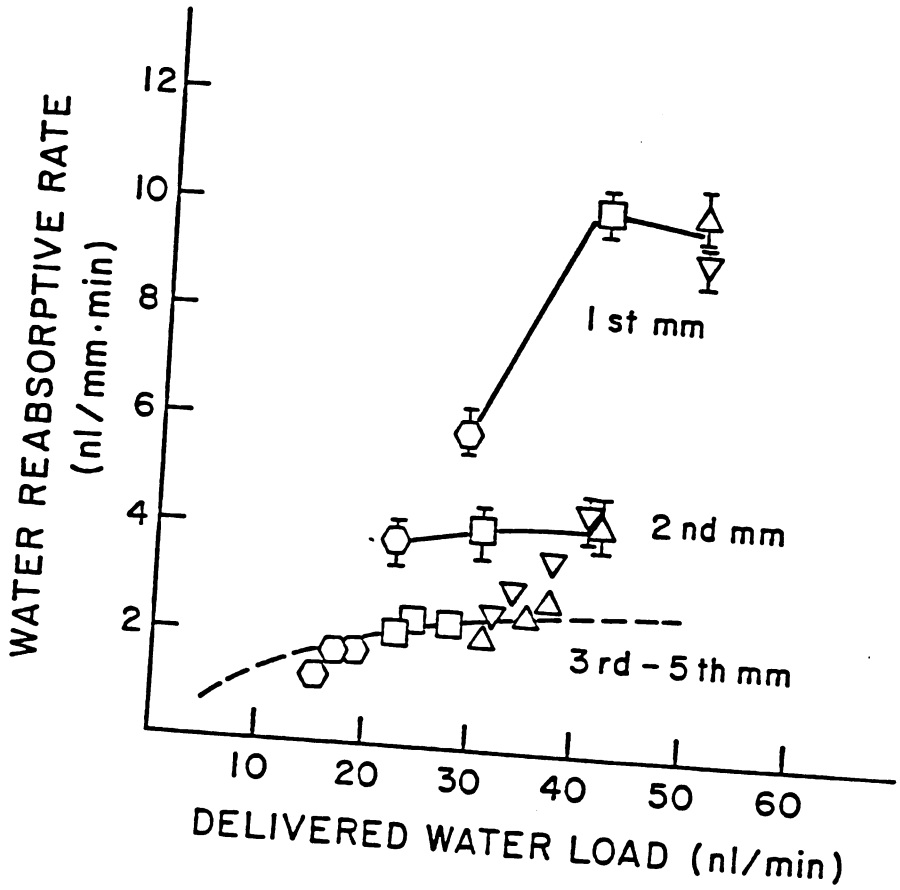
WATER REABSORPTIVE RATE
(nl/mm·min)
12
10
8
6
4
2
1 st mm
2 nd mm
3 rd - 5 th mm
10
20
30
40
50
60
DELIVERED WATER LOAD (nl/min)

Fig. 11

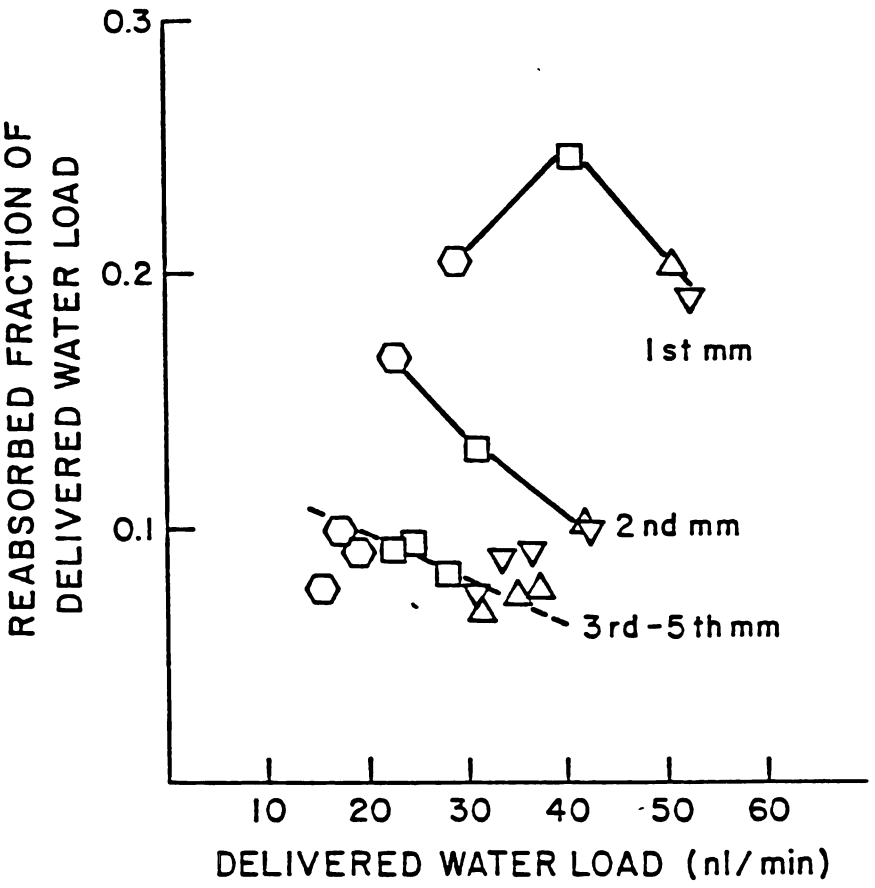
0.3
0.2
0.1
REABSORBED FRACTION OF DELIVERED WATER LOAD
1st mm
2nd mm
3rd-5th mm
10
20
30
40
50
60
DELIVERED WATER LOAD (nl/min)

FIG. 12

REFERENCES

1. Liu, F.-Y. and M. G. Cogan. Axial heterogeneity in the rat proximal convoluted tubule. 1. Bicarbonate, chloride and water transport. Am. J. Physiol. 247 (Renal Fluid and Electrolyte Physiol. 16): F816-F821, 1984.

2. Cogan, M. G. and R. J. Alpern. Regulation of proximal bicarbonate reabsorption. Am. J. Physiol. 247 (Renal Fluid Electrolyte Physiol. 16): F387-F396, 1984.

3. Liu, F.-Y. and M. G. Cogan. Axial heterogeneity in the rat proximal convoluted tubule. II. Osmolality and osmotic water permeability. Am. J. Physiol. 247 (Renal Fluid Electrolyte Physiol. 16): F822-F826, 1984.

4. Maunsbach, A. B. Observations on the segmentation of the proximal tubule in the rat kidney. J. Ultracture. Res. 16:239-258, 1966.

5. Cogan, M. G., D. A. Maddox, M. S. Lucci and F. C. Rector, Jr. Control of proximal bicarbonate reabsorption in normal and acidotic rats. J. Clin. Invest. 64:1168-1180, 1979.

6. Rector, F. C., Jr. Sodium, bicarbonate, and chloride

absorption by the proximal tubule. Am. J. Physiol. 244 (Renal Fluid Electrolyte Physiol. 13): F461-F471, 1983.

7. Chantrelle, B., M. G. Cogan and F. C. Rector, Jr. Evidence for coupled sodium/hydrogen exchange in the rat superficial proximal convoluted tubule. Pfluegers Arch. 395:186-189, 1982.

8. Alpern, R. J., M. G. Cogan and F. C. Rector, Jr. Effect of luminal bicarbonate concentration on proximal acidification in the rat. Am. J. Physiol. 243 (Renal Fluid Electrolyte Physiol. 12): F53-F59, 1982.

9. Malnic, G. and M. DeMello-Aires. Kinetic study of bicarbonate reabsorption in proximal tubule of the rat. Am. J. Physiol. 220:1759-1767, 1971.

10. Cogan, M. G. and F.-Y. Liu. Metabolic alkalosis in the rat: Evidence that reduced glomerular filtration rather than enhanced tubular bicarbonate reabsorption is responsible for maintaining the alkalotic state. J. Clin. Invest. 71:1141-1160, 1983.

11. Alpern, R. J., M. G. Cogan and F. C. Rector, Jr. Effects of extracellular fluid volume and plasma bicarbonate concentration on proximal acidification in the rat. J. Clin. Invest. 71:736-746, 1983.

12. Sasaki, S., C. A. Berry and F. C. Rector, Jr. Effect of

luminal and peritubular HCO_3^- concentrations and pCO_2 on HCO_3^- reabsorption in rabbit proximal convoluted tubules perfused in vitro. J. Clin. Invest. 70:639-649, 1982.

13. Chan, Y, L., B. Biagi and G. Giebisch. Control mechanisms of bicarbonate transport across the rat proximal convoluted tubule. Am. J. Physiol. 242 (Renal Fluid Electrolyte Physiol. 11): F532-F543, 1982.

14. Alpern, R. J., M. G. Cogan and F. C. Rector, Jr. Flow dependence of proximal tubular bicarbonate absorption. Am. J. Physiol. 245 (Renal Fluid Electrolyte Physiol. 14): F478-F484, 1983.

15. Cogan, M. G. Effects of acute alterations in pCO_2 on proximal HCO_3^-, Cl^- and H_2O reabsorption. Am. J. Physiol. 246 (Renal Fluid Electrolyte Physiol. 15): F21-F26, 1984.

16. Cogan, M. G. Chronic hypercapnia stimulates proximal bicarbonate reabsorption in the rat. J. Clin. Invest. 74:1942-1947, 1984.

17. Jacobson, H. R. Effects of CO_2 and acetazolamide on bicarbonate and fluid transport in rabbit proximal tubules. Am. J. Physiol. 240 (Renal Fluid Electrolyte Physiol. 9): F54-F62, 1981.

18. Cogan, M. G. Neurogenic regulation of proximal bicarbonate and chloride reabsorption. Am. J. Physiol. (Renal Fluid Electrolyte Physiol. 19): F22-F26, 1986.

19. Cogan, M. G., D. A. Maddox, D. G. Warnock, E. T. Lin and F. C. Rector, Jr. Effect of acetazolamide on bicarbonate reabsorption in the proximal tubule of the rat. Am. J. Physiol. 237 (Renal Fluid Electrolyte Physiol. 6): F447-F454, 1979.

20. Cogan, M. G. and F. C. Rector, Jr. Determinants of proximal bicarbonate, chloride and water reabsorption during carbonic anhydrase inhibition. Am. J. Physiol. 242 (Renal Fluid Electrolyte Physiol. 11): F274-F284, 1982.

21. Cogan, M. G. Volume expansion predominantly inhibits proximal reabsorption of NaCl rather than $NaHCO_3$. Am. J. Physiol. 245 (Renal Fluid Electrolyte Physiol. 14): F272-F275, 1983.

22. Berry, C. A. and M. G. Cogan. Influence of peritubular protein on solute absorption in the rabbit proximal tubule: A specific effect on NaCl transport. J. Clin. Invest. 68:506-516, 1981.

23. Alpern, R. J. Bicarbonate-water interactions in the rat proximal convoluted tubule: an unstirred layer effect. J. Gen. Physiol. 84:753-770, 1984.

24. Levine, D. Z., T. Walker and L.A. Nash. Effects of KCl infusions on proximal tubular function in normal and potassium-depleted rats. Kidney Intern. 4:318-325, 1973.

25. Maddox, D. A. and F. J. Gennari. Proximal tubular bicarbonate reabsorption and pCO_2 in chronic metabolic alkalosis in the rat. J. Clin. Invest. 72:1385-1395, 1983.

26. Ullrich, K. J., G. Rumrich and K. Baumann. Renal proximal tubular buffer-(glycodiazine) transport. Inhomogeneity of local transport rate, dependence on sodium, effect of inhibitors and chronic adaptation. Pfluegers Arch. 357:149-163, 1975.

27. Jacobson, H. R. Functional segmentation of the mammalian nephron. Am. J. Physiol. 241 (Renal Fluid Electrolyte Physiol. 10): F203-F218, 1981.

28. Maddox, D. A. and F. J. Gennari. Load dependence of HCO_3 and H_2O reabsorption in the early proximal tubule of the MunichWistar rat. Am. J. Physiol. 248 (Renal Fluid Electrolyte Physiol. 17):F113-F121, 1985.

29. Baum, M. and C. A. Berry. Evidence for neutral transcellular NaCl transport and neutral basolateral chloride exit in the rabbit proximal convoluted tubule. J. Clin. Invest. 74:205-211, 1984.

30. Baum, M. and C. A. Berry. Peritubular protein modulates neutral active NaCl absorption in rabbit proximal convoluted tubule. Am. J. Physiol. 248 (Renal Fluid Electrolyte Physiol. 17): F790-F795, 1985.

31. Green, R., R. J. Moriarty and G. Giebisch. Ionic requirements of proximal tubular fluid reabsorption: Flow dependence of fluid transport. Kidney Intern. 20:580-587, 1981.

32. Lucci, M. S. and D. G. Warnock. Effects of anion-transport inhibitors on NaCl reabsorption in the rat superficial proximal convoluted tubule. J. Clin Invest. 64:570-579, 1979.

33. Warnock, D. G. and J. Eveloff. NaCl entry mechanisms in the luminal membrane of the renal tubule. Am. J. Physiol. 242 (Renal Fluid Electrolyte Physiol. 11): F561-F574, 1982.

34. Chantrelle, B. M., M. G. Cogan and F. C. Rector, Jr. Active and passive components of NaCl absorption in the proximal convoluted tubule of the rat kidney. Mineral Electrolyte Metab. 11:209-214, 1985.

35. Berry, C. A. and F. C. Rector, Jr. Active and passive sodium transport in the proximal tubule. Mineral Electrolyte Metab. 4:149-160, 1980.

36. Alpern, R. J., K. J. Howlin and P. A. Preisig. Active and passive components of chloride transport in the rat proximal convoluted tubule. J. Clin. Invest. 76:1360-1366, 1985.

37. Jacobson, H. R., J. P. Kokko, D. W. Seldin and C. Holmberg. Lack of solvent drag of NaCl and $NaHCO_3$ in rabbit proximal tubules. Am. J. Physiol. 243 (Renal Fluid Electrolyte Physiol. 12): F342-F348, 1982.

38. Berry, C. A. Lack of effect of peritubular protein on passive NaCl transport in the rabbit proximal tubule. J. Clin. Invest. 71:268-281, 1983.

39. Neumann, K. H. and F. C. Rector, Jr. Mechanism of NaCl and water reabsorption in the proximal convoluted tubules of the kidney. Role of chloride concentration gradients. J. Clin. Invest. 58:1110-1118, 1976.

40. Preisig, P. and C. A. Berry. Evidence for transcellular osmotic water flow in rat proximal convoluted tubule. Am. J. Physiol. 249 (Renal Fluid Electrolyte Physiol. 18): F124-F131, 1985.

41. Schafer, J. A., C. S. Patlak, S. L. Troutman and T. E. Andreoli. Volume absorption in the pars recta. II. Hydraulic conductivity coefficient. Am. J. Physiol. 234 (Renal Fluid

Electrolyte Physiol. 3): F340-F348, 1978.

42. Andreoli, T. E., J. A. Schafer and S. L. Troutman. Perfusion rate-dependence of transepithelial osmosis in isolated proximal convoluted tubules: estimation of hydraulic conductance. Kidney Intern. 14:263-269, 1978.

43. Kokko, J. P., M. B. Burg and J. Orloff. Characteristic of NaCl and water transport in the renal proximal tubule. J. Clin. Invest. 50:69-76, 1971.

44. Wearn, J. T. and A. N. Richards. Observations on the composition of glomerular urine, with particular reference to the problem of reabsorption in the renal tubules Am. J. Physiol. 71:209-227, 1924.

45. Walker, A. M. and J. Oliver. Methods for the collection of fluid from single glomeruli and tubules of the mammalian kidney. Am. J. Physiol. 134:562-579, 1941.

46. Brenner, B. M., J. L. Troy and T. M. Daugharty. The dynamics of glomerular ultrafiltration in the rat. J. Clin Invest. 50:1776-1780, 1971.

47. Barfuss, D. W. and J. A. Schaffer. Differences in active and passive glucose transport along the proximal nephron. Am. J. Physiol. 240 (Renal Fluid Electrolyte Physiol. 10): F322-F332,

1981.

48. McKeown, J. W., P. C. Brazy and V. W. Dennis. Intrarenal heterogeneity for fluid, phosphate, and glucose absorption in the rabbit. Am. J. Physiol. 237 (Renal Fluid Electrolyte Physiol. 6): F312-F318, 1979.

49. Turner, R. J. and A. Moran. Heterogeneity of sodium-dependent D-glucose transport sites along the proximal tubule: evidence from vesicle studies. Am. J. Physiol. 242 (Renal Fluid Electrolyte Physiol. 11): F406-F414, 1982.

50. Lingard, J., G. Rumrich and J. A. Young. Reabsorption of L-glutamine and L-histidine from various regions of the rat proximal convolution studied by stationary microperfusion: evidence that the proximal convolution is not homogeneous. Pfluegers Arch. 342:1-12, 1973.

51. Brunette, M. G., L. Taleb and Carriere. Effect of parathyroid hormone on phosphate reabsorption along the nephron of the rat. Am. J. Physiol. 225:1076-1081, 1973.

52. Staum, B. B., R. J. Hamburger and M. Goldberg. Tracer microinjection study of renal tubular phosphate rabsorption in the rat. J. Clin Invest. 41:2271-2276, 1972.

53. Ramsay, J. A. and R. H. J. Brown. Simplified apparatus and

procedure for freezing-point determinations upon small volumes of fluid. J. Sci. Instrum. 32:372-375, 1955.

54. Vurek, G. G., D. G. Warnock and R. Corsey. Measurement of picomole amounts of carbon dioxide by calorimetry. Anal. Chem. 47:765-767, 1975.

55. Ramsay, J. A., R. H. J. Brown and P. C. Croghan. Electrometric titration of chloride in small volume. J. Exp. Biol. 32:822-829, 1955.

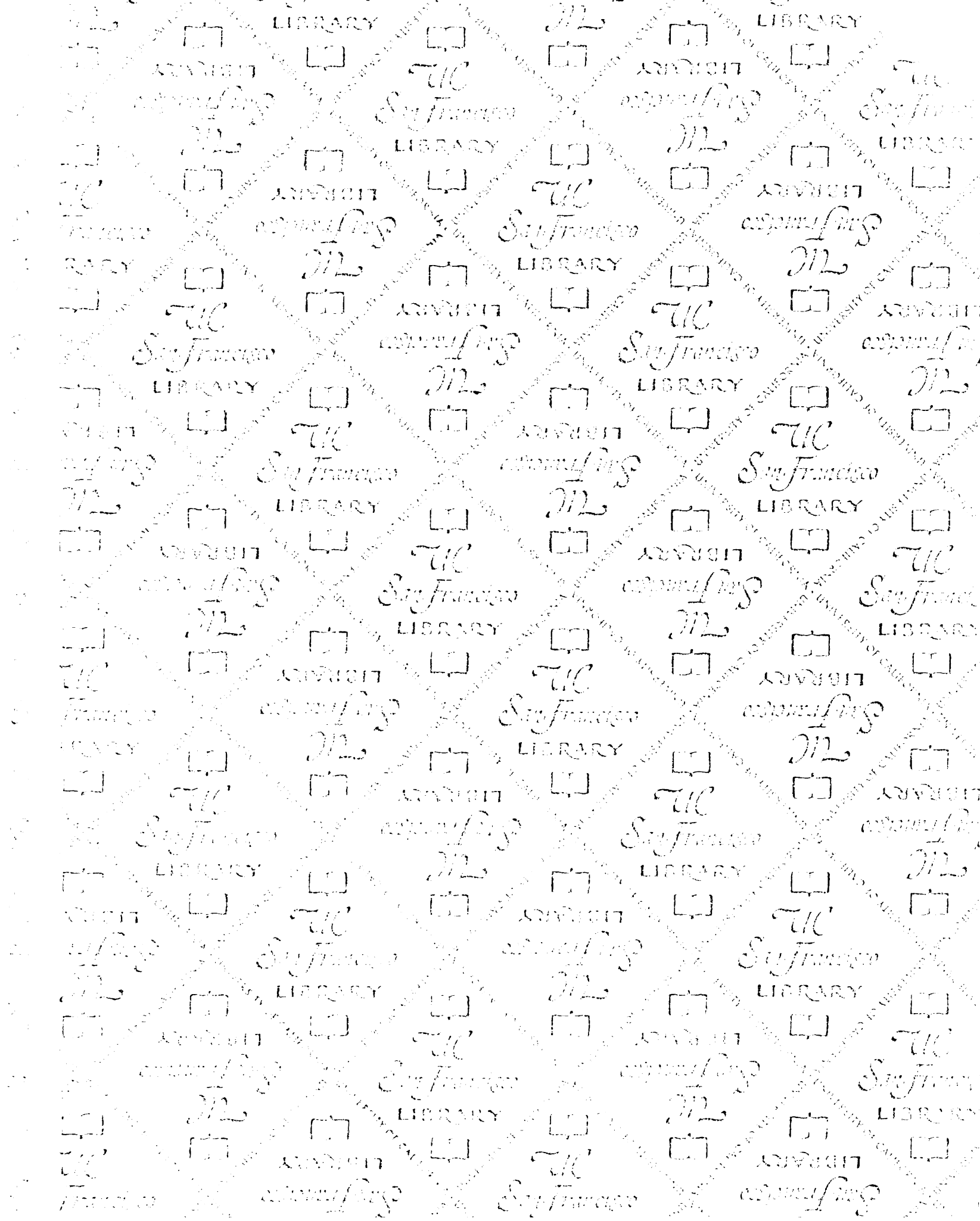
UC
San Francisco
LIBRARY